Contents

List of Tables

List of Figures

Chapter 7

Mean Field Theory of Phase Transitions

7.1 References

- M. Kardar, *Statistical Physics of Particles* (Cambridge, 2007)
  A superb modern text, with many insightful presentations of key concepts.
- M. Plischke and B. Bergersen, *Equilibrium Statistical Physics* ($3^{\rm rd}$ edition, World Scientific, 2006)
  An excellent graduate level text. Less insightful than Kardar but still a good modern treatment of the subject. Good discussion of mean field theory.
- G. Parisi, *Statistical Field Theory* (Addison-Wesley, 1988)
  An advanced text focusing on field theoretic approaches, covering mean field and Landau-Ginzburg theories before moving on to renormalization group and beyond.
- J. P. Sethna, *Entropy, Order Parameters, and Complexity* (Oxford, 2006)
  An excellent introductory text with a very modern set of topics and exercises. Available online at http://www.physics.cornell.edu/sethna/StatMech

7.2 The van der Waals system

7.2.1 Equation of state

Recall the van der Waals equation of state,

$$\left(p + \frac{a}{v^2}\right)(v - b) = RT \quad , \tag{7.1}$$

where $v = N_{\rm A}V/N$ is the molar volume. Solving for $p(v, T)$, we have

$$p = \frac{RT}{v - b} - \frac{a}{v^2} \quad . \tag{7.2}$$

Let us fix the temperature T and examine the function $p(v)$. Clearly $p(v)$ is a decreasing function of volume for v just above the minimum allowed value $v = b$, as well as for $v \to \infty$. But is $p(v)$ a monotonic function for all $v \in [b, \infty]$?

We can answer this by computing the derivative,

$$\left(\frac{\partial p}{\partial v}\right)_T = \frac{2a}{v^3} - \frac{RT}{(v - b)^2} \quad . \tag{7.3}$$

Setting this expression to zero for finite v, we obtain the equation[1]

$$\frac{2a}{bRT} = \frac{u^3}{(u - 1)^2} \quad , \tag{7.4}$$

where $u \equiv v/b$ is dimensionless. It is easy to see that the function $f(u) = u^3/(u - 1)^2$ has a unique minimum for $u > 1$. Setting $f'(u^*) = 0$ yields $u^* = 3$, and so $f_{\rm min} = f(3) = \frac{27}{4}$. Thus, for $T > T_{\rm c} = 8a/27bR$, the LHS of eqn. 7.4 lies below the minimum value of the RHS, and there is no solution. This means that $p(v, T > T_{\rm c})$ is a monotonically decreasing function of v.

At $T = T_{\rm c}$ there is a saddle-node bifurcation[2]. Setting $v_{\rm c} = bu^* = 3b$ and evaluating $p_{\rm c} = p(v_{\rm c}, T_{\rm c})$, we have that the location of the *critical point* for the van der Waals system is[3]

$$p_{\rm c} = \frac{a}{27\,b^2} \qquad , \qquad v_{\rm c} = 3b \qquad , \qquad T_{\rm c} = \frac{8a}{27\,bR} \quad . \tag{7.5}$$

For $T < T_{\rm c}$, there are two solutions to eqn. 7.4, corresponding to a local minimum and a local maximum of the function $p(v)$. The locus of points in the (v, p) plane for which $(\partial p/\partial v)_T = 0$ is obtained by setting eqn. 7.3 to zero and solving for T, then substituting this into eqn. 7.2. The result is

$$p^*(v) = \frac{a}{v^2} - \frac{2ab}{v^3} \quad . \tag{7.6}$$

[1] There is always a solution to $(\partial p/\partial v)_T = 0$ at $v = \infty$.

[2] See the appendix in §7.8.

[3] Equivalently, one can obtain the location of the saddle-node bifurcation in the local extrema of $p(T, v)$ by setting $(\partial p/\partial v)_T = 0$ and $(\partial^2 p/\partial v^2)_T = 0$. This yields two equations for the two unknowns $(T_{\rm c}, v_{\rm c})$. Invoking the van der Waals equation of state then yields $p_{\rm c} = p(T_{\rm c}, v_{\rm c})$.

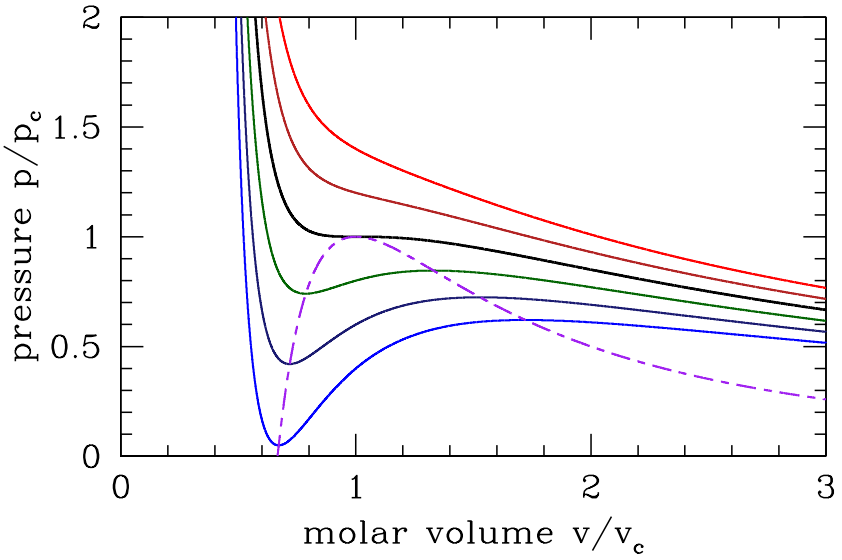

Figure 7.1: Pressure *versus* molar volume for the van der Waals gas at temperatures in equal intervals from $T = 1.10\,T_{\rm c}$ (red) to $T = 0.85\,T_{\rm c}$ (blue). The purple curve is $\bar{p}^*(\bar{v})$.

Expressed in terms of dimensionless quantities $\bar{p} = p/p_{\rm c}$ and $\bar{v} = v/v_{\rm c}$, this equation becomes

$$\bar{p}^*(\bar{v}) = \frac{3}{\bar{v}^2} - \frac{2}{\bar{v}^3} \quad . \tag{7.7}$$

Along the curve $p = p^*(v)$, the isothermal compressibility, $\kappa_T = -v^{-1}\big(\partial v/\partial p\big)_T$ diverges, heralding a *thermodynamic instability*. To understand better, let us compute the free energy of the van der Waals system, $F = E - TS$. Regarding the energy E, we showed back in chapter 2 that

$$\left(\frac{\partial \varepsilon}{\partial v}\right)_T = T\left(\frac{\partial p}{\partial T}\right)_v - p = \frac{a}{v^2} \quad , \tag{7.8}$$

which entails

$$\varepsilon(T,v) = \tfrac{1}{2}\mathfrak{f}RT - \frac{a}{v} \quad , \tag{7.9}$$

where $\varepsilon = E/\nu$ is the molar internal energy. The first term is the molar energy of an ideal gas, where $\mathfrak{f}$ is the number of molecular freedoms, which is the appropriate low density limit. The molar specific heat is then $c_V = \big(\partial\varepsilon/\partial T\big)_v = \frac{1}{2}\mathfrak{f}R$, which means that the molar entropy is

$$s(T,v) = \int^T\!\! dT'\,\frac{c_V}{T'} = \tfrac{1}{2}\mathfrak{f}R\log(T/T_{\rm c}) + s_1(v) \quad . \tag{7.10}$$

We then write $f = \varepsilon - Ts$, and we fix the function $s_1(v)$ by demanding that $p = -\big(\partial f/\partial v\big)_T$. This yields $s_1(v) = R\log(v-b) + s_0$, where s_0 is a constant. Thus[4],

$$f(T,v) = \tfrac{1}{2}\mathfrak{f}RT\left(1 - \log\big(T/T_{\rm c}\big)\right) - \frac{a}{v} - RT\log(v-b) - Ts_0 \quad . \tag{7.11}$$

gas	$a\ \left(\frac{\mathrm{L}^2\cdot\mathrm{bar}}{\mathrm{mol}^2}\right)$	$b\ \left(\frac{\mathrm{L}}{\mathrm{mol}}\right)$	p_c (bar)	T_c (K)	v_c (L/mol)
Acetone	14.09	0.0994	52.82	505.1	0.2982
Argon	1.363	0.03219	48.72	150.9	0.0966
Carbon dioxide	3.640	0.04267	7404	304.0	0.1280
Ethanol	12.18	0.08407	63.83	516.3	0.2522
Freon	10.78	0.0998	40.09	384.9	0.2994
Helium	0.03457	0.0237	2.279	5.198	0.0711
Hydrogen	0.2476	0.02661	12.95	33.16	0.0798
Mercury	8.200	0.01696	1055	1723	0.0509
Methane	2.283	0.04278	46.20	190.2	0.1283
Nitrogen	1.408	0.03913	34.06	128.2	0.1174
Oxygen	1.378	0.03183	50.37	154.3	0.0955
Water	5.536	0.03049	220.6	647.0	0.0915

Table 7.1: van der Waals parameters for some common gases. (Source: *Wikipedia*)

We know that under equilibrium conditions, f is driven to a minimum by spontaneous processes. Now suppose that $(\partial^2 f/\partial v^2)_T < 0$ over some range of v at a given temperature T. This would mean that one mole of the system at volume v and temperature T could lower its energy by rearranging into two half-moles, with respective molar volumes $v \pm \delta v$, each at temperature T, where δv is a positive infinitesimal. The total volume and temperature thus remain fixed, but the free energy changes by an amount $\Delta f = \frac{1}{2}(\partial^2 f/\partial v^2)_T(\delta v)^2 < 0$. This means that the system is unstable – it can lower its energy by dividing up into two subsystems each with different densities (*i.e.* molar volumes). Note that the onset of stability occurs when

$$\left.\frac{\partial^2 f}{\partial v^2}\right|_T = -\left.\frac{\partial p}{\partial v}\right|_T = \frac{1}{v\kappa_T} = 0 \quad , \tag{7.12}$$

which is to say when $\kappa_T = \infty$. As we saw, this occurs at $p = p^*(v)$, given in eqn. 7.6.

However, this condition, $(\partial^2 f/\partial v^2)_T < 0$, is in fact too strong. We need not limit our analysis to cases where δv is infinitesimal, in which case the system can be unstable even at molar volumes where $(\partial^2 f/\partial v^2)_T > 0$. The reason is shown graphically in fig. 7.2. At the fixed temperature T, for any molar volume v between $v_{\rm liquid} \equiv v_1$ and $v_{\rm gas} \equiv v_2$, the system can lower its free energy by *phase separating* into regions of different molar volumes. In general we can write

$$v = (1-x)\,v_1 + x\,v_2 \quad , \tag{7.13}$$

so $v = v_1$ when $x = 0$ and $v = v_2$ when $x = 1$. The free energy upon phase separation is simply

$$f = (1-x)\,f_1 + x\,f_2 \quad , \tag{7.14}$$

where $f_j = f(v_j, T)$. This function is given by the straight black line connecting the points at volumes v_1 and v_2 in fig. 7.2.

[4] Don't confuse the molar free energy (f) with the number of molecular degrees of freedom (ƒ)!

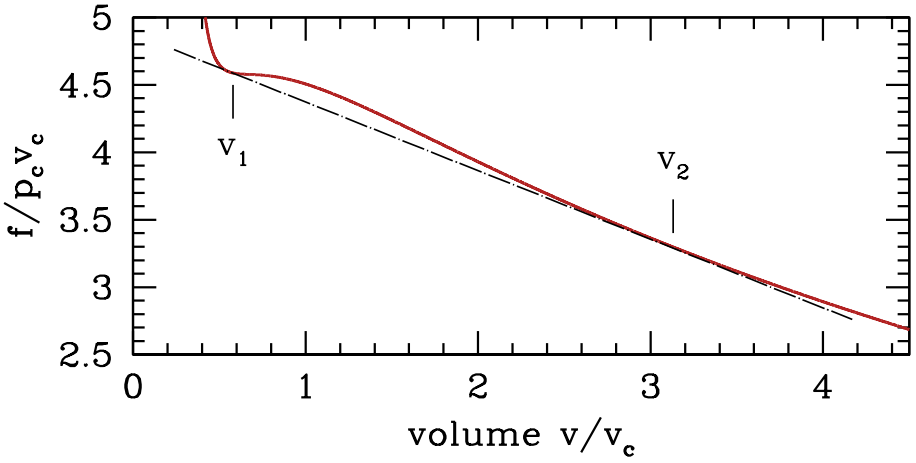

Figure 7.2: The molar free energy $f(T,v)$ of the van der Waals system at $T = 0.85\,T_{\rm c}$. The dot-dashed black line shows the Maxwell construction connecting molar volumes $v_{1,2}$ on opposite sides of the coexistence curve.

The two equations which give us v_1 and v_2 are

$$\left.\frac{\partial f}{\partial v}\right|_{v_1,T} = \left.\frac{\partial f}{\partial v}\right|_{v_2,T} = \frac{f(T,v_2)-f(T,v_1)}{(v_2-v_1)} \quad . \tag{7.15}$$

Equivalently, in terms of the pressure, $p = -\big(\partial f/\partial v\big)_T$, these equations are equivalent to

$$p(T,v_1) = p(T,v_2) = \frac{1}{v_2-v_1}\int\limits_{v_1}^{v_2} dv\, p(T,v) \quad . \tag{7.16}$$

This procedure is known as the *Maxwell construction*, and is depicted graphically in fig. 7.4. When the Maxwell construction is enforced, the isotherms resemble the curves in fig. 7.3. In this figure, all points within the purple shaded region have $\partial^2 f/\partial v^2 < 0$, hence this region is unstable to infinitesimal fluctuations. The boundary of this region is called the *spinodal*, and the spontaneous phase separation into two phases is a process known as *spinodal decomposition*. The dot-dashed orange curve, called the *coexistence curve*, marks the instability boundary for *nucleation*. In a nucleation process, an energy barrier must be overcome in order to achieve the lower free energy state. There is no energy barrier for spinodal decomposition – it is a spontaneous process.

Suppose we follow along an isotherm starting from the high molar volume (gas) phase. If $T > T_{\rm c}$, the volume v decreases continuously as the pressure p increases. If $T < T_{\rm c}$, then at the instant the isotherm first intersects the orange boundary curve in fig. 7.3, there is a discontinuous change in the molar volume from high (gas) to low (liquid). This discontinuous change is the hallmark of a *first order phase transition*. The volume discontinuity is $\Delta v \propto (T_{\rm c}-T)^{1/2}$. This is an example of a *critical behavior* in which the *order parameter* ϕ, which in this case may be taken to be the difference $\phi = v_{\rm G} - v_{\rm L}$, behaves as a power law in $\big|T-T_{\rm c}\big|$, where $T_{\rm c}$ is the *critical temperature*. In this case, we have $\phi(T) \propto (T_{\rm c}-T)_+^{\beta}$, where $\beta = \frac{1}{2}$ is the exponent, and where $(T_{\rm c}-T)_+$ is defined to be $T_{\rm c}-T$ if $T < T_{\rm c}$ and 0 otherwise. Recall the isothermal

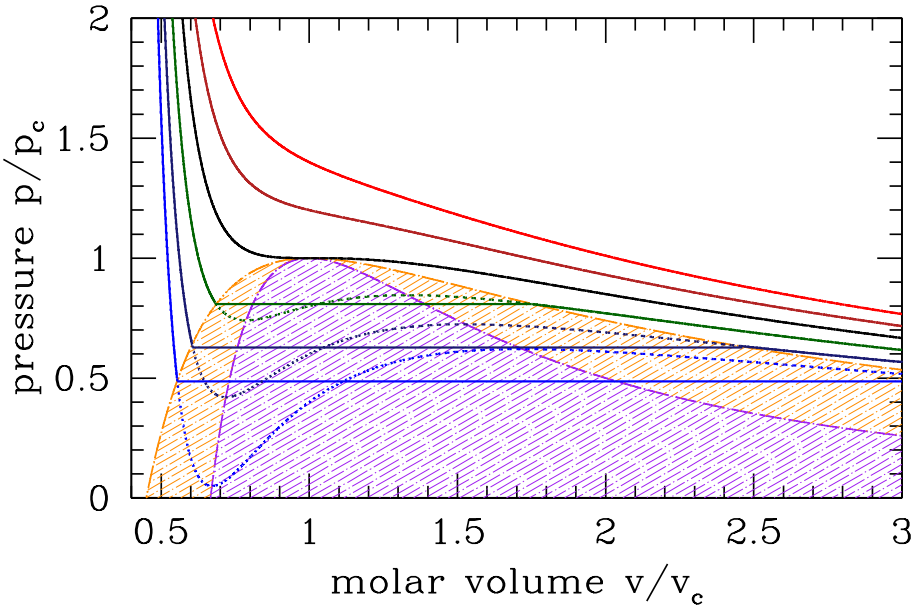

Figure 7.3: Pressure-volume isotherms for the van der Waals system, as in fig. 7.1, but corrected to account for the Maxwell construction. The boundary of the purple shaded region is the spinodal line $\bar{p}^*(\bar{v})$. The boundary of the orange shaded region is the stability boundary with respect to phase separation, and is called the *coexistence curve*.

compressibility is $\kappa_T = -v^{-1}\big(\partial v/\partial p\big)_T$. This is finite along the coexistence curve – it diverges only along the spinodal. It therefore diverges at the critical point, which lies at the intersection of the spinodal and the coexistence curve.

It is convenient to express the equation of state and the coexistence curve in terms of dimensionless variables. Writing

$$\bar{p} = \frac{p}{p_{\rm c}} \quad , \quad \bar{v} = \frac{v}{v_{\rm c}} \quad , \quad \bar{T} = \frac{T}{T_{\rm c}} \quad , \tag{7.17}$$

the dimensionless van der Waals equation of state takes the form

$$\bar{p} = \frac{8\bar{T}}{3\bar{v}-1} - \frac{3}{\bar{v}^2} \quad . \tag{7.18}$$

7.2.2 Analytic form of the coexistence curve near the critical point

Close to the critical point, the dimensionless equation of state may be written as $\pi = \pi(\epsilon, t)$, where

$$\bar{p} = 1 + \pi \quad , \quad \bar{v} = 1 + \epsilon \quad , \quad \bar{T} = 1 + t \quad , \tag{7.19}$$

where $\pi(0,0) = 0$. Equivalently,

$$\pi = \frac{p - p_{\rm c}}{p_{\rm c}} \quad , \quad \epsilon = \frac{v - v_{\rm c}}{v_{\rm c}} \quad , \quad t = \frac{T - T_{\rm c}}{T_{\rm c}} = \frac{\Theta}{T_{\rm c}} \quad . \tag{7.20}$$

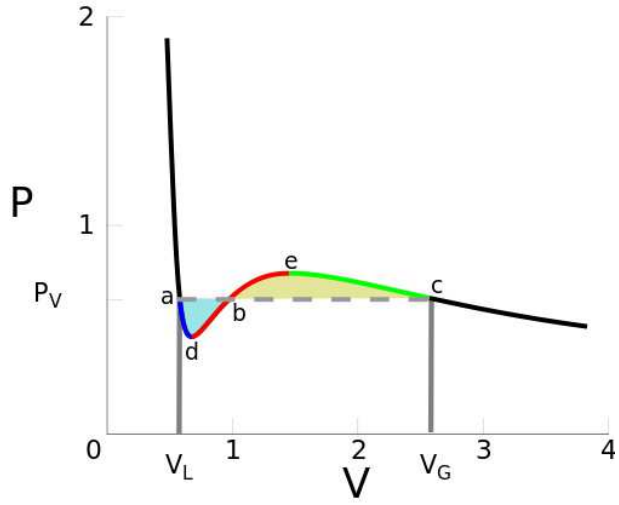

Figure 7.4: Maxwell construction in the (v, p) plane. The system is absolutely unstable between volumes $v_{\rm d}$ and $v_{\rm e}$. For $v \in [v_{\rm a}, v_{\rm d}]$ of $v \in [v_{\rm e}, v_{\rm c}]$, the solution is unstable with respect to phase separation. Source: *Wikipedia*.

Here π, ϵ, and t are, respectively, the dimensionless deviations of pressure, molar volume, and temperature from their critical point values. For the van der Waals equation of state in eqn. 7.18, we have

$$\begin{aligned}\pi(\epsilon, t) &= \frac{8(1+t)}{2+3\epsilon} - \frac{3}{(1+\epsilon)^2} - 1 \\ &= 4t - 6t\epsilon + 9\epsilon^2 t - \tfrac{3}{2}\epsilon^3 - \tfrac{27}{2}\epsilon^3 t + \tfrac{21}{4}\epsilon^4 + \tfrac{81}{4}\epsilon^4 t - \tfrac{99}{8}\epsilon^5 + \ldots \quad .\end{aligned} \tag{7.21}$$

from which we may derive

$$\epsilon_{\rm L,G}(t) = \mp 2\sqrt{-t} - \tfrac{5}{18}\, t + \ldots \quad . \tag{7.22}$$

We identify the difference $\Delta v \equiv v_{\rm L} - v_{\rm G}$ as the *order parameter* for the transition which occurs at $T = T_{\rm c}$. We see that the order parameter behaves as a power law for T just below the critical point, with $\Delta v \propto (-t)^\beta$ and $\beta = \frac{1}{2}$, which is the *order parameter critical exponent*.

The spinodal boundary for the vdW system is then given by the solution to

$$0 = \frac{\partial \pi}{\partial \epsilon} = -6t + 18\epsilon t - \tfrac{9}{2}\epsilon^2 - \tfrac{81}{2}\epsilon^2 t + 21\epsilon^3 + \ldots \quad . \tag{7.23}$$

For the spinodal, is easy to see that the lowest order nontrivial solution is $\epsilon = \mp \frac{2}{\sqrt{3}}\sqrt{-t}$. For the coexistence curve, we found $\epsilon_{\rm L,G} = \mp 2\sqrt{-t}$.

Fig. 7.5 shows the universality of the liquid-gas transition for eight different fluids: Ne, Ar, Kr, Xe, N_2, O_2, CO, and CH_4. The experimental coexistence curve expressed in dimensionless variables $\bar{n} = 1/\bar{v}$ and $\bar{T} = T/T_{\rm c}$ is fairly well-fit to the curve[5]

$$\bar{n}_{\rm L,G}(t) = 1 \pm \tfrac{7}{4}(1-\bar{T})^{1/3} + \tfrac{3}{4}(1-\bar{T}) \tag{7.24}$$

[5]See M. Schwartz, https://scholar.harvard.edu/files/schwartz/files/9-phases.pdf.

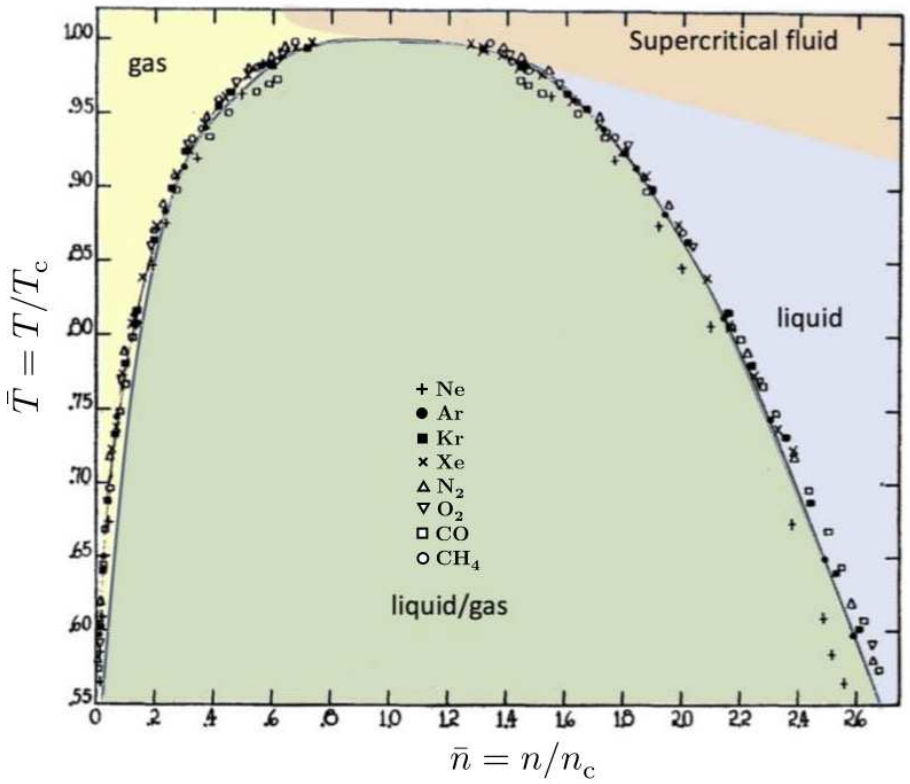

Figure 7.5: Universality of the liquid-gas transition for eight different atomic and molecular fluids, from E. A. Guggenheim, *J. Chem. Phys.* **13**, 253 (1945). Dimensionless temperature $\bar{T} = T/T_c$ *versus* dimensionless number density $\bar{n} = n/n_c = v_c/v$ is shown. The van der Waals / mean field theory gives $\Delta n = n_{\rm liquid} - q_{\rm gas} \propto (-t)^{1/2}$, while experiments show a result closer to $\Delta n \propto (-t)^{1/3}$. Here $t \equiv \bar{T} - 1 = (T - T_c)/T_c$ is the dimensionless temperature deviation with respect to the critical point. (Image adapted from Matthew Schwartz's Harvard lecture notes, adapted from Guggenheim 1945.)

which shows that the critical exponent β is much closer to $\beta = \frac{1}{3}$ than to the vdW value $\beta^{\rm vdW} = \frac{1}{2}$. The van der Waals equation is in essence a *mean field theory* of the liquid-gas transition.

7.2.3 History of the van der Waals equation

The van der Waals equation of state first appears in van der Waals' 1873 PhD thesis[6], *"Over de Continuïteit van den Gas - en Vloeistoftoestand"* ("On the continuity of the gas and liquid state"). In his Nobel lecture[7], van der Waals writes of how he was inspired by Rudolf Clausius' 1857 treatise on the nature of heat,

[6]Johannes Diderik van der Waals, the eldest of ten children, was the son of a carpenter. As a child he received only a primary school education. He worked for a living until age 25, and was able to enroll in a three-year industrial evening school for working class youth. Afterward he continued his studies independently, in his spare time, working as a teacher. By the time he obtained his PhD, he was 36 years old. He received the Nobel Prize for Physics in 1910.

[7]See http://www.nobelprize.org/nobel_prizes/physics/laureates/1910/waals-lecture.pdf

where it is posited that a gas in fact consists of microscopic particles whizzing around at high velocities. van der Waals reasoned that liquids, which result when gases are compressed, also consist of 'small moving particles': *"Thus I conceived the idea that there is no essential difference between the gaseous and the liquid state of matter..."*

Clausius' treatise showed how his kinetic theory of heat was consistent with Boyle's law for gases ($pV = \text{constant}$ at fixed temperature). van der Waals pondered why this might fail for the non-dilute liquid phase, and he reasoned that there were two principal differences: inter-particle attraction and excluded volume. These considerations prompted him to posit his famous equation,

$$p = \frac{RT}{v-b} - \frac{a}{v^2} \quad . \tag{7.25}$$

The first term on the RHS accounts for excluded volume effects, and the second for mutual attractions.

In the limiting case of $p \to \infty$, the molar volume approaches $v = b$. On physical grounds, one might expect $b = v_0/\zeta$, where $v_0 = N_{\rm A}\,\omega_0$ is $N_{\rm A}$ times the volume ω_0 of a single molecule, and the *packing fraction* is $\zeta = N\omega_0/V = v_0/v$, which is the ratio of the total molecular volume to the total system volume. In three dimensions, the maximum possible packing fraction is for fcc and hcp lattices, each of which have coordination number 12, with $\zeta_{\rm max} = \frac{\pi}{3\sqrt{2}} = 0.74078$. Dense random packing results in $\zeta_{\rm drp} = 0.634$. Expanding the vdW equation of state in inverse powers of v yields

$$p = \frac{RT}{v} + \left(b - \frac{a}{RT}\right) \cdot \frac{RT}{v^2} + \mathcal{O}\big(v^{-3}\big) \quad , \tag{7.26}$$

and we read of the second virial coefficient $B_2 = \big(b - \frac{a}{RT}\big)/N_{\rm A}$. For hard spheres, $a = 0$, and the result $B_2 = 4\omega_0$ from the Mayer cluster expansion corresponds to $b_{\rm Mayer} = 4v_0$, which is larger than the result from even the loosest regular sphere packing, *i.e.* that for a cubic lattice, with $\zeta_{\sf cub} = \frac{\pi}{6}$.

The law of corresponding states

Another of van der Waals' great achievements was his articulation of the *law of corresponding states*. Recall that the van der Waals equation of state, when written in terms of dimensionless quantities $\bar{p} = p/p_{\rm c}$, $\bar{v} = v/v_{\rm c}$, and $\bar{T} = T/T_{\rm c}$, takes the form of eqn. 7.18. Thus, while the a and b parameters are specific to each fluid – see Tab. 7.1 – when written in terms of these scaled dimensionless variables, the equation of state and all its consequent properties (*i.e.* the liquid-gas phase transition) are *universal*.

The van der Waals equation is best viewed as semi-phenomenological. Interaction and excluded volume effects surely are present, but the van der Waals equation itself only captures them in a very approximate way. It is applicable to gases, where it successfully predicts features that are not present in ideal systems (*e.g.* throttling). It is of only qualitative and pedagogical use in the study of fluids, the essential physics of which lies in the behavior of quantities like the pair distribution function $g(r)$. As we saw in chapter 6, any adequate first principles derivation of $g(r)$ - a function which can be measured in scattering experiments - involves rather complicated approximation schemes to close the BBGKY hierarchy. Else one must resort to numerical simulations such as the Monte Carlo method. Nevertheless, the lessons learned from the van der Waals system are invaluable and they provide us with a first glimpse of what is going on in the vicinity of a phase transition, and how nonanalytic behavior, such as $v_{\sf G} - v_{\sf L} \propto (T_{\rm c} - T)^\beta$ with noninteger exponent β may result due to singularities in the free energy at the critical point.

7.3 Fluids, Magnets, and the Ising Model

7.3.1 Lattice gas description of a fluid

The usual description of a fluid follows from a continuum Hamiltonian of the form

$$\hat{H}(\boldsymbol{p},\boldsymbol{x}) = \sum_{i=1}^{N} \frac{\boldsymbol{p}_i^2}{2m} + \sum_{i<j} u(\boldsymbol{x}_i - \boldsymbol{x}_j) \quad . \tag{7.27}$$

The potential $u(\boldsymbol{r})$ is typically central, depending only on the magnitude $|\boldsymbol{r}|$, and short-ranged. Now consider a discretized version of the fluid, in which we divide up space into cells (cubes, say), each of which can accommodate at most one fluid particle (due to excluded volume effects). That is, each cube has a volume on the order of a^3, where a is the diameter of the fluid particles. In a given cube i we set the occupancy $n_i = 1$ if a fluid particle is present and $n_i = 0$ if there is no fluid particle present. We then have that the potential energy is

$$U = \sum_{i<j} u(\boldsymbol{x}_i - \boldsymbol{x}_j) = \tfrac{1}{2} \sum_{\boldsymbol{R}\neq\boldsymbol{R}'} V_{\boldsymbol{R},\boldsymbol{R}'}\, n_{\boldsymbol{R}}\, n_{\boldsymbol{R}'} \quad , \tag{7.28}$$

where $V_{\boldsymbol{R},\boldsymbol{R}'} \approx u(\boldsymbol{R} - \boldsymbol{R}')$, where R_k is the position at the center of cube k. The grand partition function is then approximated as

$$\Xi(T,V,\mu) \approx \sum_{\{n_{\boldsymbol{R}}\}} \left(\prod_{\boldsymbol{R}} \xi^{n_{\boldsymbol{R}}} \right) \exp\left(-\tfrac{1}{2}\beta \sum_{\boldsymbol{R}\neq\boldsymbol{R}'} V_{\boldsymbol{R},\boldsymbol{R}'}\, n_{\boldsymbol{R}}\, n_{\boldsymbol{R}'} \right) \quad , \tag{7.29}$$

where $\xi = e^{\beta\mu}\, \lambda_T^{-d}\, a^d$, and where a is the side length of each cube (chosen to be on the order of the hard sphere diameter). The λ_T^{-d} factor arises from the integration over the momenta. Note $N = \sum_{\boldsymbol{R}} n_{\boldsymbol{R}}$ is the total number of fluid particles, so $\prod_{\boldsymbol{R}} \xi^{\,n_{\boldsymbol{R}}} = \xi^N$ where $\xi = e^{\beta\mu}(a/\lambda_T)^d$.

Thus, we arrive at $\Xi = \mathsf{Tr}\, \exp(-\beta \hat{H}_{\mathsf{LG}})$ where $\hat{H}_{\mathsf{LG}}$ is the *lattice gas Hamiltonian*,

$$\begin{aligned} \hat{H}_{\mathsf{LG}} &= \tfrac{1}{2} \sum_{\boldsymbol{R}\neq\boldsymbol{R}'} V_{\boldsymbol{R},\boldsymbol{R}'}\, n_{\boldsymbol{R}}\, n_{\boldsymbol{R}'} - k_{\mathrm{B}} T \log \xi \sum_{\boldsymbol{R}} n_{\boldsymbol{R}} \\ &= -\tfrac{1}{2} \sum_{\boldsymbol{R}\neq\boldsymbol{R}'} J_{\boldsymbol{R},\boldsymbol{R}'}\, \sigma_{\boldsymbol{R}}\, \sigma_{\boldsymbol{R}'} - H \sum_{\boldsymbol{R}} \sigma_{\boldsymbol{R}} + E_0 \quad , \end{aligned} \tag{7.30}$$

where $\sigma_{\boldsymbol{R}} \equiv 2n_{\boldsymbol{R}} - 1$ is a spin variable taking the possible values $\{-1, +1\}$, and

$$J_{\boldsymbol{R},\boldsymbol{R}'} = -\tfrac{1}{4} u(\boldsymbol{R} - \boldsymbol{R}') \qquad , \qquad H = \mu + d k_{\mathrm{B}} T \log(a/\lambda_T) - \tfrac{1}{4} {\sum_{\boldsymbol{R}}}' u(\boldsymbol{R}) \tag{7.31}$$

and $E_0 = \frac{1}{8} N_{\mathrm{c}} \, {\sum_{\boldsymbol{R}}}' u(\boldsymbol{R})$, where $N_{\mathrm{c}} = V/a^d$ is the number of unit cells, and where the prime on the sum indicates that $\boldsymbol{R} = 0$ is to be excluded. For the Lennard-Jones system, $u(\boldsymbol{R} - \boldsymbol{R}') < 0$ is due to the attractive tail of the potential, hence $J_{\boldsymbol{R},\boldsymbol{R}'} > 0$, which prefers alignment of the spins $\sigma_{\boldsymbol{R}}$ and $\sigma_{\boldsymbol{R}'}$. This interaction is therefore *ferromagnetic*. The spin Hamiltonian in eqn. 7.30 is recognized as the Ising model.

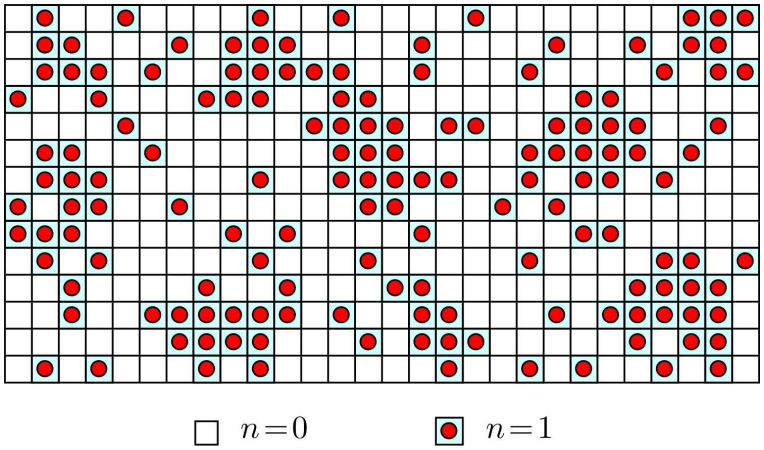

Figure 7.6: The lattice gas model. An occupied cell corresponds to $n = 1$ ($\sigma = +1$), and a vacant cell to $n = 0$ ($\sigma = -1$).

7.3.2 Phase diagrams and critical exponents

The physics of the liquid-gas transition in fact has a great deal in common with that of the transition between a magnetized and unmagnetized state of a magnetic system. The correspondences are[8] $p \leftrightarrow H$ and $v \leftrightarrow m$, where m is the magnetization density, defined here to be the total magnetization M divided by the number of lattice sites[9] $N_{\rm c}$, *viz.*

$$m = \frac{M}{N_{\rm c}} = \frac{1}{N_{\rm c}} \sum_{\boldsymbol{R}} \langle \sigma_{\boldsymbol{R}} \rangle \quad . \tag{7.32}$$

Sketches of the phase diagrams are reproduced in fig. 7.7. Of particular interest is the *critical point*, which occurs at $(T_{\rm c}, p_{\rm c})$ in the fluid system and $(T_{\rm c}, H_{\rm c})$ in the magnetic system, with $H_{\rm c} = 0$ by symmetry.

In the fluid, the coexistence curve in the (p, T) plane separates high density (liquid) and low density (vapor) phases. The specific volume v (or the density $n = v^{-1}$) jumps discontinuously across the coexistence curve. In the magnet, the coexistence curve in the (H, T) plane separates positive magnetization and negative magnetization phases. The magnetization density m jumps discontinuously across the coexistence curve. For $T > T_{\rm c}$, the latter system is a *paramagnet*, in which the magnetization varies smoothly as a function of H. This behavior is most apparent in the bottom panel of the figure, where $v(p)$ and $m(H)$ curves are shown.

For $T < T_{\rm c}$, the fluid exists in a *two phase region*, which is spatially inhomogeneous, supporting local regions of high and low density. There is no stable homogeneous thermodynamic phase for (T, v) within the two phase region shown in the middle left panel. Similarly, for the magnet, there is no stable homogeneous thermodynamic phase at fixed temperature T and magnetization m if (T, m) lies within the

[8] H is more properly analogous to μ. However, since $\mu = \mu(p, T)$, H can also be regarded as analogous to p. Note also that $\beta p = z\lambda_T^{-d}$ for the ideal gas, in which case $\xi = z\,(a/\lambda_T)^d$ is proportional to $p/k_{\rm B}T$.

[9] Note the distinction between the number of lattice sites $N_{\rm c}$ and the number of occupied cells N. According to our definitions, $N = \frac{1}{2}(M + N_{\rm c})$.

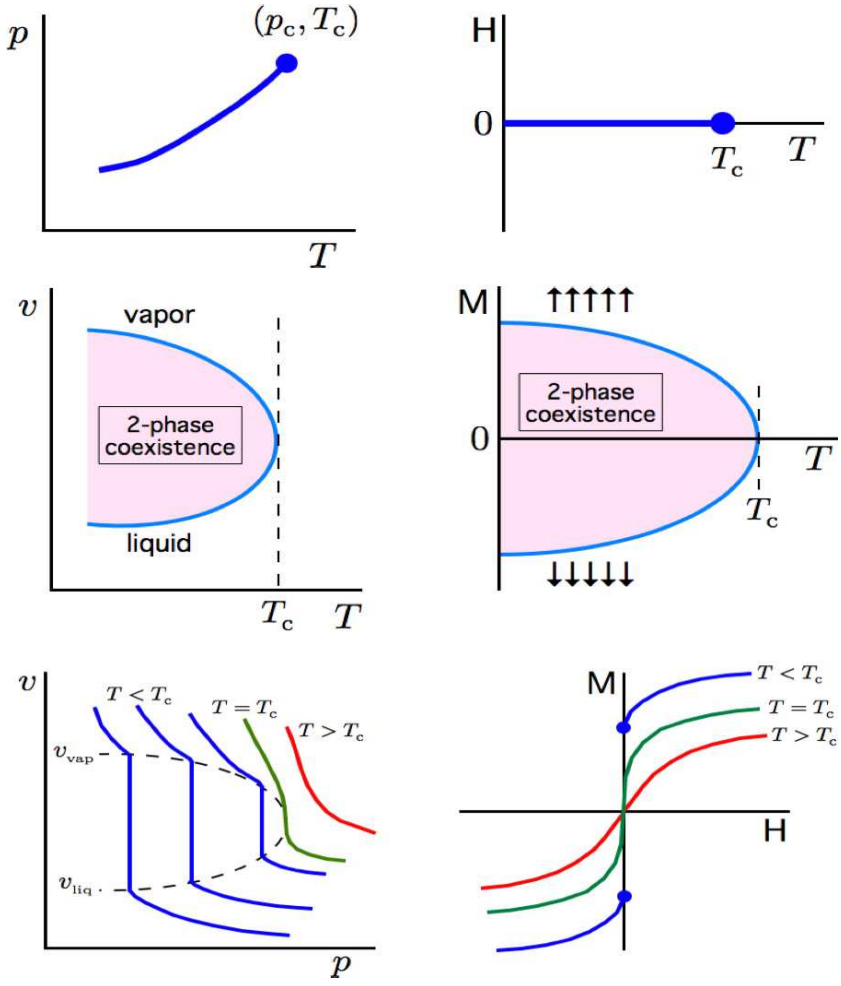

Figure 7.7: Comparison of the liquid-gas phase diagram with that of the Ising ferromagnet.

coexistence region. Rather, the system consists of blobs where the spin is predominantly up, and blobs where the spin is predominantly down.

Note also the analogy between the isothermal compressibility κ_T and the isothermal susceptibility χ_T:

$$\kappa_T = -\frac{1}{v}\left(\frac{\partial v}{\partial p}\right)_T \quad , \quad \chi_T = \left(\frac{\partial m}{\partial H}\right)_T \quad , \tag{7.33}$$

with $\kappa_T(T_c, p_c) = \infty$ and $\chi_T(T_c, H_c) = \infty$.

The *order parameter* for a second order phase transition is a quantity which vanishes in the disordered phase and is finite in the ordered phase. For the fluid, the order parameter can be chosen to be $\Psi \propto (v_{vap} - v_{liq})$, the difference in the specific volumes of the vapor and liquid phases. In the vicinity of the critical point, the system exhibits power law behavior in many physical quantities, *viz.*

$$m(T, H_c) \sim \left(T_c - T\right)_+^{\beta} \quad , \quad \chi(T, H_c) \sim |T - T_c|^{-\gamma} \quad , \quad C_M(T, H_c) \sim |T - T_c|^{-\alpha} \quad , \quad m(T_c, H) \sim \pm |H|^{1/\delta} \quad . \tag{7.34}$$

The quantities α, β, γ, and δ are the *critical exponents* associated with the transition. These exponents satisfy certain equalities, such as the Rushbrooke and Griffiths relations:

$$\alpha + 2\beta + \gamma = 2 \quad \text{(Rushbrooke)} \qquad , \qquad \beta + \gamma = \beta\delta \quad \text{(Griffiths)} \quad . \tag{7.35}$$

Originally such relations were derived as inequalities, and only after the advent of scaling and renormalization group theories it was realized that they held as equalities.

In addition to the exponents α, β, γ, and δ, one defines the *correlation length exponent* ν from the behavior of the two-point correlation function $C(\boldsymbol{r}, T) = \langle \psi(0)\, \psi(\boldsymbol{r}) \rangle$, where $\psi(\boldsymbol{r})$ is a local operator, such as the local density in a fluid or the local spin polarization in a magnet[10]. In the limits $T \to T_{\rm c}$ and $H \to H_{\rm c} = 0$, one has

$$C(\boldsymbol{r}, T, H) = r^{-(d-2+\eta)}\, \phi\big(r/\xi(T), H/\xi_H(T)\big) \quad , \tag{7.36}$$

where η is the *anomalous exponent*, $\phi(r/\xi, H/\xi_H)$ is a *scaling function*, $\xi(T) \propto |T - T_{\rm c}|^{-\nu}$ is the *correlation length*, and $\xi_H(T) \propto |T - T_{\rm c}|^{\Delta}$, with $\Delta = \beta\delta$, is a field scale. As we have seen, for the lattice gas system the effective magnetic field H is a proxy for the pressure or the chemical potential. Along with the new exponents η and ν come additional exponent relations,

$$(2 - \eta)\nu = \gamma \qquad , \qquad d\,\nu = 2 - \alpha \quad \text{(hyperscaling)} \quad . \tag{7.37}$$

Thus there are three relations among the six critical exponents α, β, γ, δ, η, and ν, which entails that there are three independent values among the six.

7.3.3 Gibbs-Duhem relation for magnetic systems

Homogeneity of $E(S, M, N)$ means $E = TS + HM + \mu N$, by Euler's theorem. After invoking the First Law $dE = T\,dS + H\,dM + \mu\,dN$, we have

$$S\,dT + M\,dH + N\,d\mu = 0 \quad . \tag{7.38}$$

Now consider two magnetic phases in coexistence. We must have $d\mu_1 = d\mu_2$, hence

$$d\mu_1 = -s_1\,dT - m_1\,dH = -s_2\,dT - m_2\,dH = d\mu_2 \quad , \tag{7.39}$$

where $m = M/N$ is the magnetization per site and $s = S/N$ is the specific entropy. Thus, we obtain the Clapeyron equation for magnetic systems,

$$\left(\frac{dH}{dT}\right)_{\rm coex} = -\frac{s_1 - s_2}{m_1 - m_2} \quad . \tag{7.40}$$

Thus, if $m_1 \neq m_2$ and $\big(dH/dT\big)_{\rm coex} = 0$, then we must have $s_1 = s_2$, which says that there is *no latent heat associated with the transition*. This absence of latent heat is a consequence of the *symmetry* which guarantees that $G(T, H, N) = G(T, -H, N)$.

[10]The local 'order parameter field' $\psi(\boldsymbol{r})$ may carry vector or tensor indices. In general, it transforms as the fundamental representation of the global symmetry group G.

Recall our discussion in §2.11.2 of the Clausius-Clapeyron relation for liquid-gas systems. From $G = E - TS + pV = G(T, p, N)$, the differential of the Gibbs free energy per particle, $\mu = G/N$, is given by $d\mu = -s\,dT + v\,dp$, where $v = V/N$ is the volume per particle[11]. This leads to the Clapeyron relation,

$$\left(\frac{dp}{dT}\right)_{\rm coex} = \frac{s_2 - s_1}{v_2 - v_1} = \frac{\ell}{T\,\Delta v} \quad , \tag{7.41}$$

which determines the slope of the coexistence curve in the (T, p) plane.

7.3.4 Order-disorder transitions

Another application of the Ising model lies in the theory of order-disorder transitions in alloys. Examples include Cu_3Au, CuZn, and other compounds. In CuZn, the Cu and Zn atoms occupy sites of a body centered cubic (BCC) lattice, forming an alloy known as β-brass. Below $T_{\rm c} \simeq 740\,{\rm K}$, the atoms are ordered, with the Cu preferentially occupying one simple cubic sublattice and the Zn preferentially occupying the other.

The energy is a sum of pairwise interactions, with a given link contributing $\varepsilon_{\rm AA}$, $\varepsilon_{\rm BB}$, or $\varepsilon_{\rm AB}$, depending on whether it is an A-A, B-B, or A-B/B-A link. Here A and B represent Cu and Zn, respectively. Thus, we can write the energy of the link $\langle ij \rangle$ as

$$E_{ij} = \varepsilon_{\rm AA}\,P_i^{\rm A}\,P_j^{\rm A} + \varepsilon_{\rm BB}\,P_i^{\rm B}\,P_j^{\rm B} + \varepsilon_{\rm AB}\left(P_i^{\rm A}\,P_j^{\rm B} + P_i^{\rm B}\,P_j^{\rm A}\right) \quad , \tag{7.42}$$

where

$$P_i^{\rm A} = \tfrac{1}{2}(1+\sigma_i) = \begin{cases} 1 & \text{if site } i \text{ contains Cu} \\ 0 & \text{if site } i \text{ contains Zn} \end{cases} \quad , \quad P_i^{\rm B} = \tfrac{1}{2}(1-\sigma_i) = \begin{cases} 1 & \text{if site } i \text{ contains Zn} \\ 0 & \text{if site } i \text{ contains Cu} \end{cases} .$$

The Hamiltonian is then

$$\begin{aligned} \hat{H} = \sum_{\langle ij \rangle} E_{ij} &= \sum_{\langle ij \rangle} \left\{ \tfrac{1}{4}\big(\varepsilon_{\rm AA} + \varepsilon_{\rm BB} - 2\varepsilon_{\rm AB}\big)\,\sigma_i\,\sigma_j + \tfrac{1}{4}\big(\varepsilon_{\rm AA} - \varepsilon_{\rm BB}\big)\,(\sigma_i + \sigma_j) + \tfrac{1}{4}\big(\varepsilon_{\rm AA} + \varepsilon_{\rm BB} + 2\varepsilon_{\rm AB}\big) \right\} \\ &= -J \sum_{\langle ij \rangle} \sigma_i\,\sigma_j - H \sum_i \sigma_i + E_0 \quad , \end{aligned} \tag{7.43}$$

where the exchange constant J and the magnetic field H are given by

$$J = \tfrac{1}{4}\big(2\varepsilon_{\rm AB} - \varepsilon_{\rm AA} - \varepsilon_{\rm BB}\big) \qquad , \qquad H = \tfrac{1}{4}\big(\varepsilon_{\rm BB} - \varepsilon_{\rm AA}\big) \quad , \tag{7.44}$$

and $E_0 = \frac{1}{8}Nz\big(\varepsilon_{\rm AA} + \varepsilon_{\rm BB} + 2\varepsilon_{\rm AB}\big)$, where N is the total number of lattice sites and $z = 8$ is the *lattice coordination number*, which is the number of nearest neighbors of any given site.

Note that

$$\begin{aligned} 2\varepsilon_{\rm AB} > \varepsilon_{\rm AA} + \varepsilon_{\rm BB} \quad &\Longrightarrow \quad J > 0 \quad \text{(ferromagnetic)} \\ 2\varepsilon_{\rm AB} < \varepsilon_{\rm AA} + \varepsilon_{\rm BB} \quad &\Longrightarrow \quad J < 0 \quad \text{(antiferromagnetic)} \quad . \end{aligned} \tag{7.45}$$

The antiferromagnetic case is depicted in fig. 7.8.

[11] In §2.11.2 we considered, equivalently, the differential of the molar free energy $g = N_{\rm A}\mu$, with v the molar volume.

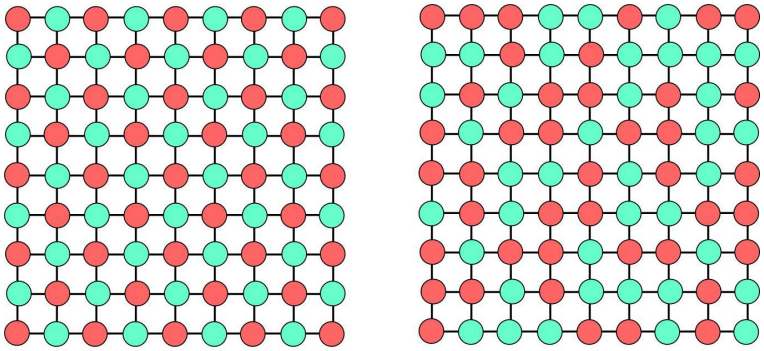

Figure 7.8: Order-disorder transition on the square lattice. Below $T = T_c$, order develops spontaneously on the two $\sqrt{2} \times \sqrt{2}$ sublattices. There is perfect sublattice order at $T = 0$ (left panel).

7.4 Mean Field Theory

7.4.1 The mean field *Ansatz*

Consider the Ising model Hamiltonian,

$$\hat{H} = -J \sum_{\langle ij \rangle} \sigma_i \, \sigma_j - H \sum_{i=1}^{N} \sigma_i \quad , \tag{7.46}$$

where the first sum on the RHS is over all links of the lattice. Each spin can be either 'up' ($\sigma = +1$) or 'down' ($\sigma = -1$). We further assume that the spins are located on a Bravais lattice[12] and that the coupling between sites i and j is $J_{ij} = J\big(|\boldsymbol{R}_i - \boldsymbol{R}_j|\big)$, where $\boldsymbol{R}_i$ is the position of the $i^{\rm th}$ spin. Here we assume $J_{ij} = 0$ beyond nearest neighbors; later we will assume a more general set of couplings. We also set the self-interaction terms to zero: $J_{ii} = 0$ for all i.

On each site i we decompose σ_i into a contribution from its thermodynamic average and a fluctuation:

$$\sigma_i = \langle \sigma_i \rangle + \delta\sigma_i \quad . \tag{7.47}$$

We will write $\langle \sigma_i \rangle \equiv m$, the local magnetization (dimensionless), and assume that m is independent of position i. Then

$$\begin{aligned} \sigma_i \, \sigma_j &= (m + \delta\sigma_i)\,(m + \delta\sigma_j) \\ &= m^2 + m\,(\delta\sigma_i + \delta\sigma_j) + \delta\sigma_i \, \delta\sigma_j \\ &= -m^2 + m\,(\sigma_i + \sigma_j) + \delta\sigma_i \, \delta\sigma_j \quad . \end{aligned} \tag{7.48}$$

[12] A Bravais lattice is one in which any site is equivalent to any other site through an appropriate discrete translation. Examples of Bravais lattices include the linear chain, square, triangular, simple cubic, face-centered cubic, *etc.* lattices. The honeycomb lattice is not a Bravais lattice, because there are two sets of inequivalent sites – those in the center of a Y and those in the center of an upside down Y.

The last term on the RHS of the second equation above is quadratic in the fluctuations, and we assume this to be negligibly small. This neglect of the fluctuations is the *mean field Ansatz*, and results in the *mean field Hamiltonian*

$$\hat{H}_{\rm MF} = \tfrac{1}{2} N z J\, m^2 - \big(H + zJm\big) \sum_{i=1}^{N} \sigma_i \quad , \tag{7.49}$$

where N is the total number of lattice sites. Note that the number of nearest-neighbor links is given by $N_{\rm links} = \frac{1}{2} zN$, where z is the lattice coordination number, *i.e.* the number of nearest neighbors for any given site, and N is the number of lattice sites[13]. The first term is a constant, although the value of m is yet to be determined. The Boltzmann weights are then completely determined by the second term, which is just what we would write down for a Hamiltonian of *noninteracting* spins in an effective 'mean field'

$$H_{\rm eff} = H + zJm \quad . \tag{7.50}$$

In other words, $H_{\rm eff} = H_{\rm ext} + H_{\rm int}$, where the external field is applied field $H_{\rm ext} = H$, and the 'internal field' is $H_{\rm int} = zJm$. The internal field accounts for the interaction with the *average* values of all other spins coupled to a spin at a given site, hence it is often called the 'mean field'. Since the spins are noninteracting, we have

$$m = \frac{e^{\beta H_{\rm eff}} - e^{-\beta H_{\rm eff}}}{e^{\beta H_{\rm eff}} + e^{-\beta H_{\rm eff}}} = \tanh\!\left(\frac{H + zJm}{k_{\rm B} T}\right) \quad . \tag{7.51}$$

It is a simple matter to solve for the free energy, given the noninteracting Hamiltonian $\hat{H}_{\rm MF}$. The partition function is

$$Z = \mathsf{Tr}\; e^{-\beta \hat{H}_{\rm MF}} = e^{-\frac{1}{2}\beta N z J\, m^2} \left(\sum_{\sigma} e^{\beta (H + zJm)\sigma} \right)^N = e^{-\beta F} \quad . \tag{7.52}$$

We now define dimensionless variables:

$$f \equiv \frac{F}{NzJ} \qquad , \qquad \theta \equiv \frac{k_{\rm B} T}{zJ} \qquad , \qquad h \equiv \frac{H}{zJ} \quad , \tag{7.53}$$

and obtain the dimensionless free energy

$$f(m, \theta, h) = \tfrac{1}{2} m^2 - \theta\, \log\cosh\!\left(\frac{m+h}{\theta}\right) - \theta \log 2 \quad . \tag{7.54}$$

Differentiating with respect to m gives the mean field equation,

$$m = \tanh\!\left(\frac{m+h}{\theta}\right) \quad , \tag{7.55}$$

which is equivalent to the self-consistency requirement, $m = \langle \sigma_i \rangle$. In terms of the dimensionless variables θ and h, the physics is universal, and independent of details such as the magnitude of J, the value of z, and Boltzmann's constant.

[13] Here we consider a finite lattice in a periodic geometry. Note that if we count each link twice, then each site is counted z times because there are z links which connect to any given site. Thus $2N_{\rm links} = zN$, which is to say $N_{\rm links} = \frac{1}{2} zN$.

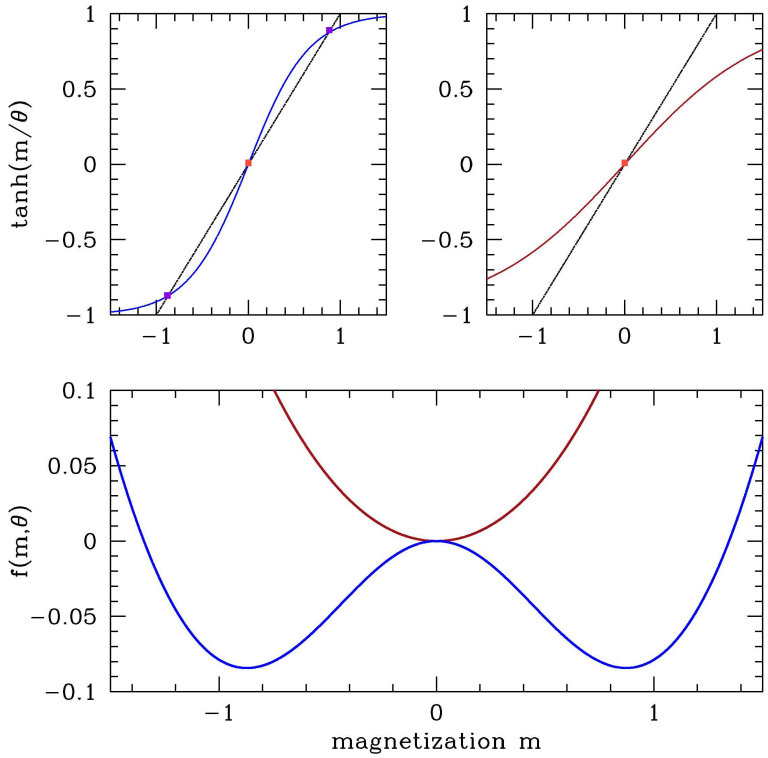

Figure 7.9: Results for $h = 0$. Upper panels: graphical solution to self-consistency equation $m = \tanh(m/\theta)$ at temperatures $\theta = 0.65$ (blue) and $\theta = 1.5$ (dark red). Lower panel: mean field free energy, with energy shifted by $\theta \log 2$ so that $f(m = 0, \theta) = 0$.

7.4.2 Zero external field

When $h = 0$ the mean field equation becomes $m = \tanh(m/\theta)$. This nonlinear equation can be solved graphically, as in the top panel of fig. 7.9. The RHS in a tanh function which gets steeper with decreasing dimensionless temperature θ. If, at $m = 0$, the slope of $\tanh(m/\theta)$ is smaller than unity, then the curve $y = \tanh(m/h)$ will intersect $y = m$ only at $m = 0$. However, if the slope is larger than unity, there will be three such intersections. Since the slope is $1/\theta$, we identify $\theta_{\rm c} = 1$ as the *mean field transition temperature*.

The mean field free energies are plotted in the bottom panel of fig. 7.9. It is possible to make analytical progress by assuming m is small and Taylor expanding the free energy $f(m, \theta)$ in powers of m when we are very close to the critical point, *i.e.* when $|\theta - \theta_{\rm c}| \ll 1$. Then we have[14]

$$f(m,\theta) = -\theta \log 2 + \tfrac{1}{2} m^2 - \theta \, \log\cosh\Big(\frac{m}{\theta}\Big) = f_0 + \tfrac{1}{2}(\theta - \theta_{\rm c})\, m^2 + \frac{m^4}{12} + \dots \quad , \tag{7.56}$$

with $f_0 = -\theta \log 2$. Note that the sign of the quadratic term is positive for $\theta > \theta_{\rm c}$ and negative for $\theta < \theta_{\rm c}$.

[14] We invoke the Taylor series expansion $\log\cosh x = \frac{1}{2}x^2 - \frac{1}{12}x^4 + \frac{1}{45}x^6 - \frac{17}{2520}x^8 + \dots$. With $\varepsilon \equiv \theta - \theta_{\rm c}$, we drop terms which are $\mathcal{O}(\varepsilon^2 m^2, \varepsilon m^4, m^6)$. As we shall see, for $\varepsilon < 0$ we have $m^2 \propto -\varepsilon$, in which case the singular part of the free energy (*i.e.* neglecting f_0) is proportional to ε^2, while the terms we are dropping are $\mathcal{O}(\varepsilon^3)$ and smaller.

Thus, the shape of the free energy $f(m,\theta)$ as a function of m qualitatively changes at $\theta = \theta_{\rm c} = 1$, the mean field transition temperature, also known as the (dimensionless) *critical temperature*. Within our mean field theory, the predicted critical temperature is $T_{\rm c} = zJ\theta_{\rm c} = zJ$.

In the high temperature phase, $\theta > \theta_{\rm c}$, and there is a unique minimum to $f(\theta, m)$ lying at $m = 0$. This is the disordered phase, where the *order parameter* m vanishes. By contrast, in the low temperature phase $\theta < \theta_{\rm c}$, there are three solutions to the mean field equations. One solution is always at $m = 0$. The other two solutions must be related by the $\mathbb{Z}_2$ symmetry of the free energy ($m \to -m$ with $h = 0$). For $\theta > \theta_{\rm c}$, the free energy $f(m,\theta)$ has a single minimum at $m = 0$. Below $\theta_{\rm c}$, the curvature at $m = 0$ reverses, and $m = 0$ becomes a local maximum. There are then two equivalent minima symmetrically displaced on either side of $m = 0$. Differentiating with respect to m, we find these additional local minima to lie at $m^2 = 3(\theta_{\rm c} - \theta) + \mathcal{O}\big((\Delta\theta)^2\big)$. Thus, we find for $|\theta - \theta_{\rm c}| \ll 1$,

$$m(\theta, h = 0) = \pm\sqrt{3}\,\big(\theta_{\rm c} - \theta\big)_+^{1/2} \quad , \tag{7.57}$$

where the $+$ subscript indicates that this solution is only for $\theta_{\rm c} - \theta > 0$. As the blue curve in fig. 7.9 shows, these nonzero solutions for m in the low temperature phase lie at a lower value of the free energy f than $m = 0$.

Again, for $\theta > \theta_{\rm c}$ the only solution is $m = 0$. The high temperature phase is thus one where the $\mathbb{Z}_2$ (*i.e.* $m \to -m$) symmetry is *unbroken*. In the low temperature phase, the magnetization m is nonzero, and takes on one of two possible values which are degenerate in free energy. The degeneracy is guaranteed by the $\mathbb{Z}_2$ symmetry present when $h = 0$. But the system must somehow choose! This is the phenomenon of *spontaneous symmetry breaking* (SSB). The exponent with which $m(\theta)$ vanishes as $\theta \to \theta_{\rm c}^-$ is denoted as β. That is, $m(\theta, h = 0) \propto (\theta_{\rm c} - \theta)_+^{\beta}$ with $\beta = \frac{1}{2}$ for our mean field theory.

Specific heat

We can now expand the free energy $f(\theta, h = 0)$. We find

$$f(\theta, h = 0) = \begin{cases} -\theta\log 2 & \text{if } \theta > \theta_{\rm c} \\ -\theta\log 2 - \frac{3}{4}(\theta_{\rm c} - \theta)^2 + \mathcal{O}\big((\theta_{\rm c} - \theta)^4\big) & \text{if } \theta < \theta_{\rm c} \end{cases} \quad . \tag{7.58}$$

Thus, if we compute the heat capacity, we find in the vicinity of $\theta = \theta_{\rm c}$

$$c_V = -\theta\,\frac{\partial^2 f}{\partial\theta^2} = \begin{cases} 0 & \text{if } \theta > \theta_{\rm c} \\ \frac{3}{2} & \text{if } \theta < \theta_{\rm c} \end{cases} \quad . \tag{7.59}$$

Thus, the specific heat is *discontinuous* at $\theta = \theta_{\rm c}$. We emphasize that our results here are only valid for $|\theta - \theta_{\rm c}| \ll 1$. The general result valid for all θ (within our mean field theory) is[15]

$$c_V(\theta) = \frac{1}{\theta}\cdot\frac{m^2(\theta) - m^4(\theta)}{\theta - 1 + m^2(\theta)} \quad , \tag{7.60}$$

[15]To obtain this result, one writes $f = f\big(\theta, m(\theta)\big)$ and then differentiates twice with respect to θ, using the chain rule. Along the way, any naked (*i.e.* undifferentiated) term proportional to $\partial f/\partial m$ may be dropped, since this vanishes at any θ by the mean field equation.

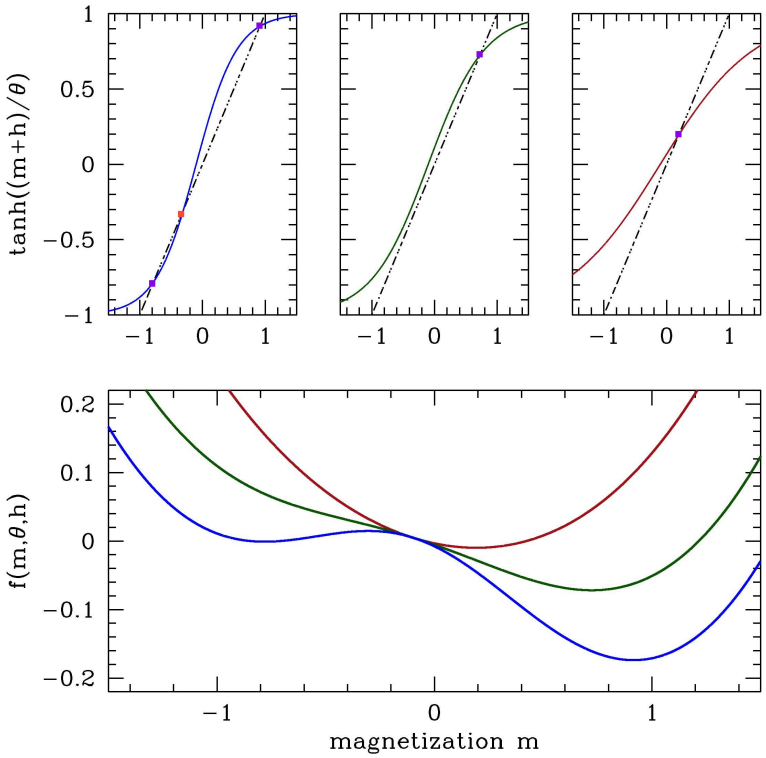

Figure 7.10: $f(m.\theta, h)$ for $h = 0.1$. Upper panels: graphical solution to the self-consistency equation $m = \tanh\big((m+h)/\theta\big)$ at temperatures $\theta = 0.65$ (blue), $\theta = 0.9$ (dark green), and $\theta = 1.5$ (dark red). Lower panel: mean field free energy, with energy shifted by $\theta \log 2$ so that $f(m = 0, \theta) = 0$.

With this expression one can check both limits $\theta \to 0$ and $\theta \to \theta_{\rm c}$. As $\theta \to 0$ the magnetization saturates and one has $m^2(\theta) \simeq 1 - 4\,e^{-2/\theta}$. The numerator then vanishes as $e^{-2/\theta}$, which overwhelms the denominator that itself vanishes as θ^2. As a result, $c_V(\theta \to 0) = 0$, as expected. As $\theta \to \theta_{\rm c}^-$, we have $m^2 = 3(\theta_{\rm c} - \theta) + \ldots$ and we recover $c_V(\theta_{\rm c}^-) = \frac{3}{2}$. In the theory of critical phenomena, $c_V(\theta) \propto |\theta - \theta_{\rm c}|^{-\alpha}$ as $\theta \to \theta_{\rm c}$. We see that mean field theory yields $\alpha = 0$.

7.4.3 Finite external field

Let us first assume $|h| \ll |\theta - 1| \ll 1$, *i.e.* that we are very close to the critical point $(\theta_{\rm c}, h_{\rm c}) = (1, 0)$. The mean field solution for $m(\theta, h)$ then be small, and we may expand the free energy from eqn. 7.54 in m and h, *viz.*

$$\begin{aligned} f(m, \theta, h) &= -\theta\,\log 2 + \tfrac{1}{2}(1 - \theta^{-1})\,m^2 + \frac{m^4}{12\,\theta^3} - \frac{hm}{\theta} \\ &= f_0 + \tfrac{1}{2}\,(\theta - \theta_{\rm c})\,m^2 + \tfrac{1}{12}m^4 - hm + \ldots \quad . \end{aligned} \tag{7.61}$$

Note that we have only gone to linear order in h. Setting $\partial f/\partial m = 0$, we obtain

$$\tfrac{1}{3}m^3 + (\theta - \theta_{\rm c}) \cdot m - h = 0 \quad . \tag{7.62}$$

If $\theta > \theta_{\rm c}$ then we have a solution $m = h/(\theta - \theta_{\rm c})$. The m^3 term can be ignored because it is higher order in h, and we have assumed $|h| \ll |\theta - \theta_{\rm c}| \ll 1$. This is known as the *Curie-Weiss law*[16]. The zero field magnetic susceptibility is then given by

$$\chi(\theta > \theta_{\rm c}) = \left.\frac{\partial m}{\partial h}\right|_{h=0} = \frac{1}{\theta - \theta_{\rm c}} \quad , \tag{7.63}$$

where the magnetization critical exponent γ is $\gamma = 1$. If $\theta < \theta_{\rm c}$ then while there is still a solution at $m = h/(\theta - \theta_{\rm c})$, it lies at a local maximum of the free energy, as shown in fig. 7.10. The minimum of the free energy occurs close to the $h = 0$ solution $m = m_0(\theta) \equiv \pm\sqrt{3}\,(\theta_{\rm c} - \theta)$, and writing $m = m_0 + \delta m$ we find δm to linear order in h as $\delta m(\theta, h) = h/2(\theta_{\rm c} - \theta)$. Thus,

$$m(\theta < \theta_{\rm c}, h) = \pm\sqrt{3}\,(\theta_{\rm c} - \theta)^{1/2} + \frac{h}{2(\theta_{\rm c} - \theta)} \quad \Rightarrow \quad \chi(\theta < \theta_{\rm c}) = \frac{1}{2(\theta_{\rm c} - \theta)} \quad . \tag{7.64}$$

Both above and below the critical temperature we find that $\chi(\theta)$ diverges as $A_\pm|\theta - \theta_{\rm c}|^{-\gamma}$ where the exponent on either side of the transition is $\gamma = 1$, but the *critical amplitudes* differ: $A_+ = 1$ and $A_- = \frac{1}{2}$.

Finally, we can set $\theta = \theta_{\rm c}$ and examine $m(h)$. We find, from eqn. 7.62,

$$m(\theta = \theta_{\rm c}, h) = (3h)^{1/3} \propto h^{1/\delta} \quad , \tag{7.65}$$

where δ is a new critical exponent. Mean field theory gives $\delta = 3$. Note that at $\theta = \theta_{\rm c} = 1$ we have $m = \tanh(m + h)$, and inverting we find

$$h(m, \theta = \theta_{\rm c}) = \tfrac{1}{2}\log\left(\frac{1+m}{1-m}\right) - m = \frac{m^3}{3} + \frac{m^5}{5} + \ldots \quad , \tag{7.66}$$

which is consistent with what we just found for $m(h, \theta = \theta_{\rm c})$.

How well does mean field theory do in describing the phase transition of the Ising model? In table 7.2 we compare our mean field results for the exponents α, β, γ, and δ with exact values for the two-dimensional Ising model, numerical work on the three-dimensional Ising model, and experiments on the liquid-gas transition in CO_2. The first thing to note is that the exponents are dependent on the dimension of space, and this is something that mean field theory completely misses. In fact, it turns out that the mean field exponents are exact provided $d > d_{\rm u}$, where $d_{\rm u}$ is the *upper critical dimension* of the theory. For the Ising model, $d_{\rm u} = 4$, and above four dimensions (which is of course unphysical) the

[16] Pierre Curie was a pioneer in the fields of crystallography, magnetism, and radiation physics. In 1880, Pierre and his older brother Jacques discovered piezoelectricity. He was 21 years old at the time. It was in 1895 that Pierre made the first systematic studies of the effects of temperature on magnetic materials, and he formulated what is known as *Curie's Law*, $\chi = C/T$, where C is a constant. Curie married Marie Sklodowska in the same year. Their research turned toward radiation, recently discovered by Becquerel and Röntgen. In 1898, Pierre and Marie Curie discovered radium. They shared the 1903 Nobel Prize in Physics with Becquerel. Marie went on to win the 1911 Nobel Prize in Chemistry and was the first person ever awarded two Nobel Prizes. Their daughter Irène Joliot Curie shared the 1935 Prize in Chemistry (with her husband), also for work on radioactivity. Pierre Curie met an untimely and unfortunate end in the Spring of 1906. Walking across the Place Dauphine, he slipped and fell under a heavy horse-drawn wagon carrying military uniforms. His skull was crushed by one of the wagon wheels, killing him instantly. Later on that year, Pierre-Ernest Weiss proposed a modification of Curie's Law to account for ferromagnetism. This became known as the Curie-Weiss law, $\chi = C/(T - T_{\rm c})$.

Exponent	MFT	2D Ising (exact)	3D Ising (numerical)	binary liquid (3D)
α	0	0	0.11008(1)	0.113(5)
β	1/2	1/8	0.326419(3)	0.316(8)
γ	1	7/4	1.237075(10)	1.240(7)
δ	3	15	4.78984(1)	–
η	0	1/3	0.036298(2)	0.016(7)
ν	1/2	1	0.629971(4)	0.625(5)

Table 7.2: Critical exponents from mean field theory as compared with exact results for the two-dimensional Ising model, numerical results for the three-dimensional Ising model, and experiments on the liquid-gas transition in the binary fluids triethylamine and water (α : D. Beysens and A. Bourgou, *Phys. Rev. A* **19**, 2407 (1979)), isobutyric acid and water (β : S. C. Greer, *Phys. Rev. A* **14**, 1770 (1976)), and 3-methylpentane-nitroethane (γ, η, ν : R. F. Chang *et al.*, *Phys. Rev. Lett.* **37**, 1481 (1976)).

mean field exponents are in fact exact. We see that all in all the MFT results compare better with the three dimensional exponent values than with the two-dimensional ones – this makes sense since MFT does better in higher dimensions. The reason for this is that higher dimensions means more nearest neighbors, which effectively reduces the relative importance of the fluctuations we neglected to include.

Metastable states at $h \neq 0$

Consider the free energy $f(m, \theta, h)$ in eqn. 7.54, now for general θ not restricted to the immediate vicinity of θ_c. When $\theta < \theta_c$ and h is sufficiently small – just how small we are about to find out – the free energy as a function of m has one local maximum and two local minima, one of which is the thermodynamically stable state (*i.e.* the one for which $mh > 0$), and the other (with $mh < 0$) is metastable. Consider the case $h > 0$. As the temperature is raised, the metastable local minimum at $m < 0$ eventually vanishes, annihilating with the local maximum in a saddle-node bifurcation. To find where this happens, one sets $\partial f/\partial m = 0$ and $\partial^2 f/\partial m^2 = 0$ simultaneously. From eqn. 7.54, we have

$$\frac{\partial f}{\partial m} = m - \tanh\Big(\frac{m+h}{\theta}\Big) \quad , \quad \frac{\partial^2 f}{\partial m^2} = 1 - \theta^{-1}\mathrm{sech}^2\Big(\frac{m+h}{\theta}\Big) \quad . \tag{7.67}$$

Thus $h = \theta\,\tanh^{-1}(m) - m$, and using $\mathrm{sech}^2 x = 1 - \tanh^2 x$, we have $m^2 = 1 - \theta$ and

$$h^*(\theta) = \sqrt{1-\theta} - \frac{\theta}{2}\log\left(\frac{1+\sqrt{1-\theta}}{1-\sqrt{1-\theta}}\right). \tag{7.68}$$

The solutions lie at $h = \pm h^*(\theta)$. For $\theta < \theta_c = 1$ and $h \in \big[-h^*(\theta)\,,\,+h^*(\theta)\big]$, there are three solutions to the mean field equation. Equivalently we could in principle invert the above expression to obtain $\theta^*(h)$. For $\theta > \theta^*(h)$, there is only a single global minimum in the free energy $f(m)$ and there is no local minimum. Note $\theta^*(h=0) = 1$. Note that we could in principle invert the above relation to obtain $\theta^*(h)$, but alas this is not analytically possible.

7.4.4 Magnetization dynamics

Dissipative processes drive physical systems to minimum energy states. We can crudely model the dissipative dynamics of a magnet by writing the phenomenological equation

$$\frac{1}{\Gamma}\frac{dm}{dt} = -\frac{\partial f}{\partial m} = \tanh\left(\frac{m+h}{\theta}\right) - m \quad , \tag{7.69}$$

where Γ has the dimensions of frequency. We may define $s = \Gamma t$ to be a dimensionless rescaled time. Under these dynamics, the free energy is never increasing:

$$\frac{df}{ds} = \frac{\partial f}{\partial m}\,\frac{dm}{ds} = -\left(\frac{\partial f}{\partial m}\right)^2 \le 0 \quad . \tag{7.70}$$

Clearly the *fixed point* of these dynamics, where $\dot{m} = 0$, is a solution to the mean field equation $\frac{\partial f}{\partial m} = 0$. The time dependent $m(s)$ thus evolves until it reaches the first fixed point encountered, which is to say the first local extremum of the function $f(m)$. This extremum could be a global minimum, but it could also be a local minimum or even an inflection point.

A first order (generally nonlinear) ordinary differential equation of the form $\dot{u} = g(u)$ is called an $N = 1$ component *dynamical system*. For a general N-component dynamical system, $\boldsymbol{u} = (u_1, \ldots, u_N)$ is an N-component vector and $\boldsymbol{V}(\boldsymbol{u})$ is an N-component *vector field*, *i.e.* a set of N functions $V_j(u_1, \ldots, u_N)$ which specify the velocity vector at each point in $\boldsymbol{u}$ space, which is $\mathbb{R}^N$ (or some other N-dimensional manifold, on which we might have to define an *atlas* of coordinate patches). We then have $\dot{\boldsymbol{u}} = \boldsymbol{V}(\boldsymbol{u})$, which is a set of N coupled first-order ODEs. The $N = 1$ case is particularly simple to understand: $u(t)$ flows to the right in regions where $g(u) > 0$ and to the left where $g(u) < 0$. The case $g(u^*) = 0$ corresponds to a *fixed point*. Linearizing about u^*, *i.e.* writing $u(t) = u^* + \eta(t)$, the linearized dynamics are $\dot{\eta} = g'(u^*)\eta$, with $\eta(t) = \eta(0)\exp\big[g'(u^*)t\big]$. Thus for $g'(u^*) > 0$, corresponding to an *unstable fixed point* (UFP), the linearized dynamics take us further and further from u^*, and the linearization soon fails. When $g'(u^*) < 0$, corresponding to a *stable fixed point* (SFP), $u(t)$ approaches u^* and the linearization gets better and better. Generically the approach to a SFP is logarithmic in time, *i.e.* $t = \log\big[\eta(0)/\eta(t)\big]/|g'(u^*)|$. Given the initial condition $u(0)$, the fate of an $N = 1$ dynamical system is to flow to the closest accessible stable fixed point[17].

Our phenomenological magnetization dynamics is described by $\dot{m} = -f'(m)$, and is thus an $N = 1$ dynamical system with $g(m) = -f'(m)$. Fixed points satisfy $f'(m^*) = 0$. Thus, local minima of the free energy as a function of m, where $f''(m^*) > 0$, correspond to stable fixed points, while local maxima, where $f''(m^*) < 0$, correspond to unstable fixed points. This phase flow is sketched in fig. 7.11. As we have seen, for any value of h there is a temperature θ^* below which the free energy $f(m)$ has two local minima and one local maximum. When $h = 0$ the minima are degenerate, but at finite h one of the minima is a global minimum. Thus, for $\theta < \theta^*(h)$ there are three solutions to the mean field equations. In the language of dynamical systems, under the dynamics of eqn. 7.69, minima of $f(m)$ correspond to attractive fixed points and maxima to repulsive fixed points. If $h > 0$, the rightmost of these fixed

[17] For the nongeneric case where $g(u^*) = 0$ and $g'(u^*) = 0$ vanish concomitantly, u^* is a *half-stable* fixed point. For example, if $g(u) = Au^2$ then $u^* = 0$ is half -stable, and for initial conditions $u(0) < 0$ the velocity $\dot{u}(t)$ is positive and the flow asymptotically approaches $u(\infty) = 0$, while for $u(0) > 0$ the velocity is also positive and the flow is to infinity, which is reached at a finite time $t_\infty = 1/Au(0)$.

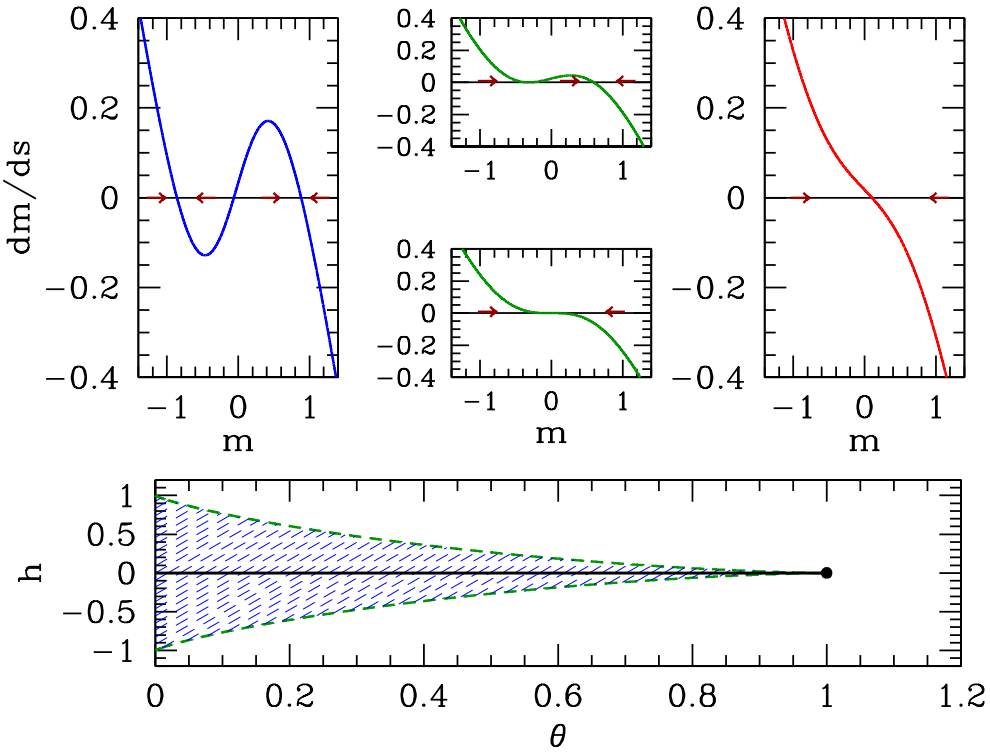

Figure 7.11: Dissipative magnetization dynamics $\dot{m} = -f'(m)$. Bottom panel shows $h^*(\theta)$ from eqn. 7.68. For (θ, h) within the blue shaded region, the free energy $f(m)$ has a global minimum plus a local minimum and a local maximum. Otherwise $f(m)$ has only a single global minimum. Top panels show an imperfect bifurcation in the magnetization dynamics at $h = 0.0215$, for which $\theta^* = 0.90$. Temperatures shown: $\theta = 0.65$ (blue), $\theta = \theta^*(h) = 0.90$ (green), and $\theta = 1.2$. The rightmost stable fixed point corresponds to the global minimum of the free energy. The bottom of the middle two upper panels shows $h = 0$, where both of the attractive fixed points and the repulsive fixed point coalesce into a single attractive fixed point (supercritical pitchfork bifurcation).

points corresponds to the global minimum of the free energy. As θ is increased, this fixed point evolves smoothly. At $\theta = \theta^*$, the (metastable) local minimum and the local maximum coalesce and annihilate in a saddle-note bifurcation. However at $h = 0$ all three fixed points coalesce at $\theta = \theta_c$ and the bifurcation is a supercritical pitchfork. As a function of θ at finite h, the dynamics are said to exhibit an *imperfect bifurcation*, which is a deformed supercritical pitchfork.

The solution set for the mean field equation is simply expressed by inverting the tanh function to obtain $h(\theta, m)$. One readily finds

$$h(\theta, m) = \frac{\theta}{2} \log\left(\frac{1+m}{1-m}\right) - m \quad . \tag{7.71}$$

As we see in the bottom panel of fig. 7.12, $m(h)$ becomes multivalued for $h \in \big[-h^*(\theta)\,,\, +h^*(\theta) \big]$, where $h^*(\theta)$ is given in eqn. 7.68. Now imagine that $\theta < \theta_c$ and we slowly ramp the field h from a large negative value to a large positive value, and then slowly back down to its original value. On the time scale of the magnetization dynamics, we can regard $h(s)$ as a constant. (Remember the time variable is

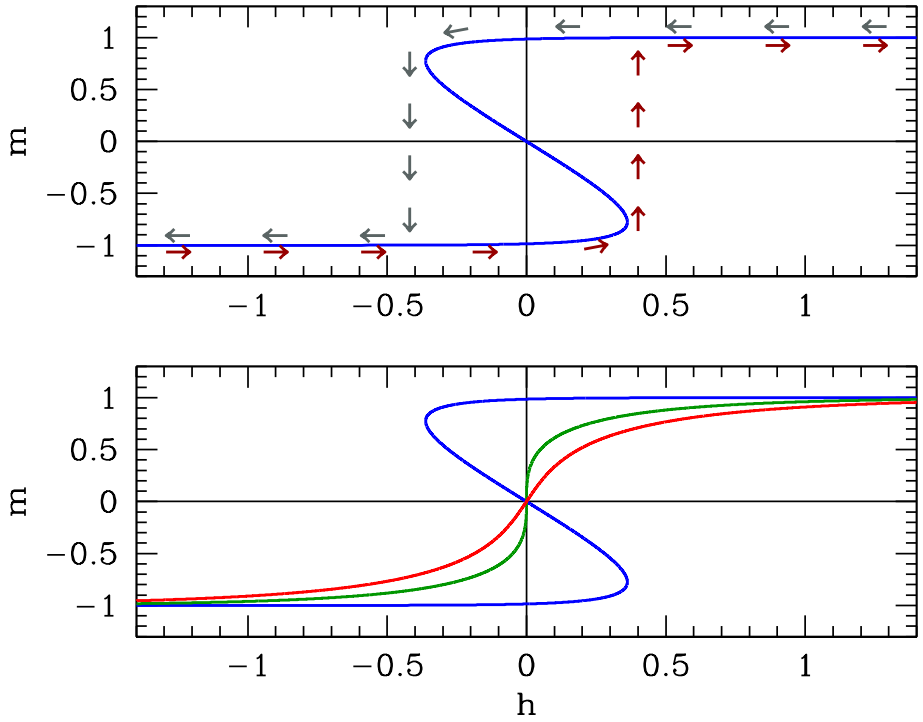

Figure 7.12: Top panel: hysteresis as a function of ramping the dimensionless magnetic field h at $\theta = 0.40$. Dark red arrows below the curve track the evolution of m upon a slow increase of h. Dark grey arrows above the curve track a slow decrease of h. Bottom panel : solution set for $m(\theta, h)$ as a function of h at temperatures $\theta = 0.40$ (blue), $\theta = \theta_c = 1.0$ (dark green), and $t = 1.25$ (red).

s here.) Thus, $m(s)$ will flow to the nearest stable fixed point. Initially the system starts with $m = -1$ and h large and negative, and there is only one fixed point, at $m^* \approx -1$. As h slowly increases, the fixed point value m^* also slowly increases. As h exceeds $-h^*(\theta)$, a saddle-node bifurcation occurs, and two new fixed points are created at positive m, one stable and one unstable. The global minimum of the free energy still lies at the fixed point with $m^* < 0$. However, when h crosses $h = 0$, the global minimum of the free energy lies at the most positive fixed point m^*. The dynamics, however, keep the system stuck in what is a metastable phase. This persists until $h = +h^*(\theta)$, at which point another saddle-note bifurcation occurs, and the attractive fixed point at $m^* < 0$ annihilates with the repulsive fixed point. The dynamics then act quickly to drive m to the only remaining fixed point. This process is depicted in the top panel of fig. 7.12. As one can see from the figure, the the system follows a stable fixed point until the fixed point disappears, even though that fixed point may not always correspond to a global minimum of the free energy. The resulting $m(h)$ curve is then not reversible as a function of time, and it possesses a characteristic shape known as a *hysteresis loop*. Etymologically, the word *hysteresis* derives from the Greek $\upsilon\sigma\tau\varepsilon\rho\eta\sigma\iota\varsigma$, which means 'lagging behind' (and not from $\iota\sigma\tau o\rho\iota\alpha$, which means 'inquiry'). Systems which are hysteretic exhibit a *history-dependence* to their status, which is not uniquely determined by external conditions. Hysteresis may be exhibited with respect to changes in applied magnetic field, changes in temperature, or changes in other externally determined parameters.

7.4.5 Beyond nearest neighbors

Up to this point we have assumed nearest-neighbor interactions on a lattice of coordination number z. Suppose, instead, that we had started with the more general model,

$$\hat{H} = -\tfrac{1}{2}\sum_{i\neq j} J_{ij}\,\sigma_i\,\sigma_j - H\sum_i \sigma_i \quad , \tag{7.72}$$

where $J_{ij} = J\big(|\boldsymbol{R}_i - \boldsymbol{R}_j|\big)$ is the coupling between spins on sites i and j[18]. In the top equation above, each pair (ij) is counted once in the interaction term; this may be replaced by a sum over all i and j if we include a factor of $\frac{1}{2}$.[19] The resulting mean field Hamiltonian is then

$$\hat{H}_{\rm MF} = \tfrac{1}{2}N\hat{J}(0)\,m^2 - \big(H + \hat{J}(0)\,m\big)\sum_{i=1}^{N}\sigma_i \quad . \tag{7.73}$$

Here, $\hat{J}(\boldsymbol{q})$ is the lattice Fourier transform of the interaction function $J(\boldsymbol{R})$:[20]

$$\hat{J}(\boldsymbol{q}) = \sum_{\boldsymbol{R}} J(\boldsymbol{R})\,e^{-i\boldsymbol{q}\cdot\boldsymbol{R}} \quad . \tag{7.74}$$

For nearest neighbor interactions only, one has $\hat{J}(0) = zJ$, where z is the *lattice coordination number*, *i.e.* the number of nearest neighbors of any given site. The scaled free energy is as in eqn. 7.54, with $f = F/N\hat{J}(0)$, $\theta = k_{\rm B}T/\hat{J}(0)$, and $h = H/\hat{J}(0)$. The analysis proceeds precisely as before, and we conclude $\theta_{\rm c} = 1$, *i.e.* $k_{\rm B}T_{\rm c}^{\rm MF} = \hat{J}(0)$. For example, on the simple cubic lattice there are six nearest neighbors and twelve next-nearest neighbors. Thus, if J is the nearest neighbor coupling and J' the next-nearest neighbor coupling, we have $\hat{J}(0) = 6J + 12J'$.

7.4.6 Ising model with long-ranged forces

Consider an Ising model where $J_{ij} = J/N$ for all i and j, so that there is a very weak interaction between every pair of spins. The Hamiltonian is then

$$\hat{H} = -\frac{J}{2N}\left(\sum_{i=1}^{N}\sigma_i\right)^2 - H\sum_{i=1}^{N}\sigma_i \quad . \tag{7.75}$$

The partition function is

$$Z = \operatorname*{Tr}_{\{\sigma_i\}} \exp\left[\frac{\beta J}{2N}\left(\sum_{i=1}^{N}\sigma_i\right)^2 + \beta H\sum_{i=1}^{N}\sigma_i\right] \quad . \tag{7.76}$$

[18]Note that we may write $\frac{1}{2}\sum_{i\neq j}A_{ij}$ as $\sum_{i<j}A_{ij}$ provided $A = A^{\rm T}$ is symmetric. Clearly $A_{ij} = \sigma_i\,\sigma_j$ is symmetric under interchange of indices i and j. Each version of the sum counts all unique *pairs* $(i,j) = (j,i)$ exactly once.

[19]The self-interaction terms with $i = j$ contribute a constant to $\hat{H}$ and may be either included or excluded. However, this property only pertains to the $\sigma_i = \pm 1$ model. For higher spin versions of the Ising model, say where $S_i \in \{-1, 0, +1\}$, then S_i^2 is not constant and we should explicitly exclude the self-interaction terms.

[20]The sum in the discrete Fourier transform is over all 'direct Bravais lattice vectors' and the wavevector $\boldsymbol{q}$ may be restricted to the 'first Brillouin zone'. These terms are familiar from elementary solid state physics.

We now invoke the Gaussian integral,

$$\int\limits_{-\infty}^{\infty} dx\, e^{-\alpha x^2 - \beta x} = \sqrt{\frac{\pi}{\alpha}}\, e^{\beta^2/4\alpha} \quad . \tag{7.77}$$

Thus,

$$\exp\left[\frac{\beta J}{2N}\Big(\sum_{i=1}^{N}\sigma_i\Big)^2\right] = \left(\frac{N\beta J}{2\pi}\right)^{1/2}\int\limits_{-\infty}^{\infty} dm\, e^{-\frac{1}{2}N\beta J m^2 + \beta J m \sum_{i=1}^{N}\sigma_i} \quad , \tag{7.78}$$

and we can write the partition function as

$$Z = \left(\frac{N\beta J}{2\pi}\right)^{1/2}\int\limits_{-\infty}^{\infty} dm\, e^{-\frac{1}{2}N\beta J m^2}\left(\sum_{\sigma} e^{\beta(H+Jm)\sigma}\right)^N = \left(\frac{N}{2\pi\theta}\right)^{1/2}\int\limits_{-\infty}^{\infty} dm\, e^{-NA(m)/\theta} \quad , \tag{7.79}$$

where $\theta = k_{\rm B}T/J$, $h = H/J$, and

$$A(m) = \tfrac{1}{2}m^2 - \theta\log\left[2\cosh\left(\frac{h+m}{\theta}\right)\right] \quad . \tag{7.80}$$

Since $N \to \infty$, we can perform the integral using the method of steepest descents. Thus, we must set

$$\left.\frac{dA}{dm}\right|_{m^*} = 0 \quad \Longrightarrow \quad m^* = \tanh\left(\frac{m^*+h}{\theta}\right) \quad . \tag{7.81}$$

Expanding about $m = m^*$, we write

$$A(m) = A(m^*) + \tfrac{1}{2}A''(m^*)\,(m-m^*)^2 + \tfrac{1}{6}\,A'''(m^*)\,(m-m^*)^3 + \ldots \quad . \tag{7.82}$$

Writing $\nu = m - m^*$ and performing the integration, we obtain

$$\begin{aligned} Z &= \left(\frac{N}{2\pi\theta}\right)^{1/2} e^{-NA(m^*)/\theta}\int\limits_{-\infty}^{\infty} d\nu\, \exp\left[-\frac{NA''(m^*)}{2\theta}\,\nu^2 - \frac{NA'''(m^*)}{6\theta}\,\nu^3 + \ldots\right] \\ &= \frac{1}{\sqrt{A''(m^*)}}\, e^{-NA(m^*)/\theta}\cdot\Big\{1 + \mathcal{O}(N^{-1})\Big\} \quad . \end{aligned} \tag{7.83}$$

The corresponding free energy per site

$$f = \frac{F}{NJ} = A(m^*) + \frac{\theta}{2N}\,\log A''(m^*) + \mathcal{O}(N^{-2}) \quad , \tag{7.84}$$

where m^* is the solution to the mean field equation which minimizes $A(m)$. Mean field theory is *exact* for this model!

7.5 Landau Theory of Phase Transitions

Landau's theory of phase transitions is based on an expansion of the free energy of a thermodynamic system in terms of an *order parameter*, which is nonzero in an ordered phase and zero in a disordered phase. For example, the magnetization density m of a ferromagnet in zero external field but at finite temperature typically vanishes for temperatures $T > T_{\rm c}$, where $T_{\rm c}$ is the *critical temperature*, also called the *Curie temperature* in a ferromagnet. A low order expansion in powers of the order parameter is appropriate sufficiently close to the phase transition, *i.e.* at temperatures such that the order parameter, if nonzero, is still small.

The order parameter m might be a scalar or a vector or even a matrix. In many cases the free energy $f(m)$ is invariant under the operations of a *symmetry group* G, such that $f(m) = f(\mathsf{g}m)$ for all $\mathsf{g} \in \mathsf{G}$, where $\mathsf{g}m$ is the action of the group element g on m. For example, we might have $\mathsf{G} = \mathbb{Z}_2$ with elements $\mathsf{g} \in \{+1, -1\}$ and $m \in \mathbb{R}$. As we saw previously, in the high temperature phase $f(m)$ has a global minimum at $m = 0$. But in the low temperature phase, $f(m)$ is minimized at $m = \pm m_0 \neq 0$, with $m = 0$ a local maximum. The free energy is symmetric under the action of $\mathbb{Z}_2$, but the system has to choose one from among the two degenerate 'vacua' $m = \pm m_0$. This is the phenomenon of *spontaneous symmetry breaking* (SSB) described in §6.2.1. The order parameter or one of its derivatives exhibits a singularity or discontinuity as a function of thermodynamic parameters, such as the temperature T. This singular behavior occurs along a subset of parameter space, identified as a *critical point* or *critical surface*. The imposition of a finite external field h *explicitly breaks* the G-symmetry, hence SSB can occur only at $h = 0$.

7.5.1 Quartic free energy with Ising symmetry

The simplest example is the quartic free energy,

$$f(m, \theta, h = 0) = f_0 + \tfrac{1}{2}am^2 + \tfrac{1}{4}bm^4 \quad , \tag{7.85}$$

where $f_0 = f_0(\theta)$, $a = a(\theta)$, and $b = b(\theta)$. Here, θ is a dimensionless measure of the temperature[21]. We assume $b > 0$, which is necessary if the free energy is to be bounded from below[22].

The equation of state, which relates the intensive quantities m and θ at $h = 0$, is then

$$\frac{\partial f}{\partial m} = 0 = am + bm^3 \quad , \tag{7.86}$$

has three solutions in the complex m plane: (i) $m = 0$, (ii) $m = \sqrt{-a/b}$, and (iii) $m = -\sqrt{-a/b}$. The latter two solutions lie along the (physical) real axis provided $a < 0$. We assume that there exists a unique temperature $\theta_{\rm c}$ where $a(\theta_{\rm c}) = 0$. Minimizing f, we find

$$\begin{aligned} a < 0 \quad (\theta < \theta_{\rm c}) \quad &: \quad f(\theta) = f_0 - \frac{a^2}{4b} \\ a > 0 \quad (\theta > \theta_{\rm c}) \quad &: \quad f(\theta) = f_0 \quad . \end{aligned} \tag{7.87}$$

[21] For example in an Ising ferromagnet we might define $\theta = k_{\rm B}T/\hat{J}(0)$, as before.

[22] It is always the case that f is bounded from below, on physical grounds. Were b negative, we'd have to consider higher order terms in the Landau expansion.

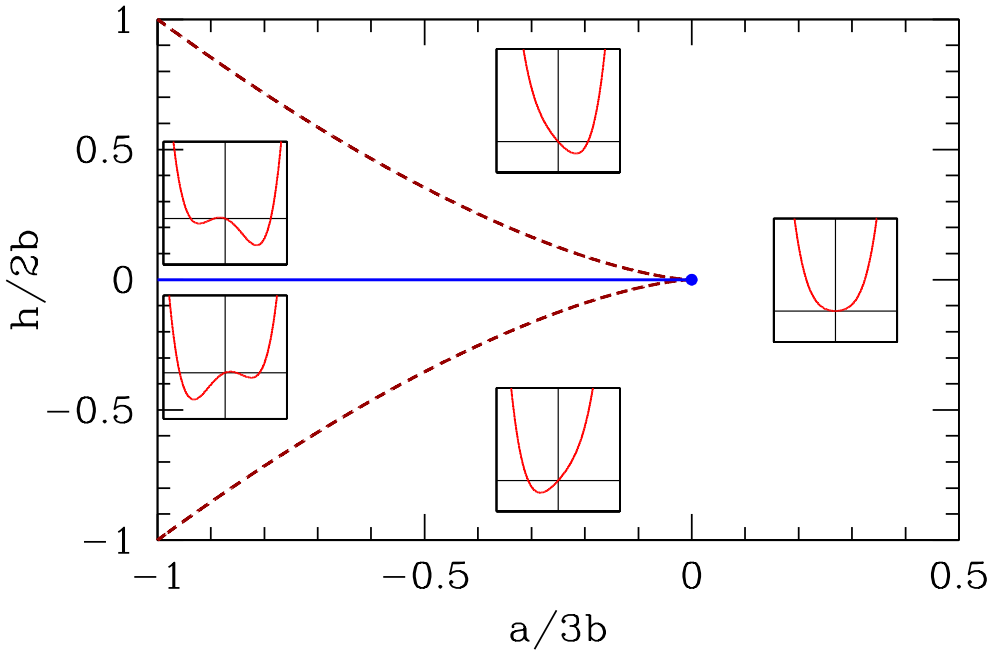

Figure 7.13: Phase diagram for the quartic Landau free energy $f = f_0 + \frac{1}{2}am^2 + \frac{1}{4}bm^4 - hm$, with $b > 0$. There is a first order line at $h = 0$ extending from $a = -\infty$ and terminating in a critical point at $a = 0$. For $|h| < h^*(a)$ (dashed red line) there are three solutions to the mean field equation, corresponding to one global minimum, one local minimum, and one local maximum. Insets show behavior of the free energy $f(m)$.

Thus $a(\theta)$ changes sign at $\theta = \theta_c$, where the free energy is continuous, since $a(\theta_c) = 0$. The specific heat, however, is discontinuous across the transition, with

$$c(\theta_c^+) - c(\theta_c^-) = -\theta_c \left.\frac{\partial^2}{\partial\theta^2}\right|_{\theta=\theta_c} \left(\frac{a^2}{4b}\right) = -\frac{\theta_c \left[a'(\theta_c)\right]^2}{2b(\theta_c)} \quad . \tag{7.88}$$

The presence of a magnetic field h breaks the $\mathbb{Z}_2$ symmetry of $m \to -m$. The free energy becomes

$$f(m, \theta, h) = f_0 + \tfrac{1}{2}am^2 + \tfrac{1}{4}bm^4 - hm \quad , \tag{7.89}$$

and the mean field equation is

$$bm^3 + am - h = 0 \quad . \tag{7.90}$$

This is a cubic equation for m with real coefficients, and as such it can either have three real solutions or one real solution and two complex solutions related by complex conjugation. Clearly we must have $a < 0$ in order to have three real roots, since $bm^3 + am$ is monotonically increasing otherwise. The boundary between these two classes of solution sets occurs when two roots coincide, which means $f''(m) = 0$ as well as $f'(m) = 0$. Simultaneously solving these two equations, we find

$$h^*(a) = \pm\frac{2}{3^{3/2}} \frac{(-a)^{3/2}}{b^{1/2}} \quad , \tag{7.91}$$

or, equivalently,

$$a^*(h) = -\frac{3}{2^{2/3}}\, b^{1/3}\, |h|^{2/3}. \tag{7.92}$$

If, for fixed h, we have $a < a^*(h)$, then there will be three real solutions to the mean field equation $f'(m) = 0$, one of which is a global minimum (the one for which $m \cdot h > 0$). For $a > a^*(h)$ there is only a single global minimum, at which m also has the same sign as h. If we solve the mean field equation perturbatively in h/a, we find

$$\begin{aligned} m(a,h) &= \frac{h}{a} - \frac{b}{a^4}\, h^3 + \mathcal{O}(h^5) \qquad\qquad (a > 0) \\ &= \pm\frac{|a|^{1/2}}{b^{1/2}} + \frac{h}{2\,|a|} \pm \frac{3\,b^{1/2}}{8\,|a|^{5/2}}\, h^2 + \mathcal{O}(h^3) \qquad (a < 0) \quad . \end{aligned} \tag{7.93}$$

7.5.2 Cubic terms in Landau theory : first order transitions

Next, consider a free energy with a cubic term,

$$f = f_0 + \tfrac{1}{2}am^2 - \tfrac{1}{3}ym^3 + \tfrac{1}{4}bm^4 \quad , \tag{7.94}$$

with $b > 0$ for stability. Without loss of generality, we may assume $y > 0$ (else send $m \to -m$). Note that we no longer have $m \to -m$ (*i.e.* $\mathbb{Z}_2$) symmetry. The cubic term favors positive m. What is the phase diagram in the (a, y) plane?

Extremizing the free energy with respect to m, we obtain

$$\frac{\partial f}{\partial m} = 0 = am - ym^2 + bm^3 \quad . \tag{7.95}$$

This cubic equation factorizes into a linear and quadratic piece, and hence may be solved simply. The three solutions are $m = 0$ and

$$m = m_\pm \equiv \frac{y}{2b} \pm \sqrt{\Big(\frac{y}{2b}\Big)^2 - \frac{a}{b}} \quad . \tag{7.96}$$

We now see that for $y^2 < 4ab$ there is only one real solution, at $m = 0$, while for $y^2 > 4ab$ there are three real solutions. Which solution has lowest free energy? To find out, we compare the energy $f(0)$ with $f(m_+)$[23]. Thus, we set

$$f(m) = f(0) \quad \Longrightarrow \quad \tfrac{1}{2}am^2 - \tfrac{1}{3}ym^3 + \tfrac{1}{4}bm^4 = 0 \quad , \tag{7.97}$$

and we now have two quadratic equations to solve simultaneously:

$$0 = a - ym + bm^2 \qquad , \qquad 0 = \tfrac{1}{2}a - \tfrac{1}{3}ym + \tfrac{1}{4}bm^2 = 0 \quad . \tag{7.98}$$

Eliminating the quadratic term gives $m = 3a/y$. Finally, substituting $m = m_+$ gives us a relation between a, b, and y:

$$y^2 = \tfrac{9}{2}\, ab \quad . \tag{7.99}$$

[23] We needn't waste our time considering the $m = m_-$ solution, since the cubic term prefers positive m.

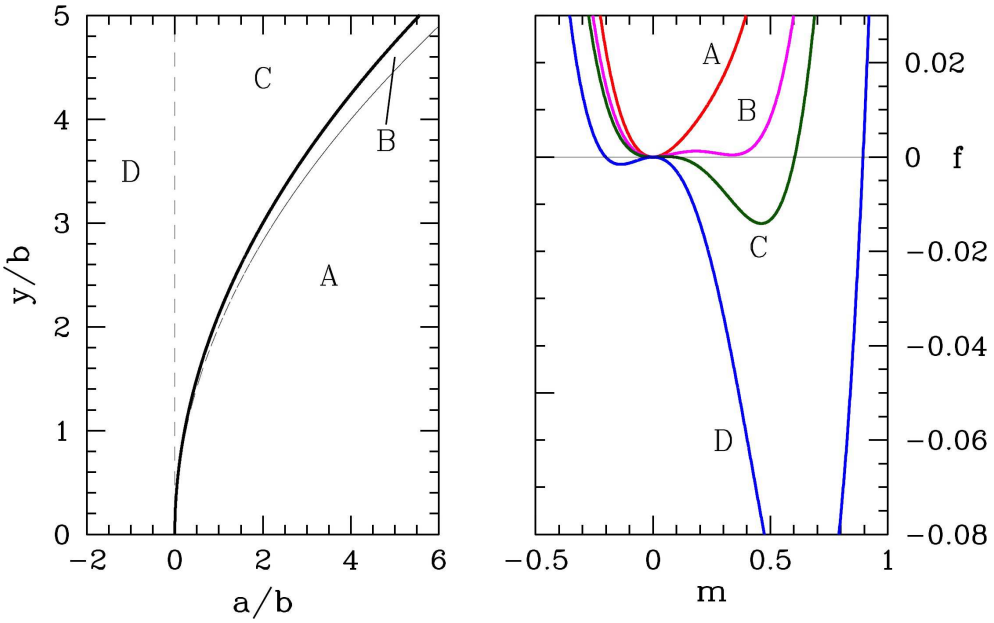

Figure 7.14: Behavior of the quartic free energy $f(m) = \frac{1}{2}am^2 - \frac{1}{3}ym^3 + \frac{1}{4}bm^4$. A: $y^2 < 4ab$; B: $4ab < y^2 < \frac{9}{2}ab$; C and D: $y^2 > \frac{9}{2}ab$. The thick black line denotes a line of first order transitions, where the order parameter is discontinuous across the transition.

Thus, we have the following:

$$\begin{aligned} a > \frac{y^2}{4b} \quad &: \quad \text{1 real root } m = 0 \\ \frac{y^2}{4b} > a > \frac{2y^2}{9b} \quad &: \quad \text{3 real roots; minimum at } m = 0 \\ \frac{2y^2}{9b} > a \quad &: \quad \text{3 real roots; minimum at } m = \frac{y}{2b} + \sqrt{\left(\frac{y}{2b}\right)^2 - \frac{a}{b}} \end{aligned} \tag{7.100}$$

The solution $m = 0$ lies at a local minimum of the free energy for $a > 0$ and at a local maximum for $a < 0$. Over the range $y^2/4b > a > 2y^2/9b$, then, there is a global minimum at $m = 0$, a local minimum at $m = m_+$, and a local maximum at $m = m_-$, with $m_+ > m_- > 0$. For $y^2/9b > a > 0$, there is a local minimum at $a = 0$, a global minimum at $m = m_+$, and a local maximum at $m = m_-$, again with $m_+ > m_- > 0$. For $a < 0$, there is a local maximum at $m = 0$, a local minimum at $m = m_-$, and a global minimum at $m = m_+$, with $m_+ > 0 > m_-$. See fig. 7.14.

With $y = 0$, we have a second order transition at $a = 0$. With $y \neq 0$, there is a discontinuous (first order) transition at $a_c = 2y^2/9b > 0$ and $m_c = 2y/3b$. This occurs before a reaches the value $a = 0$ where the curvature at $m = 0$ turns negative. If we write $a = \alpha(T - T_0)$, then the expected second order transition at $T = T_0$ is *preempted* by a first order transition at $T_c = T_0 + 2y^2/9\alpha b$.

7.5.3 Order parameter dynamics

Suppose we now impose some dynamics on the system, of the simple relaxational type

$$\frac{dm}{dt} = -\Gamma \frac{\partial f}{\partial m} \quad , \tag{7.101}$$

where Γ is a phenomenological kinetic coefficient. Assuming $y > 0$ and $b > 0$, it is convenient to adimensionalize by writing

$$m \equiv \frac{y}{b} \cdot u \qquad , \qquad a \equiv \frac{y^2}{b} \cdot r \qquad , \qquad t \equiv \frac{b}{\Gamma y^2} \cdot s \quad . \tag{7.102}$$

Then we obtain

$$\frac{du}{ds} = -\frac{\partial \varphi}{\partial u} \quad , \tag{7.103}$$

where the dimensionless free energy function is

$$\varphi(u) = \tfrac{1}{2} r u^2 - \tfrac{1}{3} u^3 + \tfrac{1}{4} u^4 \quad . \tag{7.104}$$

We see that there is a single control parameter, $r = ab/y^2$. The fixed points of the dynamics are then the stationary points of $\varphi(u)$, where $\varphi'(u) = 0$, with $\varphi'(u) = u\,(r - u + u^2)$. The solutions to $\varphi'(u) = 0$ are then given by

$$u^* = 0 \qquad , \qquad u^* = \tfrac{1}{2} \pm \left(\tfrac{1}{4} - r\right)^{1/2} \quad . \tag{7.105}$$

The second of these is a parabola $r = u(1-u)$ opening to the left in the (r, u) plane. For $r > \frac{1}{4}$ there is one fixed point at $u = 0$, which is attractive under the dynamics $\dot{u} = -\varphi'(u)$ since $\varphi''(0) = r$. At $r = \frac{1}{4}$ there occurs a saddle-node bifurcation and a pair of fixed points is generated, one stable and one unstable. As we see from fig. 7.13, the interior fixed point is always unstable and the two exterior fixed points are always stable. At $r = 0$ there is a transcritical bifurcation where two fixed points of opposite stability collide and bounce off one another (metaphorically speaking).

At the saddle-node bifurcation, $r = \frac{1}{4}$ and $u = \frac{1}{2}$, and we find $\varphi(u = \frac{1}{2}; r = \frac{1}{4}) = \frac{1}{192}$, which is positive. Thus, the thermodynamic state of the system remains at $u = 0$ until the value of $\varphi(u_+)$ crosses zero. This occurs when $\varphi(u) = 0$ and $\varphi'(u) = 0$, the simultaneous solution of which yields $r = \frac{2}{9}$ and $u = \frac{2}{3}$.

Suppose we slowly ramp the control parameter r up and down as a function of the dimensionless time s. Under the dynamics of eqn. 7.103, $u(s)$ flows to the first stable fixed point encountered – this is always the case for a dynamical system with a one-dimensional phase space. Then as r is further varied, u follows the position of whatever locally stable fixed point it initially encountered. Thus, $u\big(r(s)\big)$ evolves smoothly until a bifurcation is encountered. The situation is depicted by the arrows in fig. 7.15. The equilibrium thermodynamic value for $u(r)$ is discontinuous; there is a first order phase transition at $r = \frac{2}{9}$, as we've already seen. As r is increased, $u(r)$ follows a trajectory indicated by the magenta arrows. For an negative initial value of u, the evolution as a function of r will be *reversible*. However, if $u(0)$ is initially positive, then the system exhibits *hysteresis*, as shown. Starting with a large positive value of r, $u(s)$ quickly evolves to $u = 0^+$, which means a positive infinitesimal value. Then as r is decreased, the system remains at $u = 0^+$ even through the first order transition, because $u = 0$ is an attractive fixed point. However, once r begins to go negative, the $u = 0$ fixed point becomes repulsive,

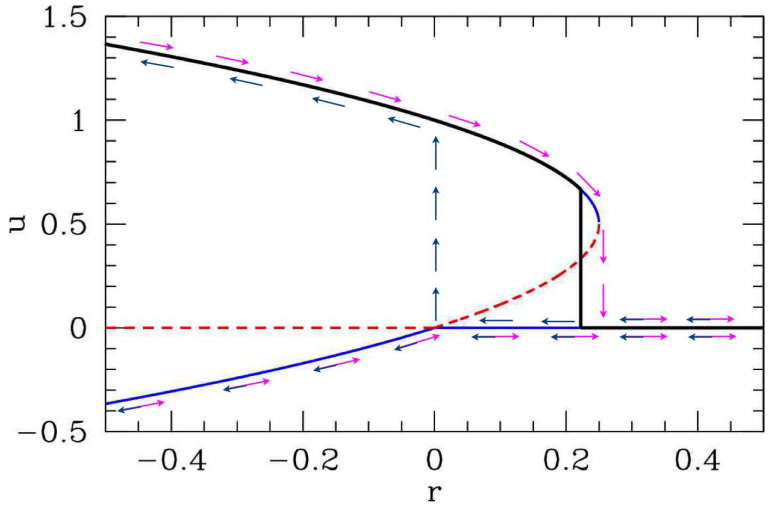

Figure 7.15: Fixed points for $\varphi(u) = \frac{1}{2}ru^2 - \frac{1}{3}u^3 + \frac{1}{4}u^4$ and flow under the dynamics $\dot{u} = -\varphi'(u)$. Solid curves represent stable fixed points and dashed curves unstable fixed points. Magenta arrows show behavior under slowly increasing control parameter r and dark blue arrows show behavior under slowly decreasing r. For $u > 0$ there is a hysteresis loop. The thick black curve shows the equilibrium thermodynamic value of $u(r)$, *i.e.* that value which minimizes the free energy $\varphi(u)$. There is a first order phase transition at $r = \frac{2}{9}$, where the thermodynamic value of u jumps from $u = 0$ to $u = \frac{2}{3}$.

and $u(s)$ quickly flows to the stable fixed point $u_+ = \frac{1}{2} + \left(\frac{1}{4} - r\right)^{1/2}$. Further decreasing r, the system remains on this branch. If r is later increased, then $u(s)$ remains on the upper branch past $r = 0$, until the u_+ fixed point annihilates with the unstable fixed point at $u_- = \frac{1}{2} - \left(\frac{1}{4} - r\right)^{1/2}$, at which time $u(s)$ quickly flows down to $u = 0^+$ again.

7.5.4 Sixth order Landau theory : tricritical point

Finally, consider a model with $\mathbb{Z}_2$ symmetry, with the Landau free energy

$$f = f_0 + \tfrac{1}{2}am^2 + \tfrac{1}{4}bm^4 + \tfrac{1}{6}cm^6 \quad , \tag{7.106}$$

with $c > 0$ for stability. We seek the phase diagram in the (a, b) plane. Extremizing f with respect to m,

$$\frac{\partial f}{\partial m} = 0 = m\left(a + bm^2 + cm^4\right) \quad , \tag{7.107}$$

which is a quintic with five solutions over the complex m plane. One solution is obviously $m = 0$. The other four are

$$m = \pm\sqrt{-\frac{b}{2c} \pm \sqrt{\left(\frac{b}{2c}\right)^2 - \frac{a}{c}}} \quad . \tag{7.108}$$

For each $\pm$ symbol in the above equation, there are two options, hence four roots in all.

If $a > 0$ and $b > 0$, then four of the roots are imaginary and there is a unique minimum at $m = 0$.

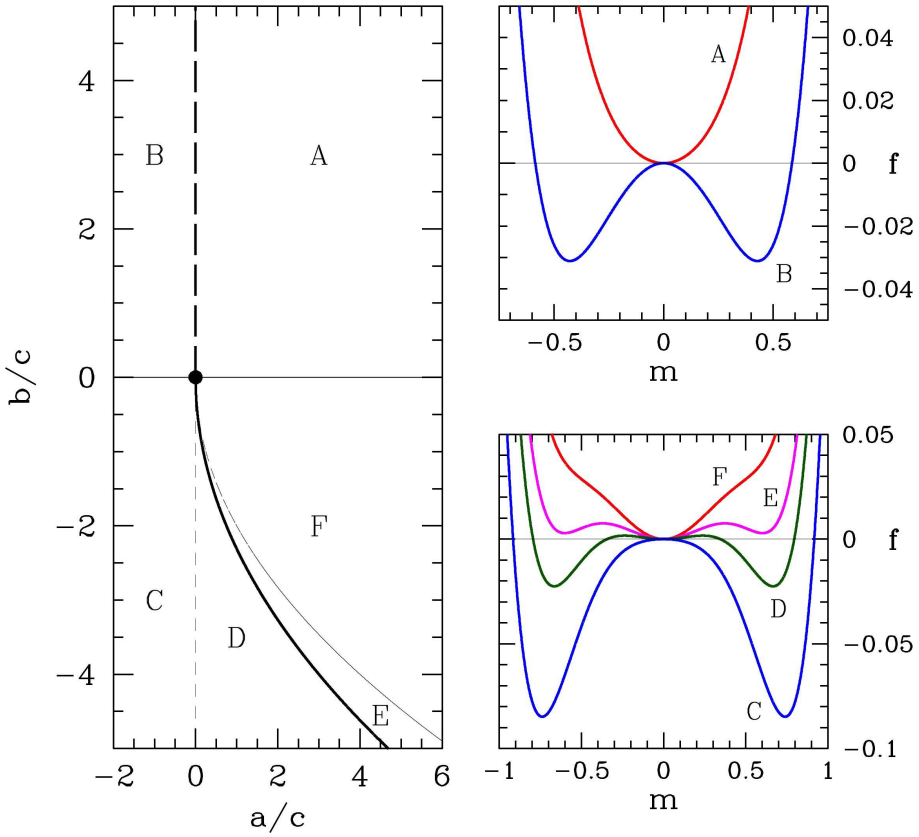

Figure 7.16: Behavior of the sextic free energy $f(m) = \frac{1}{2}am^2 + \frac{1}{4}bm^4 + \frac{1}{6}cm^6$. A: $a > 0$ and $b > 0$; B: $a < 0$ and $b > 0$; C: $a < 0$ and $b < 0$; D: $a > 0$ and $b < -\frac{4}{\sqrt{3}}\sqrt{ac}$; E: $a > 0$ and $-\frac{4}{\sqrt{3}}\sqrt{ac} < b < -2\sqrt{ac}$; F: $a > 0$ and $-2\sqrt{ac} < b < 0$. The thick dashed line is a line of second order transitions, which meets the thick solid line of first order transitions at the tricritical point, $(a, b) = (0, 0)$.

For $a < 0$, there are only three solutions to $f'(m) = 0$ for real m, regardless of the sign of b, since the minus choice for the $\pm$ sign under the radical leads to imaginary roots. One of the solutions is $m = 0$, which is a local maximum of $f(m)$. The other two are degenerate minima at

$$m = \pm\sqrt{-\frac{b}{2c} + \sqrt{\left(\frac{b}{2c}\right)^2 - \frac{a}{c}}} \quad . \tag{7.109}$$

The most interesting situation is $a > 0$ and $b < 0$. If $a > 0$ and $b < -2\sqrt{ac}$, all five roots are real. There must be three minima, separated by two local maxima. Clearly if m^* is a solution, then so is $-m^*$. Thus, the only question is whether the outer minima are of lower energy than the minimum at $m = 0$. We assess this by demanding $f(m^*) = f(0)$, where m^* is the position of the largest root (*i.e.* the rightmost minimum). This gives a second quadratic equation,

$$0 = \tfrac{1}{2}a + \tfrac{1}{4}bm^2 + \tfrac{1}{6}cm^4 \quad , \tag{7.110}$$

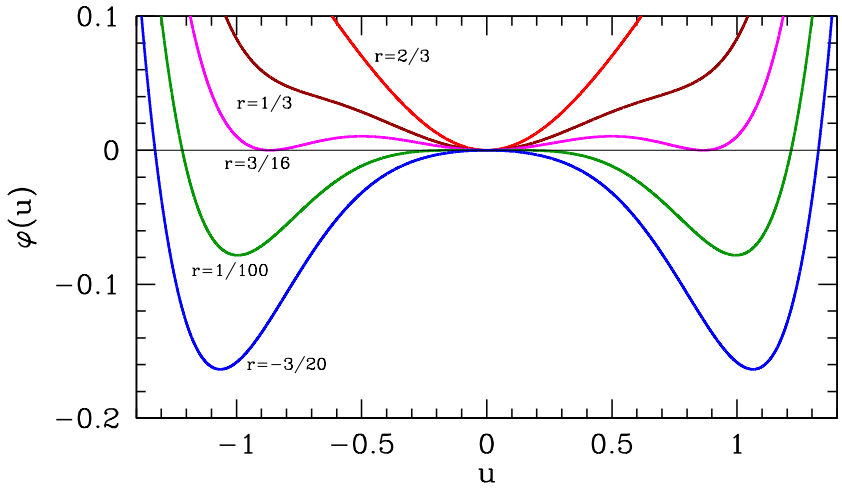

Figure 7.17: Free energy $\varphi(u) = \frac{1}{2}ru^2 - \frac{1}{4}u^4 + \frac{1}{6}u^6$ for different values of the control parameter r.

which together with equation 7.107 gives $b = -\frac{4}{\sqrt{3}}\sqrt{ac}$. Thus, we have the following, for fixed $a > 0$:

$$\begin{aligned} b > -2\sqrt{ac} \quad &: \quad \text{1 real root } m = 0 \\ -2\sqrt{ac} > b > -\tfrac{4}{\sqrt{3}}\sqrt{ac} \quad &: \quad \text{5 real roots; minimum at } m = 0 \\ -\tfrac{4}{\sqrt{3}}\sqrt{ac} > b \quad &: \quad \text{5 real roots; minima at } m = \pm\sqrt{-\frac{b}{2c} + \sqrt{\Big(\frac{b}{2c}\Big)^2 - \frac{a}{c}}} \end{aligned} \tag{7.111}$$

The point $(a, b) = (0, 0)$, which lies at the confluence of a first order line and a second order line, is known as a *tricritical point*.

7.5.5 Hysteresis for the sextic potential

Once again, we consider the dissipative dynamics $\dot{m} = -\Gamma f'(m)$. We adimensionalize by writing

$$m \equiv \sqrt{\frac{|b|}{c}} \cdot u \quad , \quad a \equiv \frac{b^2}{c} \cdot r \quad , \quad t \equiv \frac{c}{\Gamma b^2} \cdot s \quad . \tag{7.112}$$

Then we obtain once again the dimensionless equation $du/ds = -\partial\varphi/\partial u$, where

$$\varphi(u) = \tfrac{1}{2}ru^2 \pm \tfrac{1}{4}u^4 + \tfrac{1}{6}u^6 \quad . \tag{7.113}$$

Once again, as in the case of the cubic Landau theory examined in §7.5.2, there is a single control parameter, which here is given by $r = ac/b^2$, but there are two distinct sub-cases to consider. In eqn. 7.113, the coefficient of the quartic term is positive if $b > 0$ and negative if $b < 0$. That is, the coefficient is $\mathrm{sgn}(b)$. When $b > 0$ we can ignore the sextic term for sufficiently small u, and we recover the quartic free energy studied earlier. There is then a second order transition at $r = 0$. The free energy curves for various values of r are plotted in fig. 7.17.

New and interesting behavior occurs for $b > 0$. The fixed points of the dynamics are obtained by setting $\varphi'(u) = 0$. We have

$$\varphi(u) = \tfrac{1}{2}ru^2 - \tfrac{1}{4}u^4 + \tfrac{1}{6}u^6 \qquad , \qquad \varphi'(u) = u\,(r - u^2 + u^4) \quad . \tag{7.114}$$

Thus, the equation $\varphi'(u) = 0$ factorizes into a linear factor u and a quartic factor $u^4 - u^2 + r$ which is quadratic in u^2. Thus, we can easily obtain the roots:

$$\begin{aligned} r < 0 \quad &: \quad u^* = 0 \quad , \; u^* = \pm\sqrt{\tfrac{1}{2} + \sqrt{\tfrac{1}{4} - r}} \\ 0 < r < \tfrac{1}{4} \quad &: \quad u^* = 0 \quad , \; u^* = \pm\sqrt{\tfrac{1}{2} + \sqrt{\tfrac{1}{4} - r}} \quad , \; u^* = \pm\sqrt{\tfrac{1}{2} - \sqrt{\tfrac{1}{4} - r}} \\ r > \tfrac{1}{4} \quad &: \quad u^* = 0 \quad . \end{aligned} \tag{7.115}$$

In fig. 7.18, we plot the fixed points and the hysteresis loops for this system. At $r = \frac{1}{4}$, there are two symmetrically located saddle-node bifurcations at $u = \pm\frac{1}{\sqrt{2}}$. We find $\varphi(u = \pm\frac{1}{\sqrt{2}}, r = \frac{1}{4}) = \frac{1}{48}$, which is positive, indicating that the stable fixed point $u^* = 0$ remains the thermodynamic minimum for the free energy $\varphi(u)$ as r is decreased through $r = \frac{1}{4}$. Setting $\varphi(u) = 0$ and $\varphi'(u) = 0$ simultaneously, we obtain $r = \frac{3}{16}$ and $u = \pm\frac{\sqrt{3}}{2}$. The thermodynamic value for u therefore jumps discontinuously from $u = 0$ to $u = \pm\frac{\sqrt{3}}{2}$ (either branch) at $r = \frac{3}{16}$; this is a first order transition.

Under the dissipative dynamics considered here, the system exhibits hysteresis, as indicated in the figure, where the arrows show the evolution of $u(s)$ for very slowly varying $r(s)$. When the control parameter r is large and positive, the flow is toward the sole fixed point at $u^* = 0$. At $r = \frac{1}{4}$, two simultaneous saddle-node bifurcations take place at $u^* = \pm\frac{1}{\sqrt{2}}$; the outer branch is stable and the inner branch unstable in both cases. At $r = 0$ there is a subcritical pitchfork bifurcation, and the fixed point at $u^* = 0$ becomes unstable.

Suppose one starts off with $r \gg \frac{1}{4}$ with some value $u > 0$. The flow $\dot{u} = -\varphi'(u)$ then rapidly results in $u \to 0^+$. This is the 'high temperature phase' in which there is no magnetization. Now let r increase slowly, using s as the dimensionless time variable. The scaled magnetization $u(s) = u^*\big(r(s)\big)$ will remain pinned at the fixed point $u^* = 0^+$. As r passes through $r = \frac{1}{4}$, two new stable values of u^* appear, but our system remains at $u = 0^+$, since $u^* = 0$ is a stable fixed point. But after the subcritical pitchfork, $u^* = 0$ becomes unstable. The magnetization $u(s)$ then flows rapidly to the stable fixed point at $u^* = \frac{1}{\sqrt{2}}$, and follows the curve $u^*(r) = \sqrt{\frac{1}{2} + (\frac{1}{4} - r)^{1/2}}$ for all $r < 0$.

Now suppose we start increasing r (*i.e.* increasing temperature). The magnetization follows the stable fixed point $u^*(r) = \sqrt{\frac{1}{2} + (\frac{1}{4} - r)^{1/2}}$ past $r = 0$, beyond the first order phase transition point at $r = \frac{3}{16}$, and all the way up to $r = \frac{1}{4}$, at which point this fixed point is annihilated at a saddle-node bifurcation. The flow then rapidly takes $u \to u^* = 0^+$, where it remains as r continues to be increased further. Within the region $r \in \big[0, \frac{1}{4}\big]$ of control parameter space, the dynamics are said to be *irreversible* and the behavior of $u(s)$ is said to be *hysteretic*.

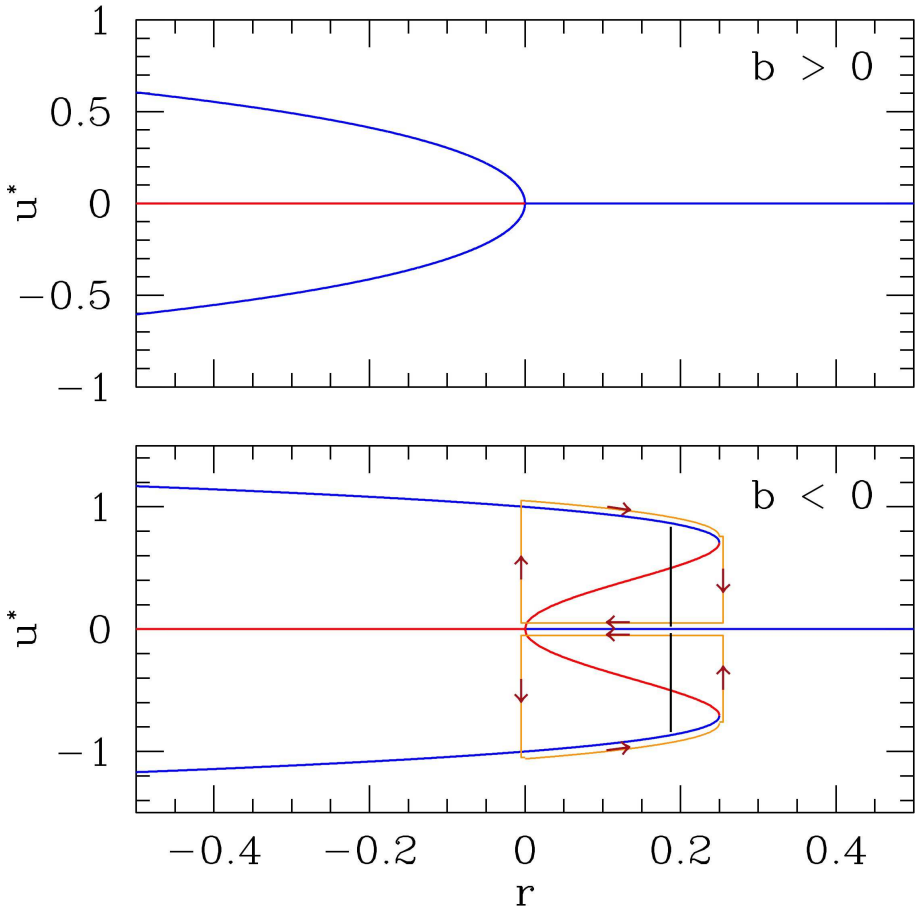

Figure 7.18: Fixed points branches $\varphi'(u^*) = 0$ for the sextic potential $\varphi(u) = \frac{1}{2}ru^2 + \frac{\sigma}{4}u^4 + \frac{1}{6}u^6$ with $\sigma = \mathrm{sgn}(b)$ (top for $\sigma = +1$, bottom for $\sigma = -1$). Blue curves indicate stable branches and red unstable branches under the dynamics $\dot{u} = -\varphi'(u)$. For $b > 0$ there is a supercritical pitchfork bifurcation at $(0, 0)$ and no hysteresis. For $b > 0$ there is a subcritical pitchfork bifurcation at $(0, 0)$ and two saddle-node bifurcations at $(\frac{1}{4}, \pm\frac{1}{\sqrt{2}})$. Solid curves show stable fixed points and dashed curves show unstable fixed points. The thick solid black segment indicates the order parameter discontinuity in u at the thermodynamic first order phase transition. Note the overall $u \to -u$ symmetry. Within the region $r \in [0, \frac{1}{4}]$ the dynamics are irreversible and the system exhibits the phenomenon of hysteresis. There is a first order phase transition at $r = \frac{3}{16}$, indicated by the thick black line segment which shows the discontinuous jump of the order parameter u at the transition.

7.6 Variational Density Matrix Method

7.6.1 The variational principle

Suppose we are given a Hamiltonian $\hat{H}$. From this we construct the free energy, F:

$$F = E - TS = \mathrm{Tr}\,(\varrho\,\hat{H}) + k_{\mathrm{B}}T\,\mathrm{Tr}\,(\varrho\,\log\varrho) \quad . \tag{7.116}$$

Here, ϱ is the *density matrix*[24]. A physical density matrix must be (i) normalized (*i.e.* $\mathrm{Tr}\,\varrho = 1$), (ii) Hermitian, and (iii) non-negative definite (*i.e.* all the eigenvalues of ϱ must be non-negative).

Our goal is to extremize the free energy subject to the various constraints on ϱ. Let us assume that ϱ is diagonal in the basis of eigenstates of $\hat{H}$, *i.e.*

$$\varrho = \sum_\gamma P_\gamma \, |\,\gamma\,\rangle\langle\,\gamma\,| \quad , \tag{7.117}$$

where P_γ is the probability that the system is in state $\big|\,\gamma\,\big\rangle$. Then

$$F = \sum_\gamma E_\gamma \, P_\gamma + k_{\rm B}T \sum_\gamma P_\gamma \log P_\gamma \quad . \tag{7.118}$$

Thus, the free energy is a function of the set $\{P_\gamma\}$. We now extremize F subject to the normalization constraint. This means we form the extended function

$$F^*\big(\{P_\gamma\},\lambda\big) = F\big(\{P_\gamma\}\big) + \lambda\Big(\sum_\gamma P_\gamma - 1\Big) \quad , \tag{7.119}$$

and then freely extremize over both the probabilities $\{P_\gamma\}$ as well as the Lagrange multiplier λ. This yields the Boltzmann distribution,

$$P_\gamma^{\rm eq} = \frac{1}{Z}\,\exp(-E_\gamma/k_{\rm B}T) \quad , \tag{7.120}$$

where $Z = \sum_\gamma e^{-E_\gamma/k_{\rm B}T} = \mathrm{Tr}\, e^{-\hat{H}/k_{\rm B}T}$ is the canonical partition function, which is related to λ through

$$\lambda = k_{\rm B}T\,(\log Z - 1) \quad . \tag{7.121}$$

Note that the Boltzmann weights are, appropriately, all positive.

If the spectrum of $\hat{H}$ is bounded from below, our extremum should in fact yield a minimum for the free energy F. Furthermore, since we have freely minimized over all the probabilities, subject to the single normalization constraint, *any distribution $\{P_\gamma\}$ other than the equilibrium one must yield a greater value of F.*

Alas, the Boltzmann distribution, while exact, is often intractable to evaluate. For one-dimensional systems, there are general methods such as the transfer matrix approach which do permit an exact evaluation of the free energy. However, beyond one dimension the situation is in general hopeless. A family of solvable ("integrable") models exists in two dimensions, but their solutions require specialized techniques and are extremely difficult. The idea behind the variational density matrix approximation is to construct a tractable *trial* density matrix ϱ which depends on a set of variational parameters $\{x_\alpha\}$, and to minimize F with respect to this set.

[24]How do we take the logarithm of a matrix? The rule is this: $A = \log B$ if $B = \exp(A)$. The exponential of a matrix may be evaluated via its Taylor expansion.

7.6.2 Variational density matrix for the Ising model

Consider once again the Ising model Hamiltonian,

$$\hat{H} = -\frac{1}{2}\sum_{i,j=1}^{N} J_{ij}\,\sigma_i\,\sigma_j - H\sum_{i=1}^{N}\sigma_i \quad . \tag{7.122}$$

The states of the system $|\boldsymbol{\sigma}\rangle$ may be labeled by the values of the spin variables: $|\boldsymbol{\sigma}\rangle = |\sigma_1, \sigma_2, \ldots, \sigma_N\rangle$. We assume the density matrix is diagonal in this basis, *i.e.*

$$\varrho_N(\boldsymbol{\sigma}\,|\,\boldsymbol{\sigma}') \equiv \varrho_N(\boldsymbol{\sigma})\,\delta_{\boldsymbol{\sigma},\boldsymbol{\sigma}'} \quad , \tag{7.123}$$

where $\delta_{\boldsymbol{\sigma},\boldsymbol{\sigma}'} = \prod_{i=1}^{N}\delta_{\sigma_i,\sigma_i'}$ and where N is the number of sites. Indeed, this is the case for the exact density matrix, which is to say the Boltzmann weight, $\varrho_N(\boldsymbol{\sigma}) = Z_N^{-1}e^{-\beta\hat{H}(\boldsymbol{\sigma})}$.

We now write a *trial density matrix* which is a product over contributions from independent single sites:

$$\varrho_N(\boldsymbol{\sigma}) = \prod_{i=1}^{N}\varrho(\sigma_i) \quad , \tag{7.124}$$

where

$$\varrho(\sigma) = \Big(\frac{1+m}{2}\Big)\,\delta_{\sigma,1} + \Big(\frac{1-m}{2}\Big)\,\delta_{\sigma,-1} \quad . \tag{7.125}$$

Note that we've changed our notation slightly. We are denoting by $\varrho(\sigma)$ the corresponding diagonal element of the matrix

$$\varrho = \frac{1}{2}\begin{pmatrix} 1+m & 0 \\ 0 & 1-m \end{pmatrix} \quad , \tag{7.126}$$

and the full density matrix is a tensor product over the single site matrices: $\varrho_N = \varrho\otimes\varrho\otimes\cdots\otimes\varrho$. Note also that ϱ and ϱ_N are normalized with unit trace.

Note that ϱ and hence ϱ_N are appropriately normalized. The variational parameter here is m, which, if ρ is to be non-negative definite, must satisfy $-1 \le m \le 1$. The quantity m has the physical interpretation of the average spin on any given site, since

$$\langle\sigma_i\rangle = \sum_{\sigma}\varrho(\sigma)\,\sigma = m. \tag{7.127}$$

We may now evaluate the average energy:

$$\begin{aligned} E = \mathsf{Tr}\,(\varrho_N\hat{H}) &= -\sum_{i<j} J_{ij}\,m^2 - H\sum_i m \\ &= -\tfrac{1}{2}N\hat{J}(0)\,m^2 - NHm \quad , \end{aligned} \tag{7.128}$$

where once again $\hat{J}(0)$ is the discrete Fourier transform of $J(\boldsymbol{R})$ at wavevector $\boldsymbol{q} = 0$. The entropy is given by

$$\begin{aligned} S &= -k_{\rm B}\,\mathsf{Tr}\,(\varrho_N\log\varrho_N) = -Nk_{\rm B}\,\mathsf{Tr}\,(\varrho\log\varrho) \\ &= -Nk_{\rm B}\Big\{\Big(\frac{1+m}{2}\Big)\log\Big(\frac{1+m}{2}\Big) + \Big(\frac{1-m}{2}\Big)\log\Big(\frac{1-m}{2}\Big)\Big\} \quad . \end{aligned} \tag{7.129}$$

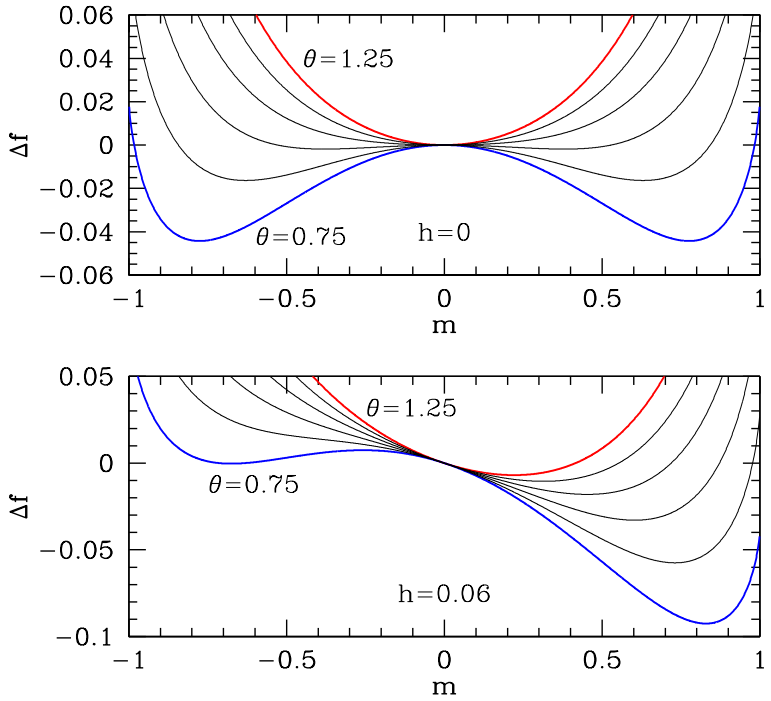

Figure 7.19: Variational field free energy $\Delta f = f(m,\theta,h) + \theta\,\log 2$ *versus* magnetization m at six equally spaced temperatures interpolating between 'high' ($\theta = 1.25$, red) and 'low' ($\theta = 0.75$, blue) values. Top panel: $h = 0$. Bottom panel: $h = 0.06$.

We now define the dimensionless free energy per site: $f \equiv F/N\hat{J}(0)$. We have

$$f(m,\theta,h) = -\tfrac{1}{2}\,m^2 - hm + \theta\left\{\left(\frac{1+m}{2}\right)\log\left(\frac{1+m}{2}\right) + \left(\frac{1-m}{2}\right)\log\left(\frac{1-m}{2}\right)\right\} \quad , \tag{7.130}$$

where $\theta \equiv k_{\rm B}T/\hat{J}(0)$ is the dimensionless temperature, and $h \equiv H/\hat{J}(0)$ the dimensionless magnetic field, as before. We extremize $f(m)$ by setting

$$\frac{\partial f}{\partial m} = 0 = -m - h + \frac{\theta}{2}\log\left(\frac{1+m}{1-m}\right) \quad . \tag{7.131}$$

Solving for m, we obtain

$$m = \tanh\left(\frac{m+h}{\theta}\right) \quad , \tag{7.132}$$

which is precisely what we found in eqn. 7.55. There is a second order phase transition at a critical temperature $\theta_{\rm c} = 1$.

Note that the optimal value of m indeed satisfies the requirement $|m| \le 1$ of non-negative probability. This nonlinear equation may be solved graphically. For $h = 0$, the unmagnetized solution $m = 0$ always applies. However, for $\theta < 1$ there are two additional solutions at $m = \pm m_{\rm A}(\theta)$, with $m_{\rm A}(\theta) = \sqrt{3(1-\theta)} + \mathcal{O}\big((1-\theta)^{3/2}\big)$ for t close to (but less than) one. These solutions, which are related by the $\mathbb{Z}_2$ symmetry of the $h = 0$ model, are in fact the low energy solutions. This is shown clearly in figure

7.19, where the variational free energy $f(m,\theta)$ is plotted as a function of m for a range of temperatures interpolating between 'high' and 'low' values. At the *critical temperature* $\theta_{\rm c} = 1$, the lowest energy state changes from being unmagnetized (high temperature) to magnetized (low temperature).

For $h > 0$, there is no longer a $\mathbb{Z}_2$ symmetry (*i.e.* $\sigma_i \to -\sigma_i \;\forall\; i$). The high temperature solution now has $m > 0$ (or $m < 0$ if $h < 0$), and this smoothly varies as t is lowered, approaching the completely polarized limit $m = 1$ as $\theta \to 0$. At very high temperatures, the argument of the $\tanh$ function is small, and we may approximate $\tanh(x) \simeq x$, in which case

$$m(h,\theta) = \frac{h}{\theta - \theta_{\rm c}} \quad . \tag{7.133}$$

This is called the *Curie-Weiss law.* One can infer $\theta_{\rm c}$ from the high temperature susceptibility $\chi(\theta) = (\partial m/\partial h)_{h=0}$ by plotting χ^{-1} *versus* θ and extrapolating to obtain the θ-intercept. In our case, $\chi(\theta) = (\theta - \theta_{\rm c})^{-1}$. For low θ and weak h, there are two inequivalent minima in the free energy.

When m is small, it is appropriate to expand $f(m,\theta,h)$, obtaining

$$f(m,\theta,h) = -\theta\,\log 2 - hm + \tfrac{1}{2}\,(\theta - 1)\,m^2 + \tfrac{\theta}{12}\,m^4 + \tfrac{\theta}{30}\,m^6 + \tfrac{\theta}{56}\,m^8 + \ldots \quad . \tag{7.134}$$

This is known as the *Landau expansion* of the free energy in terms of the *order parameter* m. An order parameter is a thermodynamic variable ϕ which distinguishes ordered and disordered phases. Typically $\phi = 0$ in the disordered (high temperature) phase, and $\phi \neq 0$ in the ordered (low temperature) phase. When the order sets in continuously, *i.e.* when ϕ is continuous across $\theta_{\rm c}$, the phase transition is said to be *second order.* When ϕ changes abruptly, the transition is *first order.* It is also quite commonplace to observe phase transitions between two ordered states. For example, a crystal, which is an ordered state, may change its lattice structure, say from a high temperature tetragonal phase to a low temperature orthorhombic phase. When the high T phase possesses the same symmetries as the low T phase, as in the tetragonal-to-orthorhombic example, the transition may be second order. When the two symmetries are completely unrelated, for example in a hexagonal-to-tetragonal transition, or in a transition between a ferromagnet and an antiferromagnet, the transition is in general first order.

Throughout this discussion, we have assumed that the interactions J_{ij} are predominantly *ferromagnetic*, *i.e.* $J_{ij} > 0$, so that all the spins prefer to align. When $J_{ij} < 0$, the interaction is said to be *antiferromagnetic* and prefers anti-alignment of the spins (*i.e.* $\sigma_i\,\sigma_j = -1$). Clearly not every pair of spins can be anti-aligned – there are two possible spin states and a thermodynamically extensive number of spins. But on the square lattice, for example, if the only interactions J_{ij} are between nearest neighbors and the interactions are antiferromagnetic, then the lowest energy configuration ($T = 0$ ground state) will be one in which spins on opposite sublattices are anti-aligned. The square lattice is *bipartite* – it breaks up into two interpenetrating sublattices A and B (which are themselves square lattices, rotated by 45° with respect to the original, and with a larger lattice constant by a factor of $\sqrt{2}$), such that any site in A has nearest neighbors in B, and *vice versa*. The honeycomb lattice is another example of a bipartite lattice. So is the simple cubic lattice. The triangular lattice, however, is not bipartite (it is *tripartite*). Consequently, with nearest neighbor antiferromagnetic interactions, the triangular lattice Ising model is highly *frustrated*. The moral of the story is this: antiferromagnetic interactions can give rise to complicated magnetic ordering, and, when frustrated by the lattice geometry, may have finite specific entropy even at $T = 0$.

7.6.3 q-state Potts model

The Hamiltonian for the Potts model is

$$\hat{H} = -\frac{1}{2}\sum_{i,j=1}^{N} J_{ij}\,\delta_{\sigma_i,\sigma_j} - H\sum_{i=1}^{N}\delta_{\sigma_i,1} \quad . \tag{7.135}$$

Here, $\sigma_i \in \{1,\ldots,q\}$, with integer q. This is the so-called 'q-state Potts model'. The quantity H is analogous to an external magnetic field, and preferentially aligns (for $H > 0$) the local spins in the $\sigma = 1$ direction. We will assume $H \geq 0$.

The q-component set is conveniently taken to be the set $\{1,\ldots,q\}$, but it could be anything, such as

$$\sigma_i \in \{\text{tomato, penny, ostrich, Grateful Dead ticket from 1987, } \ldots\} \quad . \tag{7.136}$$

The interaction energy is $-J_{ij}$ if sites i and j contain the same object (q possibilities), and 0 if i and j contain different objects ($q^2 - q$ possibilities).

The two-state Potts model is equivalent to the Ising model. Let the allowed values of σ be ± 1. Then the quantity

$$\delta_{\sigma,\sigma'} = \tfrac{1}{2} + \tfrac{1}{2}\,\sigma\sigma' \tag{7.137}$$

equals 1 if $\sigma = \sigma'$, and is zero otherwise. The three-state Potts model cannot be written as a simple three-state Ising model, *i.e.* one with a bilinear interaction $\sigma\,\sigma'$ where $\sigma \in \{-1, 0, +1\}$. However, it is straightforward to verify the identity

$$\delta_{\sigma,\sigma'} = 1 + \tfrac{1}{2}\,\sigma\sigma' + \tfrac{3}{2}\,\sigma^2\sigma'^2 - (\sigma^2 + \sigma'^2) \quad . \tag{7.138}$$

Thus, the $q = 3$-state Potts model is equivalent to a $S = 1$ (three-state) Ising model which includes both bilinear ($\sigma\sigma'$) and biquadratic ($\sigma^2\sigma'^2$) interactions, as well as a local field term which couples to the square of the spin, σ^2. In general one can find such correspondences for higher q Potts models, but, as should be expected, the interactions become increasingly complex, with bi-cubic, bi-quartic, bi-quintic, *etc.* terms. Such a formulation, however, obscures the beautiful S_q symmetry inherent in the model, where S_q is the permutation group on q symbols, which has $q!$ elements.

Getting back to the mean field theory, we write the single site variational density matrix ϱ as a diagonal matrix with entries

$$\varrho(\sigma) = x\,\delta_{\sigma,1} + \left(\frac{1-x}{q-1}\right)\left(1 - \delta_{\sigma,1}\right) \quad , \tag{7.139}$$

with $\varrho_N(\sigma_1,\ldots,\sigma_N) = \varrho(\sigma_1)\cdots\varrho(\sigma_N)$. Note that $\mathsf{Tr}\,(\varrho) = 1$. The variational parameter is x. When $x = q^{-1}$, all states are equally probable. But for $x > q^{-1}$, the state $\sigma = 1$ is preferred, and the other $(q-1)$ states have identical but smaller probabilities. It is a simple matter to compute the energy and entropy:

$$\begin{aligned} E &= \mathsf{Tr}\,(\varrho_N \hat{H}) = -\tfrac{1}{2}N\hat{J}(0)\left\{x^2 + \frac{(1-x)^2}{q-1}\right\} - NHx \\ S &= -k_{\rm B}\,\mathsf{Tr}\,(\varrho_N \log \varrho_N) = -Nk_{\rm B}\left\{x\log x + (1-x)\log\left(\frac{1-x}{q-1}\right)\right\} \quad . \end{aligned} \tag{7.140}$$

The dimensionless free energy per site is then

$$f(x,\theta,h) = -\tfrac{1}{2}\left\{x^2 + \frac{(1-x)^2}{q-1}\right\} + \theta\left\{x\log x + (1-x)\log\left(\frac{1-x}{q-1}\right)\right\} - hx \quad , \tag{7.141}$$

where $\theta = k_{\rm B}T/\hat{J}(0)$ and $h = H/\hat{J}(0)$. We now extremize with respect to x to obtain the mean field equation,

$$\frac{\partial f}{\partial x} = 0 = -x + \frac{1-x}{q-1} + \theta\,\log x - \theta\,\log\left(\frac{1-x}{q-1}\right) - h \quad . \tag{7.142}$$

For reference, the second derivative of f with respect to x is given by

$$\frac{\partial^2 f}{\partial x^2} = -\frac{q}{q-1} + \frac{\theta}{x(1-x)} \quad , \tag{7.143}$$

and solving for $f''(x) = 0$, we obtain

$$x_\pm = \frac{1}{2} \pm \frac{1}{2}\sqrt{1 - \frac{\theta}{\theta_0}} \qquad , \qquad \theta_0 = \frac{q}{4(q-1)} \quad . \tag{7.144}$$

Note that when $h = 0$, $x = q^{-1}$ is a solution to $f'(x) = 0$, corresponding to a S_q-symmetric disordered state in which all states are equally probable. At high temperatures, for small h, we expect $x - q^{-1} \propto h$. Using `Mathematica`, one can set $x \equiv q^{-1} + u$ and expand the mean field equation in powers of u. One obtains

$$h = \frac{q\,(q\theta - 1)}{q-1}\,u + \frac{q^3\,(q-2)\,\theta}{2\,(q-1)^2}\,u^2 + \mathcal{O}(u^3) \quad . \tag{7.145}$$

For weak fields, $|h| \ll 1$, and in the high temperature phase we have

$$u(\theta) = \frac{(q-1)\,h}{q\,(q\theta - 1)} + \mathcal{O}(h^2) \quad , \tag{7.146}$$

which again is of the Curie-Weiss form, with a Curie temperature $\theta_{\rm C} = q^{-1}$. The difference $u = x - q^{-1}$ is the order parameter for the transition. However, for $q > 2$ we expect the transition to be first order, which we can see by expanding the free energy in powers of u, obtaining the Landau expansion. Expressed in terms of the order parameter u (rather than $x = q^{-1} + u$), the free energy $f(u,\theta,h)$ is

$$f(u,\theta,h) = f_0 - \frac{qu^2}{2(q-1)} - hu + \theta\,(q^{-1}+u)\log(1+qu) - \theta\,(1-q^{-1}-u)\log\left(1 - \frac{qu}{q-1}\right) \quad , \tag{7.147}$$

with $f_0 = -\theta\log q - (h + \frac{1}{2})\,q^{-1}$; note that $f(u=0,\theta,h) = f_0$. Expanding in powers of u, we find

$$\begin{aligned} f(u,\theta,h) = f_0 - hu + \frac{q^2\,(\theta - q^{-1})}{2\,(q-1)}\,u^2 - \frac{(q-2)\,q^3\,\theta}{6\,(q-1)^2}\,u^3 \\ + \frac{q^3\theta}{12}\Big[1 + (q-1)^{-3}\Big]u^4 - \frac{q^4\theta}{20}\Big[1 - (q-1)^{-4}\Big]u^5 + \frac{q^5\theta}{30}\Big[1 + (q-1)^{-5}\Big]u^6 + \ldots \quad . \end{aligned} \tag{7.148}$$

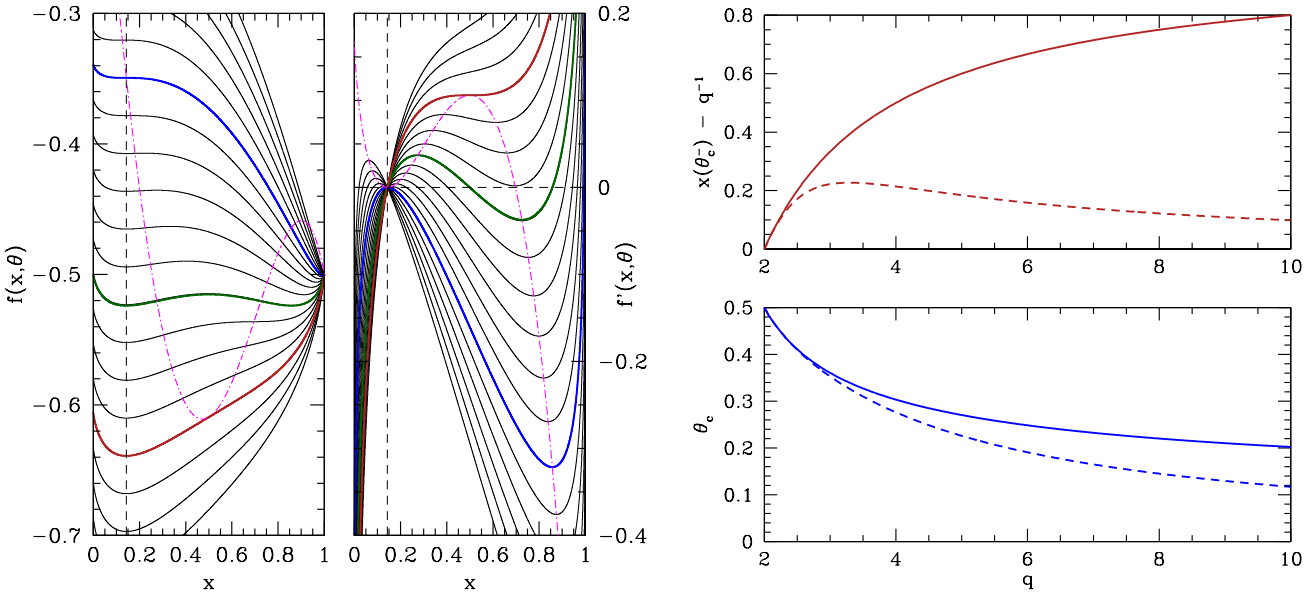

Figure 7.20: The left panels show the variational free energy $f(x,\theta)$ of the $q = 7$ state Potts model and its $x-$derivative $f'(x,\theta)$ *versus* the variational parameter x, for a set of equally spaced temperatures. The vertical dashed black line is at $x = q^{-1} = \frac{1}{7}$. The dot-dash magenta curve in both cases is the locus of points for which the second derivative $f''(x,\theta)$ with respect to x vanishes. Three characteristic temperatures are marked: (i) $\theta = q^{-1}$ (blue), where the coefficient of the quadratic term in the Landau expansion changes sign, (ii) $\theta = \theta_0$ (red), where there is a saddle-node bifurcation and above which the free energy has only one minimum at $x = q^{-1}$ (symmetric phase), and (iii) $\theta = \theta_c$ (green), where the first order transition occurs. The right panels show comparisons of the order parameter jump at θ_c (top) and critical temperature θ_c (bottom) *versus* q for untruncated (solid lines) and truncated (dashed lines) expansions of the mean field free energy. Note the agreement as $q \to 2$, where the jump is small and a truncated expansion is then valid.

Note that, for $q = 2$, the coefficients of u^3, u^5, and higher order odd powers of u vanish in the Landau expansion. This is consistent with what we found for the Ising model, and is related to the $\mathbb{Z}_2$ symmetry of that model. For $q > 3$, there is a cubic term in the mean field free energy, and thus we generically expect a first order transition, as we found in §7.5.2. It is important to understand that while the mean field theory which yields the free energy function $f(u,\theta,h)$ is an approximation to a full interacting theory for which no analytic solutions may exist, truncating the MF free energy to yield a low-order polynomial in u and h, *i.e.* a Landau free energy, constitutes a further approximation to the mean field theory itself. In particular, if at $h = 0$ we include only terms in $f(u,\theta)$ up to fourth order in u, we will obtain a free energy of the form $f(u) = \frac{1}{2}au^2 - \frac{1}{3}yu^3 + \frac{1}{4}bu^4$, where $\{a, y, b\}$ may be read off from eqn. 7.148. We found earlier that such a free energy results in a first order transition at $a = 2y^2/9b$. One can thusly compute expressions for the critical temperature $\theta_c^{\rm L}$ and order parameter discontinuity $u(\theta_c^{\rm L-})$ as functions of q, but these will not be the same as what one obtains by working with the untruncated mean field free energy. For $q = 2$ there is a $\mathbb{Z}_2$ symmetry and our Potts model mean field theory predicts a second order transition at $\theta_c = \frac{1}{2}$.[25] For $q > 2$, the mean field critical point is obtained by simultaneously solving the equations $f'(u) = 0$ and $f(0) = f(u)$, both at $h = 0$. These are two equations for the two unknowns u_c and θ_c, with $u_c > 0$ the value of the order parameter just inside the ordered phase. This

[25] In §7.6.2 we found $\theta_c = 1$ for the Ising model. So why do we find $\theta_c = \frac{1}{2}$ for the $q = 2$ Potts model?

can be done numerically, but there is an analytic solution (see fig. 7.20):

$$\theta_{\rm c} = \frac{q-2}{2(q-1)\log(q-1)} \qquad , \qquad u_{\rm c} = u(\theta_{\rm c}^-) = 1 - \frac{2}{q} \quad . \tag{7.149}$$

In fig. 7.20 we plot the mean field free energy $f(x,\theta)$ and its x-derivative $f'(x,\theta)$ *versus* x for an equally spaced set of temperatures. Also plotted are the critical temperature $\theta_{\rm c}$ and the order parameter discontinuity $u(\theta_{\rm c}^-)$ *versus* q for the q-state Potts model MFT. For comparison, $\theta_{\rm c}$ and $u(\theta_{\rm c}^-)$ are also plotted for the truncated quartic free energy Landau theory.

7.6.4 XY Model

Variational density matrix

Consider the so-called XY model, in which each site contains a continuous planar spin, represented by an angular variable $\phi_i \in [-\pi, \pi]$:

$$\hat{H} = -\frac{1}{2}\sum_{i\neq j}^{N} J_{ij}\cos\big(\phi_i - \phi_j\big) - H\sum_{i=1}^{N}\cos\phi_i \quad . \tag{7.150}$$

We write the (diagonal elements of the) full density matrix once again as a product:

$$\varrho_N(\boldsymbol{\phi}) = \prod_{i=1}^{N}\varrho(\phi_i) \quad . \tag{7.151}$$

Our goal will be to extremize the free energy with respect to the *function* $\varrho(\phi)$. To this end, we compute

$$E = \mathsf{Tr}\,(\varrho_N\,\hat{H}) = -\tfrac{1}{2}N\hat{J}(0)\,\Big|\mathsf{Tr}\,\big(\varrho\,e^{i\phi}\big)\Big|^2 - NH\,\mathsf{Tr}\,\big(\varrho\,\cos\phi\big) \quad . \tag{7.152}$$

The entropy is $S = -Nk_{\rm B}\,\mathsf{Tr}\,(\varrho\,\log\varrho)$. Note that for any function $A(\phi)$, we have[26]

$$\mathsf{Tr}\,\big(\varrho\,A\big) \equiv \int_{-\pi}^{\pi}\frac{d\phi}{2\pi}\,\varrho(\phi)\,A(\phi) \quad . \tag{7.153}$$

We now extremize the *functional* $F\big[\varrho(\phi)\big] = E - TS$ with respect to $\varrho(\phi)$, under the condition that $\mathsf{Tr}\;\varrho = 1$. We therefore use Lagrange's method of undetermined multipliers, writing

$$F^* = F - Nk_{\rm B}T\,\lambda\,\Big(\mathsf{Tr}\,\varrho - 1\Big) \quad . \tag{7.154}$$

[26]The denominator of 2π in the measure is not necessary, and in fact it is even slightly cumbersome. It divides out whenever we take a ratio to compute a thermodynamic average. I introduce this factor to preserve the relation $\mathsf{Tr}\;1 = 1$. I personally find unnormalized traces to be profoundly unsettling on purely aesthetic grounds.

Note that F^* is a *function* of the Lagrange multiplier λ and a *functional* of the density matrix $\varrho(\phi)$. The prefactor $Nk_{\rm B}T$ which multiplies λ is of no mathematical consequence – we could always redefine the multiplier to be $\lambda' \equiv Nk_{\rm B}T\lambda$. It is present only to maintain homogeneity and proper dimensionality of F^* with λ itself dimensionless and of order N^0. We now have

$$\frac{\delta F^*}{\delta\varrho(\phi)} = \frac{\delta}{\delta\varrho(\phi)}\Bigg\{ -\tfrac{1}{2}N\hat{J}(0)\,\Big|\mathsf{Tr}\big(\varrho\,e^{i\phi}\big)\Big|^2 - NH\,\mathsf{Tr}\big(\varrho\,\cos\phi\big) + Nk_{\rm B}T\;\mathsf{Tr}\,\big(\varrho\,\log\varrho\big) - Nk_{\rm B}T\,\lambda\,\Big(\,\mathsf{Tr}\,\varrho - 1\Big)\Bigg\} \quad . \tag{7.155}$$

To this end, we note that

$$\frac{\delta}{\delta\varrho(\phi)}\,\mathsf{Tr}\,(\varrho\,A) = \frac{\delta}{\delta\varrho(\phi)}\int\limits_{-\pi}^{\pi}\frac{d\phi}{2\pi}\,\varrho(\phi)\,A(\phi) = \frac{1}{2\pi}\,A(\phi) \quad . \tag{7.156}$$

Thus, we have

$$\frac{\delta\tilde{F}}{\delta\varrho(\phi)} = -\frac{N\hat{J}(0)}{4\pi}\left[\mathop{\mathsf{Tr}}_{\phi'}\big(\varrho\,e^{i\phi'}\big)\,e^{-i\phi} + \mathop{\mathsf{Tr}}_{\phi'}\big(\varrho\,e^{-i\phi'}\big)\,e^{i\phi}\right] - \frac{NH}{2\pi}\cos\phi + \frac{Nk_{\rm B}T}{2\pi}\Big[\,\log\varrho(\phi) + 1 - \lambda\Big] \quad . \tag{7.157}$$

Now let us define

$$\mathop{\mathsf{Tr}}_{\phi}\big(\varrho\,e^{i\phi}\big) = \int\limits_{-\pi}^{\pi}\frac{d\phi}{2\pi}\,\varrho(\phi)\,e^{i\phi} \equiv m\,e^{i\phi_0} \quad . \tag{7.158}$$

We then have

$$\log\varrho(\phi) = \frac{\hat{J}(0)}{k_{\rm B}T}\,m\,\cos(\phi-\phi_0) + \frac{H}{k_{\rm B}T}\,\cos\phi + \lambda - 1. \tag{7.159}$$

Clearly the free energy will be reduced if $\phi_0 = 0$ so that the mean field is maximal and aligns with the external field, which prefers $\phi = 0$. Thus, we conclude

$$\varrho(\phi) = \mathcal{C}\,\exp\!\left(\frac{H_{\rm eff}}{k_{\rm B}T}\,\cos\phi\right) \quad , \tag{7.160}$$

where $H_{\rm eff} = \hat{J}(0)\,m + H$ and $\mathcal{C} = e^{\lambda-1}$. The value of λ is then determined by invoking the constraint,

$$\mathsf{Tr}\,\varrho = 1 = \mathcal{C}\int\limits_{-\pi}^{\pi}\frac{d\phi}{2\pi}\,\exp\!\left(\frac{H_{\rm eff}}{k_{\rm B}T}\,\cos\phi\right) = \mathcal{C}\,I_0(H_{\rm eff}/k_{\rm B}T) \quad , \tag{7.161}$$

where $I_0(z)$ is the Bessel function. We are free to define $\varepsilon \equiv H_{\rm eff}/k_{\rm B}T$, and treat ε as our single variational parameter. We then have the normalized single site density matrix

$$\varrho(\phi) = \frac{\exp(\varepsilon\cos\phi)}{\int\limits_{-\pi}^{\pi}\frac{d\phi'}{2\pi}\,\exp(\varepsilon\cos\phi')} = \frac{\exp(\varepsilon\cos\phi)}{I_0(\varepsilon)} \quad . \tag{7.162}$$

We next compute the following averages:

$$\left\langle\, e^{\pm i\phi}\,\right\rangle = \int\limits_{-\pi}^{\pi} \frac{d\phi}{2\pi}\, \varrho(\phi)\, e^{\pm i\phi} = \frac{I_1(\varepsilon)}{I_0(\varepsilon)} \tag{7.163}$$

$$\left\langle \cos(\phi - \phi')\right\rangle = \mathsf{Re}\left\langle e^{i\phi}\, e^{-i\phi'}\right\rangle = \left(\frac{I_1(\varepsilon)}{I_0(\varepsilon)}\right)^2 \quad , \tag{7.164}$$

as well as

$$\mathsf{Tr}\,(\varrho\,\log\varrho) = \int\limits_{-\pi}^{\pi} \frac{d\phi}{2\pi}\, \frac{e^{\varepsilon\cos\phi}}{I_0(\varepsilon)} \Big\{ \varepsilon\cos\phi - \log I_0(\varepsilon)\Big\} = \varepsilon\,\frac{I_1(\varepsilon)}{I_0(\varepsilon)} - \log I_0(\varepsilon) \quad . \tag{7.165}$$

The dimensionless free energy per site is therefore

$$f(\varepsilon,\theta,h) = -\frac{1}{2}\left(\frac{I_1(\varepsilon)}{I_0(\varepsilon)}\right)^2 + (\theta\varepsilon - h)\,\frac{I_1(\varepsilon)}{I_0(\varepsilon)} - \theta\,\log I_0(\varepsilon) \quad , \tag{7.166}$$

with $\theta = k_{\rm B}T/\hat{J}(0)$ and $h = H/\hat{J}(0)$ and $f = F/N\hat{J}(0)$ as before. Note that the mean field equation is $m = \theta\varepsilon - h = \left\langle\, e^{i\phi}\,\right\rangle$, *i.e.*

$$\theta\varepsilon - h = \frac{I_1(\varepsilon)}{I_0(\varepsilon)} \quad . \tag{7.167}$$

For small ε, we may expand the Bessel functions, using

$$I_\nu(z) = (\tfrac{1}{2}z)^\nu \sum_{k=0}^{\infty} \frac{(\frac{1}{4}z^2)^k}{k!\,\Gamma(k+\nu+1)} \quad , \tag{7.168}$$

to obtain

$$f(\varepsilon,\theta,h) = \tfrac{1}{4}\left(\theta - \tfrac{1}{2}\right)\varepsilon^2 + \tfrac{1}{64}\left(2 - 3\theta\right)\varepsilon^4 - \tfrac{1}{2}\,h\varepsilon + \tfrac{1}{16}\,h\varepsilon^3 + \ldots \quad . \tag{7.169}$$

This predicts a second order phase transition at $\theta_{\rm c} = \frac{1}{2}$.[27] Note also the Curie-Weiss form of the susceptibility at high θ:

$$\frac{\partial f}{\partial\varepsilon} = 0 \quad\Longrightarrow\quad \varepsilon = \frac{h}{\theta - \theta_{\rm c}} + \ldots \quad . \tag{7.170}$$

Neglect of fluctuations method

Consider again the Hamiltonian of eqn. 7.150. Define $z_i \equiv \exp(i\phi_i)$ and write $z_i = w + \delta z_i$, where $w \equiv \langle z_i\rangle$ and $\delta z_i \equiv z_i - w$. Of course we also have the complex conjugate relations $z_i^* = w^* + \delta z_i^*$ and $w^* = \langle z_i^*\rangle$. Writing $\cos(\phi_i - \phi_j) = \mathsf{Re}\,(z_i^* z_j)$, by neglecting the terms proportional to $\delta z_i^*\,\delta z_j$ in $\hat{H}$ we arrive at the mean field Hamiltonian,

$$\hat{H}^{\rm MF} = \tfrac{1}{2}N\hat{J}(0)\,|w|^2 - \tfrac{1}{2}\hat{J}(0)\,|w| \sum_{i=1}^{N}\left(w^* z_i + w z_i^*\right) - \tfrac{1}{2}H\sum_{i=1}^{N}\left(z_i^* + z_i\right) \tag{7.171}$$

[27] Note that the coefficient of the quartic term in ε is negative for $\theta > \frac{2}{3}$. At $\theta = \theta_{\rm c} = \frac{1}{2}$, the coefficient is positive, but for larger θ one must include higher order terms in the Landau expansion.

It is clear that the free energy will be minimized if the mean field w breaks the $\mathsf{O}(2)$ symmetry in the same direction as the external field H, which means $w \in \mathbb{R}$ and

$$\hat{H}^{\rm MF} = \tfrac{1}{2} N \hat{J}(0)\,|w|^2 - \big(H + \hat{J}(0)\,|w|\big) \sum_{i=1}^{N} \cos\phi_i \quad . \tag{7.172}$$

The dimensionless free energy per site is then

$$f = \tfrac{1}{2}|w|^2 - \theta \log I_0\left(\frac{h+|w|}{\theta}\right) \quad . \tag{7.173}$$

Differentiating with respect to $|w|$, one obtains

$$|w| \equiv m = I_1\left(\frac{h+m}{\theta}\right) \Big/ I_0\left(\frac{h+m}{\theta}\right) \quad , \tag{7.174}$$

which is the same equation as eqn. 7.167. The two mean field theories yield the same results in every detail (see §**??**).

7.7 Mean Field Theory of Fluctuations

7.7.1 Correlation and response in mean field theory

We now consider the matter of correlation and response functions within mean field theory. A correlation function is a thermodynamic average of fields at various sites, such as $\langle \sigma_i \sigma_j \rangle$ (two-point correlation function), $\langle \sigma_i \sigma_j \sigma_k \sigma_l \rangle$ (four-point correlation function), *etc.* A response function describes the influence of external fields on thermodynamic averages, such as $\partial m_i / \partial H_j$, the variation of the local magnetization $m_i = \langle \sigma_i$ at site i due to the presence of a local field H_j at site j. We shall see that there is a direct relation between correlation and response functions.

Consider the Ising model,

$$\hat{H} = -\tfrac{1}{2} \sum_{i,j=1}^{N} J_{ij}\,\sigma_i\,\sigma_j - \sum_{i=1}^{N} H_i\,\sigma_k \quad , \tag{7.175}$$

where the local magnetic field on site k is now H_k. We assume without loss of generality that the diagonal terms vanish: $J_{ii} = 0$. Now consider the partition function $Z = \mathsf{Tr}\; e^{-\beta \hat{H}}$ as a function of the temperature T and the local field values $\{H_i\}$. We have

$$\begin{aligned} \frac{\partial Z}{\partial H_i} &= \beta\;\mathsf{Tr}\,\Big[\sigma_i\, e^{-\beta\hat{H}}\Big] = \beta Z\,\langle \sigma_i \rangle \\ \frac{\partial^2 Z}{\partial H_i\,\partial H_j} &= \beta^2\;\mathsf{Tr}\,\Big[\sigma_i\,\sigma_j\, e^{-\beta\hat{H}}\Big] = \beta^2 Z\,\langle \sigma_i\,\sigma_j \rangle \quad . \end{aligned} \tag{7.176}$$

Thus,

$$\begin{aligned} m_i &= -\frac{\partial F}{\partial H_i} = \langle \sigma_i \rangle \\ \chi_{ij} &= \frac{\partial m_i}{\partial H_j} = -\frac{\partial^2 F}{\partial H_i\,\partial H_j} = \frac{1}{k_{\rm B}T} \cdot \Big\{ \langle \sigma_i\,\sigma_j \rangle - \langle \sigma_i \rangle\,\langle \sigma_j \rangle \Big\} \quad . \end{aligned} \tag{7.177}$$

Expressions such as $\langle \sigma_i \rangle$, $\langle \sigma_i \, \sigma_j \rangle$, *etc.* are in general called *correlation functions*. For example, we define the *spin-spin correlation function* C_{ij} as

$$C_{ij} \equiv \langle \sigma_i \, \sigma_j \rangle - \langle \sigma_i \rangle \, \langle \sigma_j \rangle \quad . \tag{7.178}$$

Expressions such as $\partial F / \partial H_i$ and $\partial^2 F / \partial H_i \, \partial H_j$ are called *response functions*. The above relation between correlation functions and response functions, $C_{ij} = k_{\rm B} T \, \chi_{ij}$, is valid *only for the equilibrium distribution*. In particular, this relationship is *invalid* if one uses an approximate distribution, such as the variational density matrix formalism of mean field theory.

The question then arises: within mean field theory, which is more accurate – correlation functions or response functions? A simple argument suggests that the *response functions* are more accurate representations of the real physics. To see this, let's write the variational density matrix $\varrho^{\rm var}$ as the sum of the exact equilibrium (Boltzmann) distribution $\varrho^{\rm eq} = Z^{-1} \exp(-\beta \hat{H})$ plus a deviation $\delta\varrho$:

$$\varrho^{\rm var} = \varrho^{\rm eq} + \delta\varrho \quad . \tag{7.179}$$

Then if we calculate a correlator using the variational distribution, we have

$$\langle \sigma_i \, \sigma_j \rangle_{\rm var} = \mathsf{Tr} \left[\varrho^{\rm var} \, \sigma_i \, \sigma_j \right] = \mathsf{Tr} \left[\varrho^{\rm eq} \, \sigma_i \, \sigma_j \right] + \mathsf{Tr} \left[\delta\varrho \, \sigma_i \, \sigma_j \right] \quad . \tag{7.180}$$

Thus, the variational density matrix gets the correlator right to first order in $\delta\varrho$. On the other hand, the free energy is given by

$$F^{\rm var} = F^{\rm eq} + \sum_{\boldsymbol{\sigma}} \frac{\partial F}{\partial \varrho_{\boldsymbol{\sigma}}} \bigg|_{\varrho^{\rm eq}} \delta\varrho_{\boldsymbol{\sigma}} + \frac{1}{2} \sum_{\boldsymbol{\sigma}, \boldsymbol{\sigma}'} \frac{\partial^2 F}{\partial \varrho_{\boldsymbol{\sigma}} \partial \varrho_{\boldsymbol{\sigma}'}} \bigg|_{\varrho^{\rm eq}} \delta\varrho_{\boldsymbol{\sigma}} \, \delta\varrho_{\boldsymbol{\sigma}'} + \ldots \quad . \tag{7.181}$$

Here $\boldsymbol{\sigma}$ denotes a state of the system, *i.e.* $| \, \boldsymbol{\sigma} \, \rangle = | \, \sigma_1, \ldots, \sigma_N \, \rangle$, where every spin polarization is specified. Since the free energy is an extremum (and in fact an absolute minimum) with respect to the distribution, the second term on the RHS vanishes. This means that the free energy is accurate to second order in the deviation $\delta\varrho$.

7.7.2 Calculation of the response functions

Consider the variational density matrix $\varrho(\boldsymbol{\sigma}) = \prod_{i=1}^N \varrho_i(\sigma_i)$, where

$$\varrho_i(\sigma_i) = \left(\frac{1 + m_i}{2} \right) \delta_{\sigma_i, 1} + \left(\frac{1 - m_i}{2} \right) \delta_{\sigma_i, -1} \quad . \tag{7.182}$$

The variational energy $E = \mathsf{Tr} \, (\varrho \, \hat{H})$ is

$$E = -\tfrac{1}{2} \sum_{i,j=1^N} J_{ij} \, m_i \, m_j - \sum_{i=1}^N H_i \, m_i \tag{7.183}$$

and the entropy $S = -k_{\rm B} T \, \mathsf{Tr} \, (\varrho \log \varrho)$ is

$$S = -k_{\rm B} \sum_{i=1}^N \left\{ \left(\frac{1 + m_i}{2} \right) \log \left(\frac{1 + m_i}{2} \right) + \left(\frac{1 - m_i}{2} \right) \log \left(\frac{1 - m_i}{2} \right) \right\} \quad . \tag{7.184}$$

Setting the variation $\partial F/\partial m_i = 0$, with $F = E - TS$, we obtain the mean field equations,

$$m_i = \tanh\left(\beta J_{ij}\, m_j + \beta H_i\right) \quad , \tag{7.185}$$

where we use the summation convention: $J_{ij}\, m_j \equiv \sum_j J_{ij}\, m_j$. Suppose $T > T_{\rm c}$ and m_i is small. Then we can expand the RHS of the above mean field equations, obtaining

$$\left(\delta_{ij} - \beta J_{ij}\right) m_j = \beta H_i \quad . \tag{7.186}$$

Thus, the susceptibility tensor χ is the inverse of the matrix $(k_{\rm B}T\,\mathbb{1} - \mathbb{J})$:

$$\chi_{ij} = \frac{\partial m_i}{\partial H_j} = \left(k_{\rm B}T\,\mathbb{1} - \mathbb{J}\right)^{-1}_{ij} \quad , \tag{7.187}$$

where $\mathbb{1}$ is the identity. Note also that so-called *connected averages* of the kind in eqn. 7.178 vanish identically if we compute them using our variational density matrix, since all the sites are independent, hence

$$\langle \sigma_i\, \sigma_j \rangle = \mathsf{Tr}\left(\varrho^{\rm var}\, \sigma_i\, \sigma_j\right) = \mathsf{Tr}\left(\varrho_i^{\rm var}\, \sigma_i\right) \mathsf{Tr}\left(\varrho_j^{\rm var}\, \sigma_j\right) = \langle \sigma_i \rangle \langle \sigma_j \rangle \quad , \tag{7.188}$$

and therefore $\chi_{ij} = 0$ if we compute the correlation functions themselves from the variational density matrix, rather than from the free energy F. As we have argued above, the latter approximation is more accurate.

Assuming $J_{ij} = J(\boldsymbol{R}_i - \boldsymbol{R}_j)$, where $\boldsymbol{R}_i$ is a Bravais lattice site, we can Fourier transform the above equation, resulting in

$$\hat{m}(\boldsymbol{q}) = \frac{\hat{H}(\boldsymbol{q})}{k_{\rm B}T - \hat{J}(\boldsymbol{q})} \equiv \hat{\chi}(\boldsymbol{q})\, \hat{H}(\boldsymbol{q}) \quad . \tag{7.189}$$

Once again, our definition of lattice Fourier transform of a function $\phi(\boldsymbol{R})$ is

$$\hat{\phi}(\boldsymbol{q}) \equiv \sum_{\boldsymbol{R}} \phi(\boldsymbol{R})\, e^{-i\boldsymbol{q}\cdot\boldsymbol{R}} \qquad , \qquad \phi(\boldsymbol{R}) = \Omega \int\limits_{\hat{\Omega}} \frac{d^d q}{(2\pi)^d}\, \hat{\phi}(\boldsymbol{q})\, e^{i\boldsymbol{q}\cdot\boldsymbol{R}} \quad , \tag{7.190}$$

where Ω is the unit cell in real space, called the *Wigner-Seitz cell*, and $\hat{\Omega}$ is the first Brillouin zone, which is the unit cell in *reciprocal space*. Similarly, we have

$$\begin{aligned} \hat{J}(\boldsymbol{q}) &= \sum_{\boldsymbol{R}} J(\boldsymbol{R}) \Big(1 - i\boldsymbol{q}\cdot\boldsymbol{R} - \tfrac{1}{2}(\boldsymbol{q}\cdot\boldsymbol{R})^2 + \ldots\Big) \\ &= \hat{J}(0) \cdot \Big\{1 - q^2 R_*^2 + \mathcal{O}(q^4)\Big\} \quad , \end{aligned} \tag{7.191}$$

where

$$R_*^2 = \frac{\sum_{\boldsymbol{R}} \boldsymbol{R}^2 J(\boldsymbol{R})}{2d \sum_{\boldsymbol{R}} J(\boldsymbol{R})} \quad . \tag{7.192}$$

Here we have assumed inversion symmetry for the lattice, in which case

$$\sum_{\boldsymbol{R}} R^\mu R^\nu J(\boldsymbol{R}) = \frac{1}{d} \cdot \delta^{\mu\nu} \sum_{\boldsymbol{R}} \boldsymbol{R}^2 J(\boldsymbol{R}) \quad . \tag{7.193}$$

On cubic lattices with nearest neighbor interactions only, one has $R_* = a/\sqrt{2d}$, where a is the lattice constant and d is the dimension of space.

Thus, with the identification $k_{\rm B}T_{\rm c} = \hat{J}(0)$, we have

$$\hat{\chi}(\boldsymbol{q}) = \frac{1}{k_{\rm B}(T - T_{\rm c}) + k_{\rm B}T_{\rm c}\, R_*^2\, \boldsymbol{q}^2 + \mathcal{O}(q^4)} = \frac{1}{k_{\rm B}T_{\rm c}\, R_*^2} \cdot \frac{1}{\xi^{-2} + q^2 + \mathcal{O}(q^4)} \quad , \tag{7.194}$$

where

$$\xi(T) = R_* \cdot \left(\frac{T - T_{\rm c}}{T_{\rm c}}\right)^{-1/2} \tag{7.195}$$

is the *correlation length*. With the definition $\xi(T) \propto |T - T_{\rm c}|^{-\nu}$ as $T \to T_{\rm c}$, we obtain the mean field correlation length exponent $\nu = \frac{1}{2}$. The exact result for the two-dimensional Ising model is $\nu = 1$, whereas $\nu \approx 0.6$ for the $d = 3$ Ising model. Note that $\hat{\chi}(\boldsymbol{q} = 0, T)$ diverges as $(T - T_{\rm c})^{-1}$ for $T > T_{\rm c}$.

In real space, we have

$$m_i = \sum_j \chi_{ij}\, H_j \qquad , \qquad \chi_{ij} = \Omega \int\limits_{\hat{\Omega}} \frac{d^d q}{(2\pi)^d}\, \hat{\chi}(\boldsymbol{q})\, e^{i\boldsymbol{q}\cdot(\boldsymbol{R}_i - \boldsymbol{R}_j)} \quad . \tag{7.196}$$

Note that $\hat{\chi}(\boldsymbol{q})$ is properly periodic under $\boldsymbol{q} \to \boldsymbol{q} + \boldsymbol{G}$, where $\boldsymbol{G}$ is a reciprocal lattice vector, which satisfies $e^{i\boldsymbol{G}\cdot\boldsymbol{R}} = 1$ for any direct Bravais lattice vector $\boldsymbol{R}$. Indeed, we have

$$\hat{\chi}^{-1}(\boldsymbol{q}) = k_{\rm B}T - \hat{J}(\boldsymbol{q}) = k_{\rm B}T - J \sum_{\boldsymbol{\delta}} e^{i\boldsymbol{q}\cdot\boldsymbol{\delta}} \quad , \tag{7.197}$$

where $\boldsymbol{\delta}$ is a nearest neighbor separation vector, and where in the second line we have assumed nearest neighbor interactions only. On cubic lattices in d dimensions, there are $2d$ nearest neighbor separation vectors, $\boldsymbol{\delta} = \pm a\, \hat{\mathbf{e}}_\mu$, where $\mu \in \{1, \ldots, d\}$. The real space susceptibility is then

$$\chi(\boldsymbol{R}, H = 0) = \int\limits_{-\pi}^{\pi} \frac{d\theta_1}{2\pi} \cdots \int\limits_{-\pi}^{\pi} \frac{d\theta_d}{2\pi}\, \frac{e^{in_1\theta_1} \cdots e^{in_d\theta_d}}{k_{\rm B}T - (2J\cos\theta_1 + \ldots + 2J\cos\theta_d)} \quad , \tag{7.198}$$

where $\boldsymbol{R} = a\sum_{\mu=1}^d n_\mu\, \hat{\mathbf{e}}_\mu$ is a general direct lattice vector for the cubic Bravais lattice in d dimensions, and the $\{n_\mu\}$ are integers.

The long distance behavior was discussed in chapter 6 (see §6.5.7 on Ornstein-Zernike theory[28]). For convenience we reiterate those results:

- In $d = 1$,

$$\chi_{d=1}(x) = \left(\frac{\xi}{2k_{\rm B}T_{\rm c}R_*^2}\right) e^{-|x|/\xi} \quad . \tag{7.199}$$

[28]There is a sign difference between the particle susceptibility defined in chapter 6 and the spin susceptibility defined here. The origin of the difference is that the single particle potential v as defined was repulsive for $v > 0$, meaning the local density response δn should be negative, while in the current discussion a positive magnetic field H prefers $m > 0$.

- In $d > 1$, with $r \to \infty$ and ξ fixed,

$$\chi_d^{\rm OZ}(\boldsymbol{r}) \simeq C_d \cdot \frac{\xi^{(3-d)/2}}{k_{\rm B}T\,R_*^2} \cdot \frac{e^{-r/\xi}}{r^{(d-1)/2}} \cdot \left\{1 + \mathcal{O}\left(\frac{d-3}{r/\xi}\right)\right\} \quad , \tag{7.200}$$

  where the C_d are dimensionless constants.

- In $d > 2$, with $\xi \to \infty$ and r fixed (*i.e.* $T \to T_{\rm c}$ at fixed separation $\boldsymbol{r}$),

$$\chi_d(\boldsymbol{r}) \simeq \frac{C_d'}{k_{\rm B}TR_*^2} \cdot \frac{e^{-r/\xi}}{r^{d-2}} \cdot \left\{1 + \mathcal{O}\left(\frac{d-3}{r/\xi}\right)\right\} \quad . \tag{7.201}$$

  In $d = 2$ dimensions we obtain

$$\chi_{d=2}(\boldsymbol{r}) \simeq \frac{C_2'}{k_{\rm B}TR_*^2} \cdot \log\left(\frac{r}{\xi}\right) e^{-r/\xi} \cdot \left\{1 + \mathcal{O}\left(\frac{1}{\log(r/\xi)}\right)\right\} \quad , \tag{7.202}$$

  where the C_d' are dimensionless constants.

Close to the critical point the spatial dependence of the two-point correlation $C(\boldsymbol{r},T) = k_{\rm B}T\,\chi(\boldsymbol{r},T)$ is given by

$$C(\boldsymbol{r},T) = r^{-(d-2+\eta)}\,\phi\big(r/\xi(T)\big) \quad , \tag{7.203}$$

where η is the *anomalous critical exponent* and $\phi(r/\xi)$ is a *scaling function*. The condition $T \approx T_{\rm c}$ means that $\xi(T) \gg a$, where a is a microscopic length, such as a lattice constant[29]. Thus, we've encountered in this section two additional critical exponents, the anomalous exponent η and the correlation length exponent ν, which we first met in §7.3.2, whose mean field values are $\eta = 0$ and $\nu = \frac{1}{2}$.

7.8 Appendix : Bifurcations

7.8.1 $N = 1$ dynamical systems

A dynamical system with a $N = 1$ dimensional phase space is a first order ODE $\dot u = g(u)$, where $g(u)$ is in general a nonlinear function of u. The dynamics are simple: $\dot u > 0$ for values of u where $g(u) > 0$ (flow to the right), and $\dot u < 0$ for values of u where $g(u) < 0$ (flow to the left). For $u = u^*$ where $g(u^*) = 0$ we have a *fixed point*. Linearizing about the fixed point, we write $u = u^* + \eta$, in which case $\dot\eta = g'(u^*)\,\eta$. Thus $\eta(t) = \eta(0)\,\exp\big[g'(u^*)t\big]$, which says that $|\eta(t)|$ grows exponentially if $g'(u^*) > 0$ and $|\eta(t)|$ shrinks exponentially if $g'(u^*) < 0$. Thus, for $g'(u^*) > 0$ we say that u^* is an *unstable fixed point* (UFP), while for $g'(u^*) < 0$ we say that u^* is a *stable fixed point* (SFP). The linearization about a UFP rapidly fails due to the exponential increase of the distance from u^*, while the linearization about a SFP gets ever more accurate as $\eta(t) \to 0$.

[29] The scaling functions on the high and low temperature sides of the transition may be different, and are denoted as $\phi_\pm(r/\xi)$, respectively.

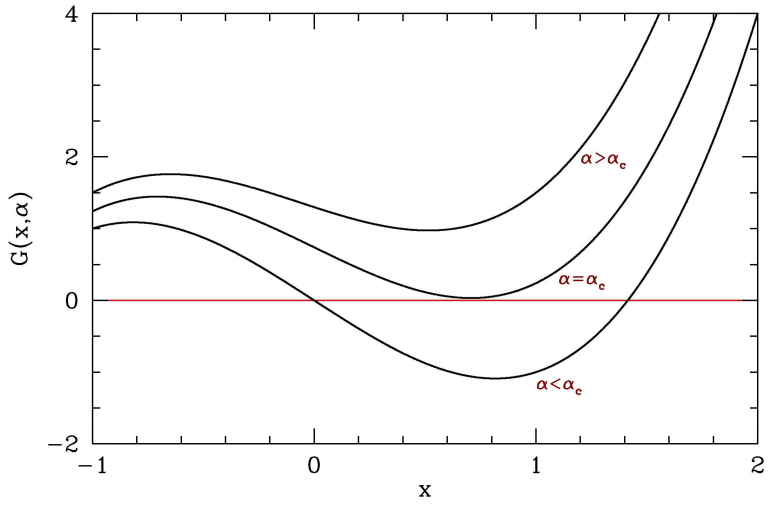

Figure 7.21: Evolution of $G(x,\alpha)$ as a function of the control parameter α.

7.8.2 Saddle-node bifurcation

Generically, $g'(u^*) \neq 0$ at points where $g(u^*) = 0$, since two equations in a single unknown is an overdetermined set. However, consider the function $G(x,\alpha)$, where α is a control parameter. If we demand $G(x,\alpha) = 0$ and $\partial_x G(x,\alpha) = 0$, we have two equations in two unknowns, and in general there will be a zero-dimensional solution set consisting of points $(x_{\rm c}, \alpha_{\rm c})$. The situation is depicted in Fig. 7.21.

Let's expand $G(x,\alpha)$ in the vicinity of such a point $(x_{\rm c}, \alpha_{\rm c})$:

$$\begin{aligned} G(x,\alpha) &= G(x_{\rm c},\alpha_{\rm c}) + \left.\frac{\partial G}{\partial x}\right|_{(x_{\rm c},\alpha_{\rm c})} (x-x_{\rm c}) + \left.\frac{\partial G}{\partial \alpha}\right|_{(x_{\rm c},\alpha_{\rm c})} (\alpha-\alpha_{\rm c}) + \frac{1}{2}\left.\frac{\partial^2 G}{\partial x^2}\right|_{(x_{\rm c},\alpha_{\rm c})} (x-x_{\rm c})^2 \\ &\qquad + \left.\frac{\partial^2 G}{\partial x\,\partial \alpha}\right|_{(x_{\rm c},\alpha_{\rm c})} (x-x_{\rm c})\,(\alpha-\alpha_{\rm c}) + \frac{1}{2}\left.\frac{\partial^2 G}{\partial \alpha^2}\right|_{(x_{\rm c},\alpha_{\rm c})} (\alpha-\alpha_{\rm c})^2 + \ldots \\ &= A\,(\alpha-\alpha_{\rm c}) + B\,(x-x_{\rm c})^2 + \ldots \quad , \end{aligned} \tag{7.204}$$

where we keep terms of lowest order in the deviations δx and $\delta\alpha$. Note that we can separately change the signs of A and B by redefining $\alpha \to -\alpha$ and/or $x \to -x$, so without loss of generality we may assume both A and B are positive. If we now rescale $u \equiv \sqrt{B/A}\,(x - x_{\rm c})$, $r \equiv \alpha - \alpha_{\rm c}$, and $\tau = \sqrt{AB}\,t$, we have, neglecting the higher order terms, we obtain the 'normal form' of the saddle-node bifurcation,

$$\frac{du}{d\tau} = r + u^2 \quad . \tag{7.205}$$

The evolution of the flow is depicted in Fig. 7.22. For $r < 0$ there are two fixed points – one stable ($u^* = -\sqrt{-r}$) and one unstable ($u = +\sqrt{-r}$). At $r = 0$ these two nodes coalesce and annihilate each other. (The point $u^* = 0$ is half-stable precisely at $r = 0$.) For $r > 0$ there are no longer any fixed points in the vicinity of $u = 0$. In the left panel of Fig. 7.23 we show the flow in the extended (r,u) plane. The unstable and stable nodes annihilate at $r = 0$.

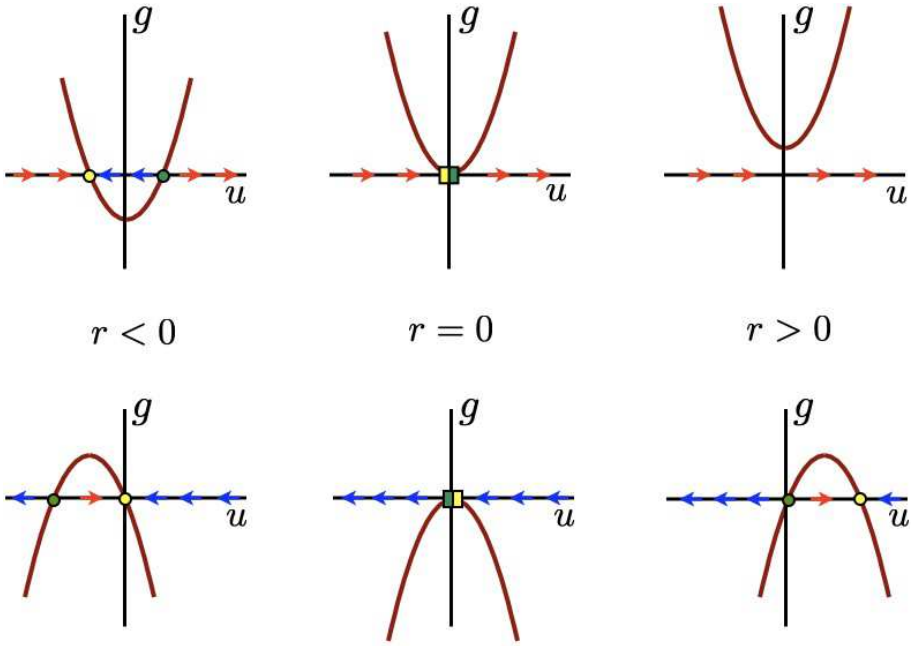

Figure 7.22: Flow diagrams for the saddle-node bifurcation $\dot{u} = r + u^2$ (top) and the transcritical bifurcation $\dot{u} = ru - u^2$ (bottom).

7.8.3 Transcritical bifurcation

Another situation which arises frequently is the *transcritical bifurcation*. Consider the equation $\dot{x} = g(x)$ in the vicinity of a fixed point x^*.

$$\frac{dx}{dt} = g'(x^*)\,(x - x^*) + \tfrac{1}{2}\,g''(x^*)(x - x^*)^2 + \dots \quad . \tag{7.206}$$

We rescale $u \equiv \beta\,(x - x^*)$ with $\beta = -\frac{1}{2}\,g''(x^*)$ and define $r \equiv g'(x^*)$ as the control parameter, to obtain, to order u^2,

$$\frac{du}{dt} = ru - u^2 \quad . \tag{7.207}$$

Note that the sign of the u^2 term can be reversed relative to the others by sending $u \to -u$.

Consider a crude model of a laser threshold. Let n be the number of photons in the laser cavity, and N the number of excited atoms in the cavity. The dynamics of the laser are approximated by the equations

$$\begin{aligned} \dot{n} &= \gamma N n - k n \\ N &= N_0 - \alpha n \quad . \end{aligned} \tag{7.208}$$

Here γ is the gain coefficient and k the photon decay rate. N_0 is the pump strength, and α is a numerical factor. The first equation tells us that the number of photons in the cavity grows with a rate $\gamma N - k$, *i.e.* gain is proportional to the number of excited atoms, and the loss rate is a constant cavity-dependent quantity (typically through the ends, which are semi-transparent). The second equation says that the

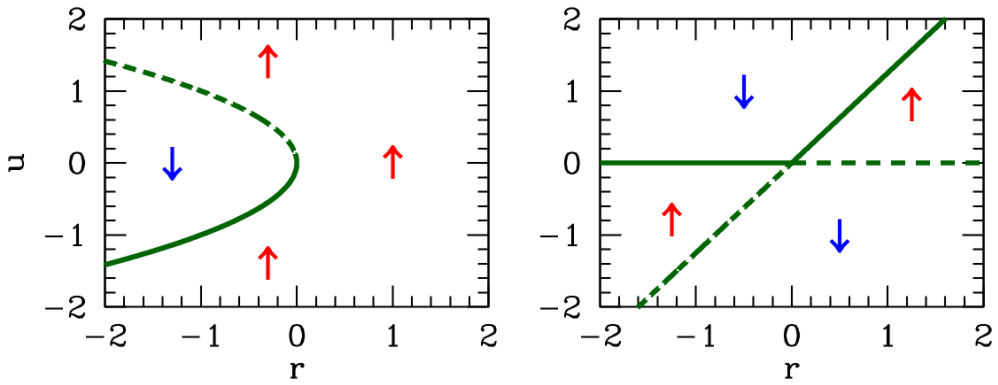

Figure 7.23: Extended phase space (r, u) flow diagrams for the saddle-node bifurcation $\dot{u} = r + u^2$ (left) and the transcritical bifurcation $\dot{u} = ru - u^2$ (right).

number of excited atoms is equal to the pump strength minus a term proportional to the number of photons (since the presence of a photon means an excited atom has decayed). Putting them together,

$$\dot{n} = (\gamma N_0 - k)\, n - \alpha\gamma n^2 \quad , \tag{7.209}$$

which exhibits a transcritical bifurcation at pump strength $N_0 = k/\gamma$. For $N_0 < k/\gamma$ the system acts as a lamp; for $N_0 > k/\gamma$ the system acts as a laser.

What happens in the transcritical bifurcation is an exchange of stability of the fixed points at $u^* = 0$ and $u^* = r$ as r passes through zero. This is depicted graphically in the bottom panel of Fig. 7.22.

7.8.4 Pitchfork bifurcation

The pitchfork bifurcation is commonly encountered in systems in which there is an overall parity symmetry ($u \to -u$). There are two classes of pitchfork: supercritical and subcritical. The normal form of the supercritical bifurcation is

$$\dot{u} = ru - u^3 \quad , \tag{7.210}$$

which has fixed points at $u^* = 0$ and $u^* = \pm\sqrt{r}$. Thus, the situation is as depicted in fig. 7.24 (top panel). For $r < 0$ there is a single stable fixed point at $u^* = 0$. For $r > 0$, $u^* = 0$ is unstable, and flanked by two stable fixed points at $u^* = \pm\sqrt{r}$.

If we send $u \to -u$, $r \to -r$, and $t \to -t$, we obtain the *subcritical pitchfork*, depicted in the bottom panel of fig. 7.24. The normal form of the subcritical pitchfork bifurcation is $\dot{u} = ru + u^3$. The fixed point structure in both supercritical and subcritical cases is shown in Fig. 7.25.

7.8.5 Imperfect bifurcation

The imperfect bifurcation occurs when a symmetry-breaking term is added to the pitchfork. The normal form contains two control parameters: $\dot{u} = h + ru - u^3$. The constant h explicitly breaks the $\mathbb{Z}_2$ parity symmetry $u \to -u$.

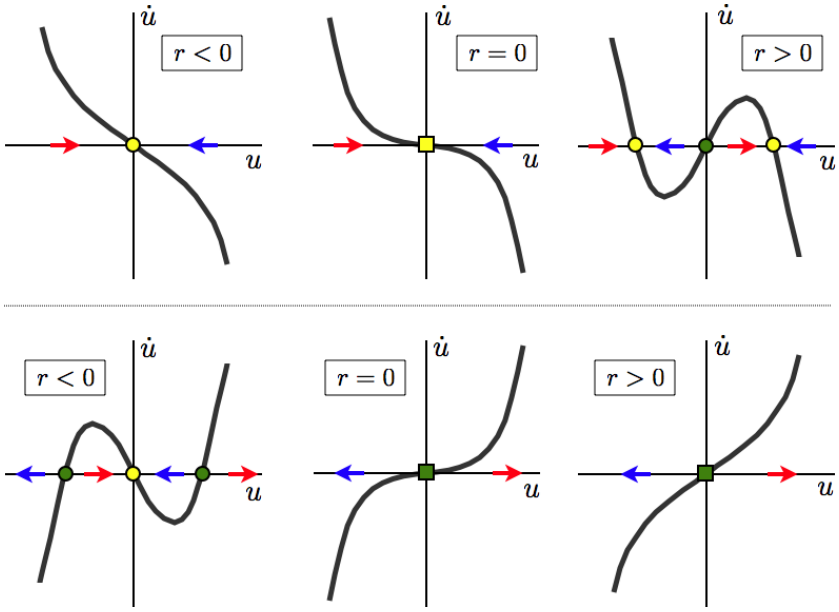

Figure 7.24: Top: supercritical pitchfork bifurcation $\dot{u} = ru - u^3$. Bottom: subcritical pitchfork bifurcation $\dot{u} = ru + u^3$.

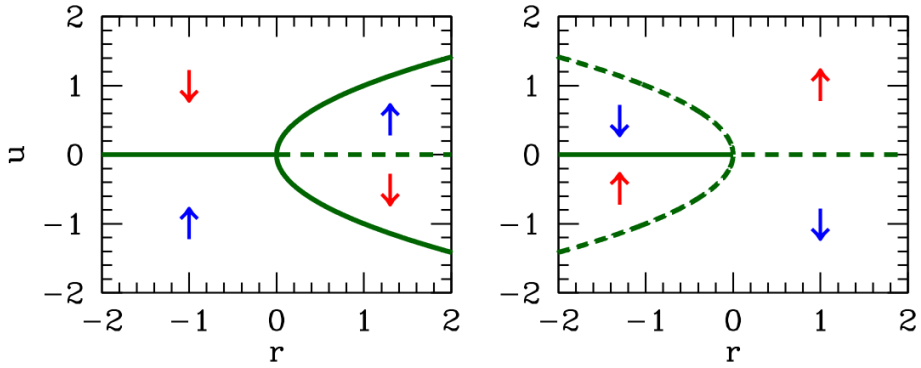

Figure 7.25: Extended phase space (r, u) flow diagrams for the pitchfork bifurcation. Left: supercritical pitchfork $\dot{u} = ru - u^3$. Right: subcritical pitchfork $\dot{u} = ru + u^3$.

This equation arises from a crude model of magnetization dynamics. Let m be the magnetization density of a sample, and $f(m)$ the free energy density. Assuming m is small, we can expand $f(m)$ as

$$f(m) = \tfrac{1}{2}am^2 + \tfrac{1}{4}bm^4 - Hm + \dots \quad , \tag{7.211}$$

where H is the external magnetic field, and a and b are temperature-dependent constants. This is called the *Landau expansion* of the free energy. We assume $b > 0$ in order that the minimum of $f(m)$ not lie at infinity. The dynamics of $m(t)$ are modeled by

$$\frac{dm}{dt} = -\Gamma \frac{\partial f}{\partial m} \quad , \tag{7.212}$$

with $\Gamma > 0$. Thus, the magnetization evolves toward a local minimum in the free energy. Note that the

free energy is a decreasing function of time:

$$\frac{df}{dt} = \frac{\partial f}{\partial m}\frac{dm}{dt} = -\Gamma\left(\frac{\partial f}{\partial m}\right)^2 \quad . \tag{7.213}$$

By rescaling $\tau \equiv \Gamma t$, $m \equiv b^{-1/2}u$, $h \equiv b^{1/2}H$, and defining $r \equiv -a$, we obtain the normal form of the bifurcation,

$$\dot{u} = h + ru - u^3 = -\frac{\partial\varphi}{\partial u} \quad , \tag{7.214}$$

where

$$\varphi(u) = -\tfrac{1}{2}ru^2 + \tfrac{1}{4}u^4 - hu \tag{7.215}$$

is a scaled version of the free energy. Fixed points satisfy the equation

$$u^3 - ru - h = 0 \quad , \tag{7.216}$$

and correspond to extrema in $\varphi(u)$. By the fundamental theorem of algebra, this cubic polynomial may be uniquely factorized over the complex plane. Since the coefficients are real, the complex conjugate $\bar{u}$ satisfies the same equation as u, hence there are two possibilities for the roots: either (i) all three roots are real, or (ii) one root is real and the other two are a complex conjugate pair. Clearly for $r < 0$ we are in situation (ii) since $u^3 - ru$ is then monotonically increasing for $u \in \mathbb{R}$, and therefore takes the value h precisely once for u real. For $r > 0$, there is a region $h \in \big[-h_{\rm c}(r), h_{\rm c}(r)\big]$ over which there are three real roots. To find $h_{\rm c}(r)$, we demand $\varphi''(u) = 0$ as well as $\varphi'(u) = 0$, which says that two roots have merged in a saddle-node bifurcation, forming an inflection point. Thus $\varphi''(u) = 3u^2 - r = 0$ yields $u = \pm(r/3)^{1/2}$, which requires $r > 0$, and using this to eliminate u from the equation $\varphi(u) = 0$ yields the critical value of h as a function of r, *viz.* $h_{\rm c}(r) = \frac{2}{3\sqrt{3}}\, r^{3/2}\,\Theta(r)$.

Examples of the function $\varphi(u)$ for $r > 0$ are shown in the left panel of Fig. 7.26 for three different values of h. For $|h| < h_{\rm c}(r)$ there are three extrema satisfying $\varphi'(u^*) = 0$: $u_1^* < u_2^* < 0 < u_3^*$, assuming

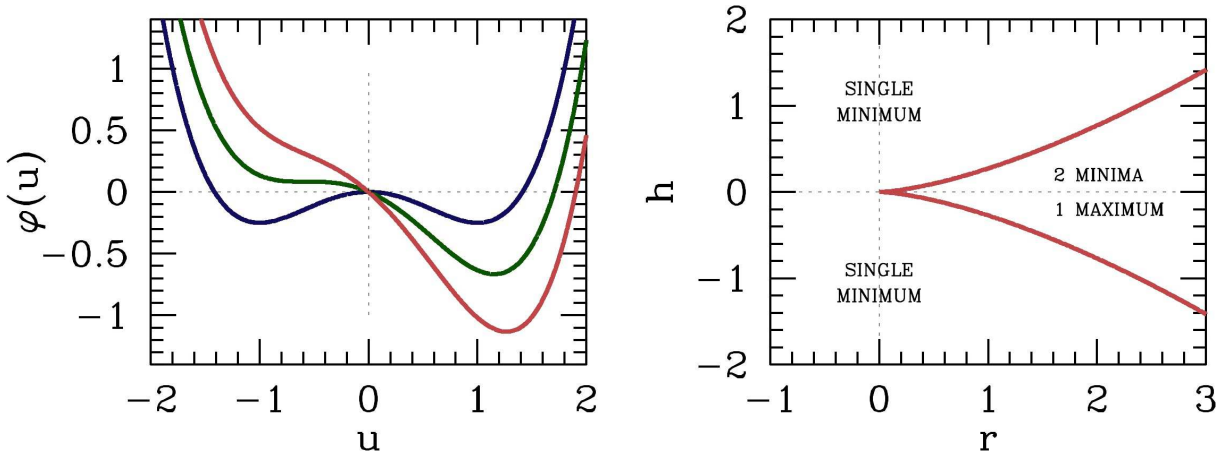

Figure 7.26: Left: scaled free energy $\varphi(u) = -\frac{1}{2}ru^2 + \frac{1}{4}u^4 - hu$, with $h = 0$ (blue), $h = h_{\rm c}$ (green), and $h = 2\,h_{\rm c}$ (red), where $h_{\rm c} = \frac{2}{3\sqrt{3}}\, r^{3/2}$. Right: phase diagram for the imperfect bifurcation $\dot{u} = -\varphi'(u) = h + ru - u^3$ in the (r, h) plane.

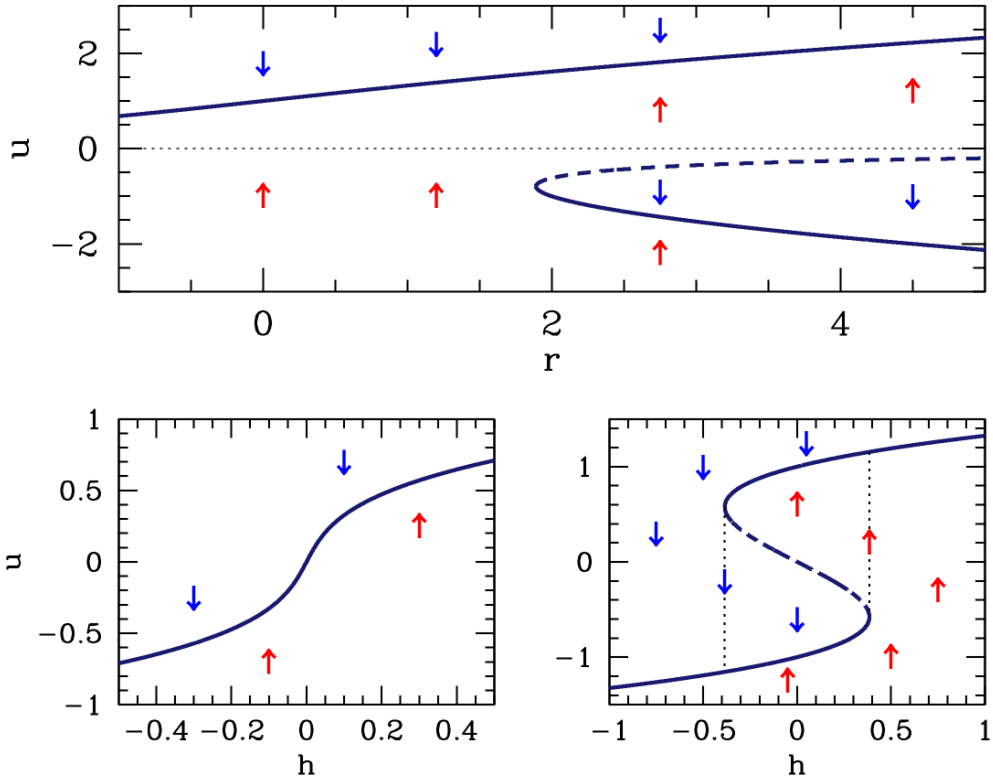

Figure 7.27: Top: extended phase space (r, u) flow diagram for $\dot{u} = h + ru - u^3$, the imperfect pitchfork bifurcation, at $h = 1$. This is in a sense a deformed supercritical pitchfork. The saddle-node bifurcation occurs at $r_c = (3/2^{2/3})|h|^{2/3} = 1.8899$. Bottom: extended phase space (h, u) flow diagram for the imperfect pitchfork bifurcation $r = -0.2$ (left panel) and $r = 1$ (right panel). For $r < 0$ the behavior is completely reversible. For $r > 0$, a regime of irreversibility sets in between $-h_c$ and $+h_c$, where $h_c = 2(r/3)^{3/2}$. The system then exhibits the phenomenon of hysteresis. The dotted vertical lines show the boundaries of the hysteresis loop.

(without loss of generality) that $h > 0$. Clearly u_1^* is a local minimum, u_2^* a local maximum, and u_3^* the global minimum of the function $f(u)$. The 'phase diagram' for this system, plotted in the (r, h) control parameter space, is shown in the right panel of Fig. 7.26.

In Fig. 7.27 we plot the fixed points $u^*(r)$ for fixed h. A saddle-node bifurcation occurs at $r = r_c(h) = \frac{3}{2^{2/3}}|h|^{2/3}$. For $h = 0$ this reduces to the supercritical pitchfork; for finite h the pitchfork is deformed and even changed topologically. Finally, in Fig. 7.27 we show the behavior of $u^*(h)$ for fixed r. When $r < 0$ the curve retraces itself as h is ramped up and down, but for $r > 0$ the system exhibits the phenomenon of *hysteresis*, *i.e.* there is an irreversible aspect to the behavior. Fig, 7.27 shows a *hysteresis loop* when $r > 0$.